Point 4

M = 142E6

ϕ^P = 0.0149 - 142E6/27.7 (30,172)

= 0.01479

CASK LAP JOINTS

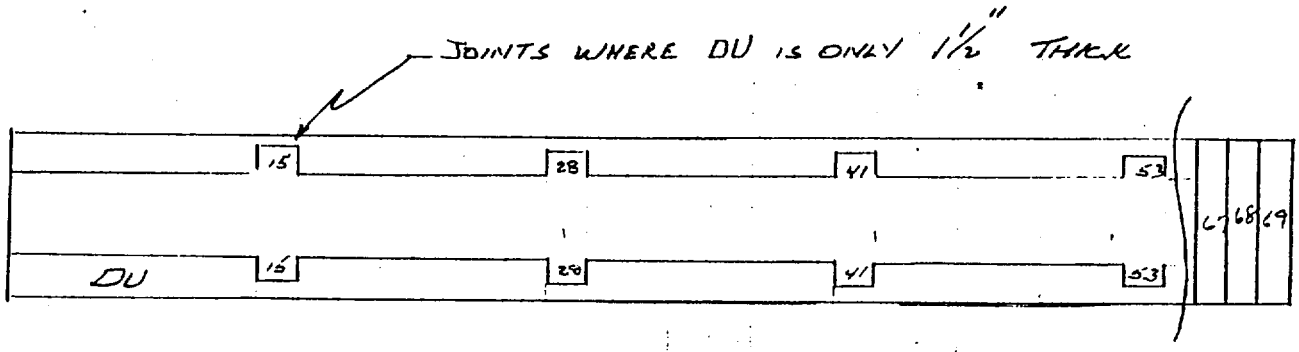

JOINTS 15, 28, 41, AND 53 URANIUM JOINTS

SEE CODE M VS ϕ UNEQUAL TEN/COMP
FOR: $I_{X_{AV}}$ (21500 LB IN SEC²)
V_{BAR} (X 3 IN.)

2.7.1.5 Unequal Sectioned Cask (M vs θ)

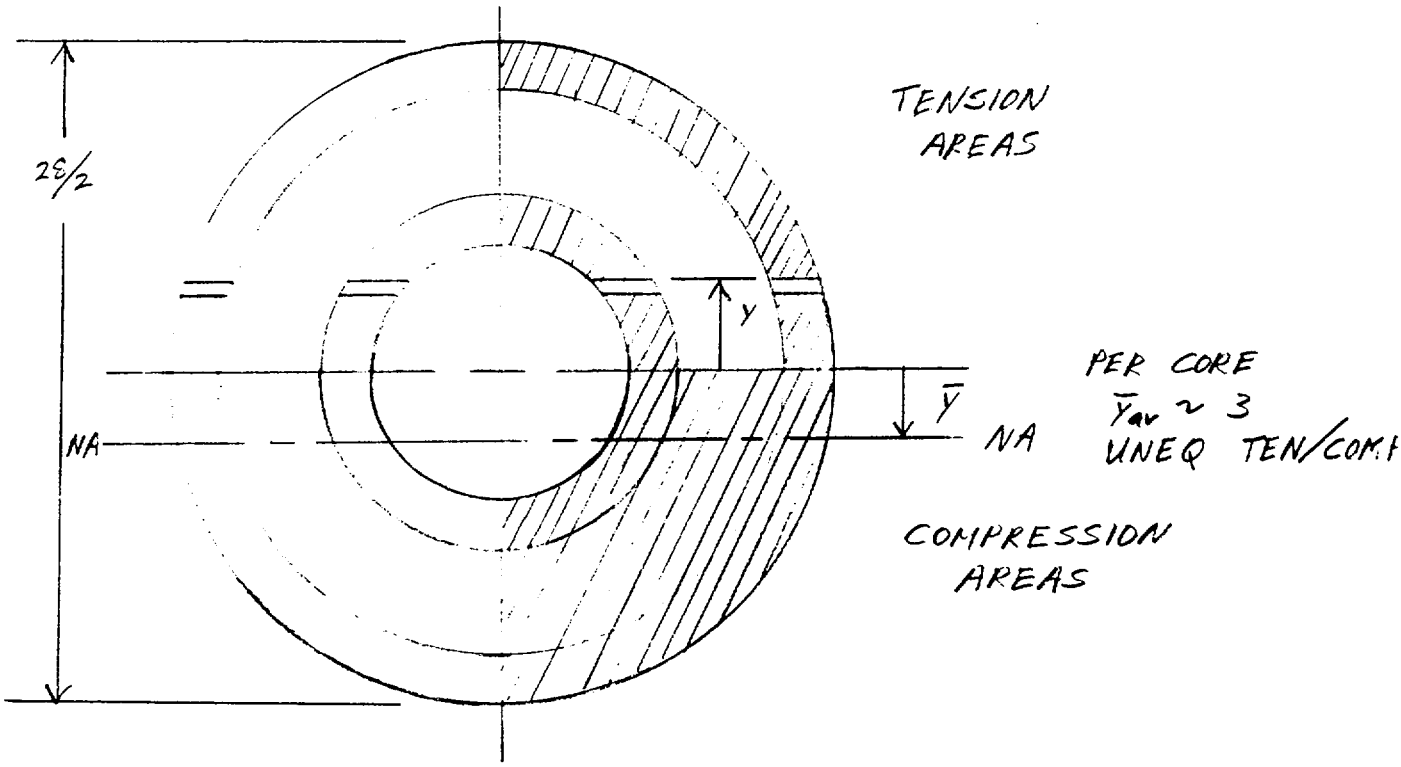

$$M = \int_{-R_o}^{R_o} (y - \bar{y}) \times \sigma\ (\varepsilon(y) \times B(y)\ dy$$

$$F = \int_{-R_o}^{R} \sigma\ (\varepsilon(y) \times B(y)\ dy = 0$$

$$\varepsilon(y) = \phi \times (y - \bar{y})$$

Maximum strain: side drop unequal case

$$2.848 \times 10^{-3} * \left[(28/2) + 3\right] = 4.84\% < 8\%$$

Code input plastic curvature vs moment

Point 1

$M = 48.0 \times 10^6$ $\phi^P = \underline{0.0}$

Point 2

$M = \underline{71.5} \times 10^6$

$\phi^P = 0.0021 - 71.5 \times 10^6/(21{,}500 \times 27.7 \times 10^6)$

$= \underline{0.00198}$

Point 3

$M = \underline{89.5 \times 10^6}$

$\phi^P = 0.0053 - 89.5 \times 10^6/(21{,}500 \times 27.7 \times 10^6)$

$= \underline{0.00515}$

Point 4

$M = \underline{105 \times 10^6}$

$\phi^P = 0.010 - 105 \times 10^6/(21{,}500 \times 27.7 \times 10^6)$

$= \underline{0.00982}$

2.7.1.6 Inner Closure & Cask Bulkhead 30-ft Side Drop (Solid Section)

Results of Computer Analysis

Maximum Load Factors:

Uranium shield, inner closure: 2017 g

4340 alloy steel outer closure: 1133 g

Uranium shield, inner closure:

σ_c = 26,100 psi < S_y = 48,000 psi @ 300°F

4340 alloy steel outer closure: bolts take load

$\sigma_{s_{bolt}}$ = 41,125 psi

Max. strain:

Element 15 plastic curve = 2.032×10^{-3}

03A side drop code (solid)

Strain = $2.033 \times 10^{-3} \times 14$ = 2.8% < 8%

$$\phi = \frac{\varepsilon}{R_o}$$

2.7.1.7 Unequal Tension Compression 30-ft Side Drop

Results of Computer Analysis

Max Load Factors

Uranium shield, inner closure = 2094 g

4340 alloy steel outer closure = 1351 g

Max Stress

Uranium shield, inner closure:

σ_c = 27,100 psi < S$_y$ = 48 ksi at 300 °F

4340 alloy steel outer closure

Hold down bolts take load in shear:

$\sigma_{s_{bolts}}$ = 49,035 psi

Max Strain

Element 15 plastic curvature - 3.925×10^{3}

Strain: 3.925×10^{-3} (28/2 + 3) = 6.7% < 8%

(Neutral axis averages 3 in. below centerline)

$$\phi = \frac{\varepsilon}{R_o}$$

02A side drop code 3.92×10^{-3}

2.7.1.8. Cask Side Drop Equation Derivation

The development of the side drop equations used in the computer code is presented in the following writeup.

The cask is divided into 69 lumped masses joined by a line beam with the appropriate representative section properties, i.e., the initial cask drop velocity is that realized when dropped 30 ft height, making a simultaneous head and tail ground strike. As the cask has a plywood impact limiter of larger diameter than the body proper only the head and tail section make initial ground contact. Then as the beam deflects additional base reactive forces are imparted to the beam as shown in the line element sketched below.

The beam element force and the dynamic equilibrium of each mass element is generated in terms of the bending moment at the mass point. A second central difference is used to approximate the curvature of the beam segments. The bending moment is related to the curvature through a one-dimensional yield criteria and associated flow rule.

GENERAL DEVELOPMENT

DERIVATION OF DYNAMIC RESPONSE OF BEAM

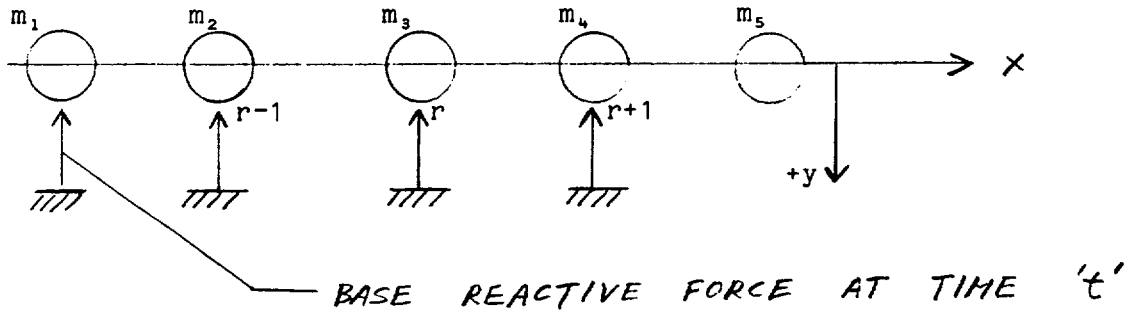

Beam element (between masses) forces

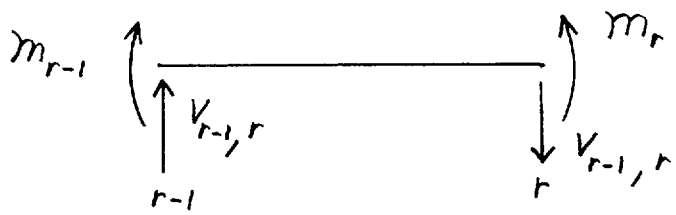

Dynamic Equilibrium of Mass r

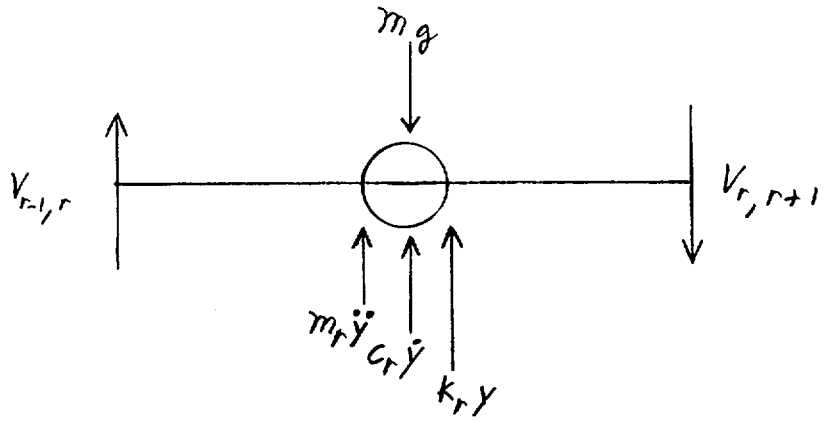

The curvature at point r is approximated by the second central difference for interior points.

$$\left(\frac{d^2y}{dx^2}\right)_r \approx -\frac{1}{\Delta x^2}\left(y_{r+1} - 2y_r + y_{r-1}\right)$$

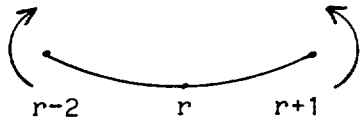

The Moment m is Defined

$$m_r = EI\frac{d^2y}{dx^2} \approx -\frac{EI}{\Delta x^2}\left(y_{r+1} - 2y_r + y_{r-1}\right) \qquad (1)$$

Interior Nodes' Dynamic Equilibrium

$$V_{r1,r} = \frac{m_r - m_{r-1}}{\Delta x} \qquad (2)$$

$$m_r \ddot{y} + V_{r-1,r} - V_{r,r+1} + C \dot{y}_r + K y_r = m_r g$$

Substituting the shear expression in the above yields:

$$m_r \ddot{y}_r - \frac{(m_{r-1} - 2 m_r + m_{r+1})}{\Delta x} + C \dot{y}_r + K y_r = m_r g$$

At the first node

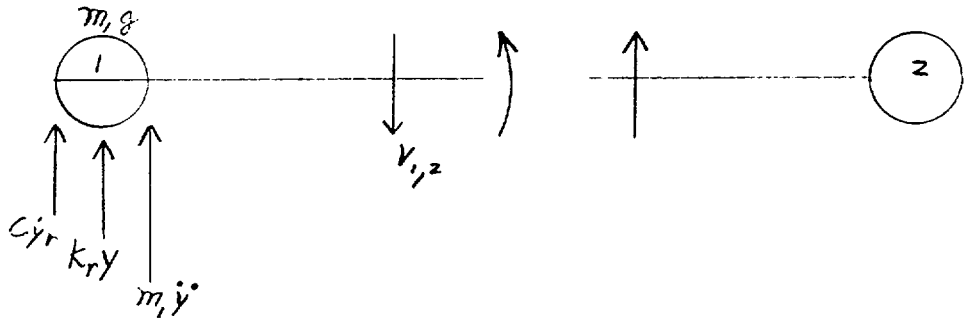

Then for Node 1

$$m_1 \ddot{y} - V_{1,2} + C_1 \dot{y} + k_1 y = m, g \qquad (3)$$

Substituting as before but with the moment on one side only of the mass.

$$m_1 \ddot{y} - \frac{m_2}{\Delta x} + C_1 \dot{y}_1 + k_1 y = m, g$$

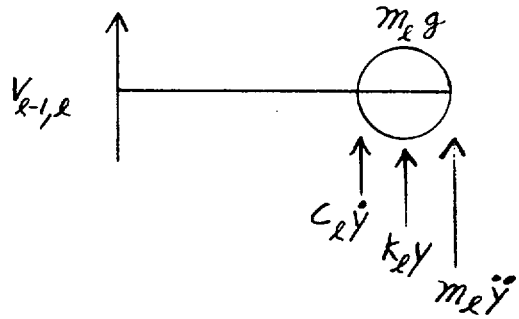

and in similar fashion, the last mass

equation is defined:

$$m_\ell \ddot{y}_\ell - \frac{m_{\ell-1}}{\Delta x} + c \dot{y}_\ell + k y_\ell = m_\ell g \tag{4}$$

The second difference scheme and predicting algorithm are indicated below (see Ref. 2-14) for the Δt time stations:

$$y^{(s+1)} = 2y^{(s)} - y^{(s-1)} + \ddot{y}^{(s)} \Delta t^2 \tag{5}$$

and

$$\dot{y}^{(s)} = \frac{y^{(s)} - y^{(s-1)}}{\Delta t} + \ddot{y}^{(s)} \frac{\Delta t}{2} \tag{6}$$

Substituting Eq. (6) into Eq. (2) gives the following:

$$\ddot{y}^{(s)} = \frac{m, g - k\, y^{(s)} - c\, (y^{(s)} - y^{(s-1)}/\Delta t + \dfrac{m_{r-1} - 2\, m_r + m_{r+1}}{\Delta t}}{(m_r + c\, \Delta t/2)} \tag{7}$$

To start assume (Ref. 2-14, p. 6)

$$y^{(2)} = \frac{1}{6} \left[2\, \ddot{y}^{(1)} + \ddot{y}^{(2)}\right] \Delta t^2 + \dot{y}^{(1)} \Delta t \tag{8}$$

As $\ddot{y}^{(2)}$ is not known the first value is assumed and then Eq. (7) may be solved for a corrected $\ddot{y}^{(2)}$. This process is repeated until no change is noted in $\ddot{y}^{(2)}$.

2.7.1.9 Determination of Stress During Elasto-Plastic Straining

Considering the elastic strain

$$d\varepsilon_e = D^{-1}\, d\sigma \qquad D = \text{elastic constant matrix}$$

If yield is reached

$$F(\sigma, \varepsilon_p, k) = 0$$

where σ = relevant stress comp,
ε_p = accumulated plastic strain, and
k = strain hardening parameter.

Plastic straining may occur and the total strain changes are given as:

$$d\varepsilon = d\varepsilon_e + d\varepsilon_p$$

For added generality the plastic potential to which the normally principles is applicable,

$$Q(\sigma, \varepsilon_p, k_o) = 0$$

where $F \equiv Q$

During plastic deformation by the normality rule:

$$d\,\varepsilon_p = d\lambda\,\frac{\partial Q}{\partial \sigma} = d\lambda\;\bar{a}\;;\;\bar{a} = \left\{\begin{matrix}\partial Q/\partial x \\ \vdots \end{matrix}\right\} = \frac{|M|}{M}$$

and is a vector defined at any stress state. During plastic deformation $F = 0$ and

$$dF = (\partial F/\partial \sigma)^T \, d\sigma + \partial F/\partial k \, dk + \{\partial F/\partial \varepsilon_p\}^T \, d\varepsilon_p = 0$$

If $a = \begin{Bmatrix} \partial F/\partial F \\ \vdots \end{Bmatrix}$ and $A = \frac{-1}{d\lambda}\left[\frac{\partial F}{\partial k} \, dk + (\partial F/\partial \varepsilon_p)^T \, d\varepsilon_p\right]$

dF may be defined: $dF = a^T \, d\sigma - A \, d\lambda = 0$ so that

$$\underline{d\varepsilon = D^{-1} \, d\sigma + d\lambda \, \bar{a}}$$

Premultiplying the aforementioned $d\varepsilon$ expression by $a^T D$ and eliminating $d\sigma$ by $dF = 0$, the following is obtained

$$d^T \, d\varepsilon = A \, d\lambda + d\lambda \, \bar{\beta}$$

where $d = Da$, $\bar{\beta} = A^T \, \bar{d}$ $\bar{d} = D \, \bar{a}$, now the plastic multiplier is:

$$d\lambda = \frac{1}{A + \bar{\beta}} \, d^T \, d\varepsilon$$

substituting $d\lambda$ in the $d\varepsilon$ expression and rearranging

$$d\sigma = (D - D_p) \, d\varepsilon = D\varepsilon_p \, d\varepsilon$$

where

$$D = \frac{1}{A + \bar{\beta}} \bar{d}\, d^T \qquad (D\, d\varepsilon = d\lambda\, \bar{d})$$

In the $d\sigma$ expression above, the stresses are uniquely determined during any iteration in which known finite changes or strain are imposed.

Isotropic hardening assumes a uniform expansion of the initial yield surface, assuming $\partial F/\partial \varepsilon_p = 0$ with k defined $dk = d\bar{e}$. Then for the isotropic work hardening $A = \frac{1}{d\lambda} M' \frac{d\varepsilon_u^P}{dk} dk = H'$ where H' is the scope of the curve relating the uniaxial stress and the corresponding plastic strain.

$$d\lambda = \frac{1}{A + \bar{\beta}} d^T dk = \frac{1}{H' + \bar{\beta}} d^T dk \qquad a = ABS(M)/M$$

with $d^T = Da$, $D = H = EI$

$$\beta = \bar{a}\, d, \quad \bar{d}^T = D\bar{a}$$

$$d\lambda = \frac{H\ ABS(M)/M}{H' + H} dk \qquad d = H\ ABS(M)/M$$

$$H' = \frac{H^*H}{H - H^*} = \frac{H^*}{1 - H^*/H}$$

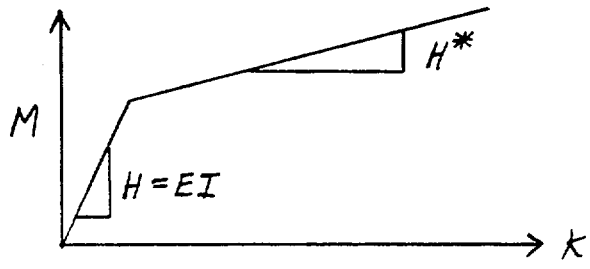

2.7.1.10 Corner Drop-Bottom Corner

In the corner drop calculations the assumption is made that the ungula developed at the impact position represents the total compressive effects at a focal point, rather than the actual nonlinear distribution of strain throughout the whole impacting mass, both elastic and plastic. It allows calculation of maximum stress values, etc., without regard for actual distribution of stress and strain at noncritical values.

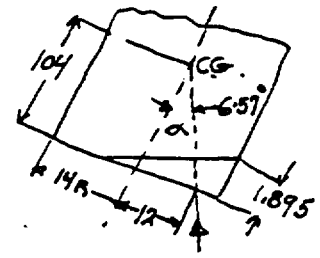

$\alpha = \arctan \frac{12}{104} = .1152$

$= 6.57°$

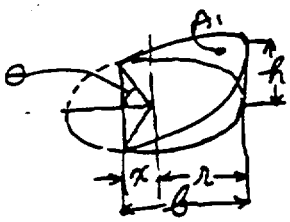

The calculated ungula is a greater volume than will actually result from impact, for this reason.

$$V_{(ungula)} = \frac{h}{b} r^3 [\sin\theta - \frac{\sin^3\theta}{3} - \theta\cos\theta]$$

$\frac{h}{b} = 0.1152$ $\qquad r^3 = 14^3 = 2744$

$\therefore$ $= (0.1152)2744[\ ] = 317[\ ]$

Assume center of impact 2 in. from edge, at R = 12 in.

Total weight impacting on SS bottom plate = 46024 lb

KE = (46024)(360 in.) = 16,600,000 in. lb

Mean flow stress for SS. (Approximately)

P = 53,800 psi

$$\frac{KE}{P} = \frac{16,600,000}{53,800} = 308 \text{ in.}^3$$

This is the calculated ungula volume

$\therefore$ Vol = 317 [ ] = 308 $\qquad [\ ] = \frac{308}{317} = 0.972$

Let $\theta = 100°$, then $[0.9848^3 - \frac{0.9848^3}{3} - (1.745)(-0.1736)] = 0.970$

and $\theta = 1.745$ radians

$x = r \cos\theta = 14(0.1736) = \underline{2.43 \text{ in.}}$

$b = r + x = 14 + 2.43 = \underline{16.43 \text{ in.}}$

$h = b\ (0.1153) = 1.895$ in.

Contact area A_1 = approx. $\frac{\pi r^2}{2} + 2rx = \frac{615.75}{2} + 28\ (2.43)$

$A_1 = 307.9 + 68 = \underline{375.9 \text{ in.}^2}$

$F_{max} = A_1 P_1 = (375.9)(53{,}800) = \underline{20{,}200{,}000 \text{ lb}}$

$F/wt = \frac{20{,}200{,}000}{46{,}024} = \underline{438 \text{ G}}$ vertically,

Component along axis:

$(438 \text{ G})(\cos 6.57°) = 438\ (0.99343) = \underline{435 \text{ G}}$

Bottom Plug Bolt Stresses:

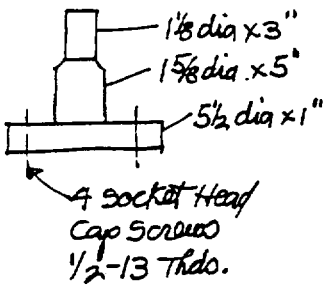

$\pi/4\ (1.125)^2 \times 3 = 3.0 \text{ in}^3$
$\pi/4\ (1.625)^2 \times 5 = 10.4$
$\pi/4\ (5.5)^2 \times 1 = 23.8$
$37.2 \text{ in}^3 \times .284 = 10.57 \text{ LBS}$

Component of deceleration along axis of cask in corner drop is 435G.

Impact force on bottom plug is:

$F = W \cdot G = (10.57)\ (435) = \underline{4600\ lb}$

Each socket head cap screw has a tensile yield strength of:

20,400 lb (high strength steel - 130,000 psi yield)
4,700 lb (stainless steel - 30,000 psi yield)
Minimum strength: 4 x 4,700 = 18,800 lb

$$\text{Margin: } \frac{18,800}{4,600} - 1 = 3.08$$

2.7.2 Puncture

This cask has uranium as shielding between the inner and outer shells. Therefore, piercing of the outer shell with potential loss of shielding in the fire case cannot occur.

Instead, a shallow indent appears on the stainless steel outer shell where the edge of the 6-in. diameter pin partly cuts into it. This is clearly shown in report KY-546 by Clifford, Ref. 2-15. Actually, the pin is more damaged than the cask.

Energy is, however, absorbed in the three concentric shells of the cask in bending, with the possible formation of a plastic hinge.

The approximate distribution of moments among the shells can be made, assuming elastic deflections and an extreme fiber stress of 30,000 psi for both uranium and stainless steel inner and outer shells, with the same deflections, of course. Relative values follow:

34.2%	25,300 in. lb	1 in. SS outer shell
59%	43,500 in. lb	3-1/2 in. uranium
6.8%	5,030 in. lb	5/8-in. inner shell
100%	73,830 in. lb	

Reference 2-16 in the Handbook of the Engineering Sciences - Vol. I - "The Basic Sciences" (pg. 1302-1307) gives the plastic region diagram in a beam when the midsection is just completely plastic.

For the uranium cylinder

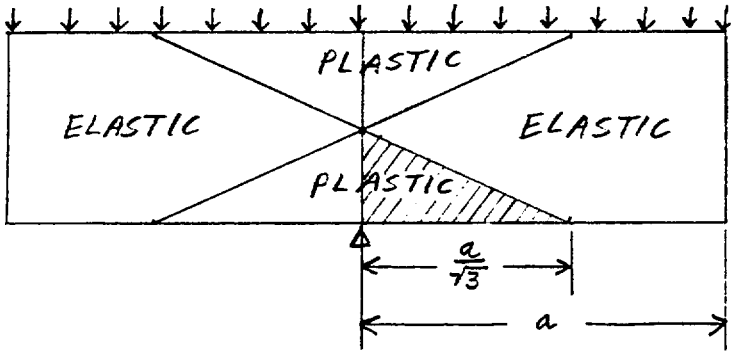

$a = \frac{190}{2}$"
$r_o = 13$"
$r_i = 9.5$"
$H = \frac{a}{\sqrt{3}} = 55$"

The plastic volume = 4 x volume of shaded ungula

$$= 4 \left(\frac{2}{3}\right)(r_o^2 - r_i^2)\, H = 4\left(\frac{2}{3}\right)(13^2 - 9.5^2)\, 55$$

$$= 11{,}520 \text{ in.}^3$$

Each plastic cubic inch has been elongated 0.2% to reach a terminal stress of 30,000 psi (yield point for uranium).

The energy absorbed is

$$U = \frac{30{,}000}{2} (11{,}520)\ (0.002) = \underline{345{,}600 \text{ in. lb}}$$

The total energy of the 40-in. fall is

$$U_{tot} = (46{,}500 \text{ lb})\ 40 \text{ in.} = 1{,}860{,}000 \text{ in. lb}$$

The difference must be absorbed in bending of the "plastic hinge."

$$U_B = 1{,}860{,}000 - 345{,}600 = \underline{1{,}514{,}400 \text{ in. lb}}$$

Determination of plastic section modulus

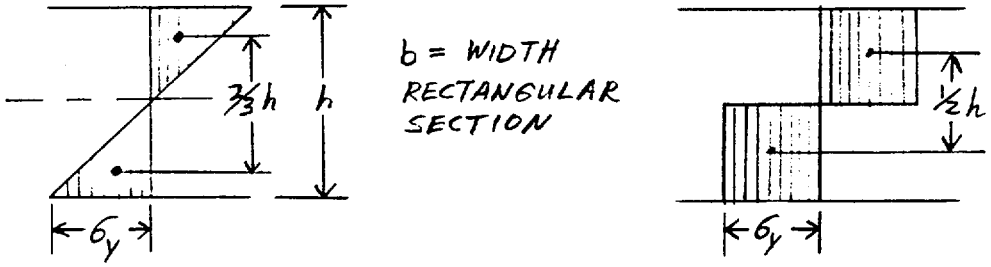

<u>Elastic</u>

$$M_E = \frac{\sigma_y}{2} \times \frac{h}{2}\left(\frac{2}{3}h\right) b$$

$$= \sigma_y \frac{bh^2}{6}$$

<u>Plastic</u>

$$M_p = \sigma_y \times \frac{h}{2}\left(\frac{h}{2}b\right) \qquad \therefore\ M_p = \frac{3}{2} M_E$$

$$= \sigma_y \frac{bh^2}{4}$$

For the <u>circular</u> section of the uranium cylinder

$$I = \frac{\pi}{4}(r_o^4 - r_i^4) \qquad Z_E = \frac{\pi}{4}\frac{(r_o^4 - r_i^4)}{r_o}$$

and

$$Z_p = \frac{3}{2}\,\frac{\pi}{4}\,\frac{(r_o^4 - r_i^4)}{r_o}$$

$$= \frac{3\pi}{8}\,\frac{(13^4 - 9.5^4)}{13} = 1860$$

The plastic moment at the midplane is

$$M_p = \sigma_p Z_p$$

$$= (30{,}000)(1860) = 55{,}800{,}000 \text{ in. lb}$$

But $U_B = M\theta$

or $1{,}574{,}400 = 55{,}800{,}000\ (\theta)$

$$\theta = \frac{1{,}514{,}400}{55{,}800{,}000} = 0.0271 \text{ radians} = \underline{1.56°}$$

Estimated Actual Angle of Bend and Elongation

We are now justified in assuming that the actual conditions, showing loadings on all three shells, would reduce their common angle of bend to

$$(0.59\ (1.56°) = 0.925°\ \theta$$

For the outer fibers of the outer shell this gives

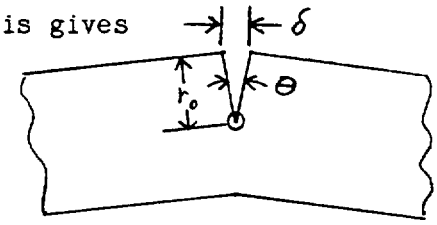

$r_o = 14 \quad \delta = r_o\theta = (14)(0.925)\ (0.01745) = 0.226$ in.

Consider this to be the measured elongation over a 2-in. gage length tension test piece.

$$\frac{0.226}{2} = 11.3\% \text{ elongation}$$

Stainless steel has 40% elongation o.k. No Rupture

Uranium elongation 13/14 in. (11.3) = 10.5% elong. at R = 13 in.

10.5/14 in. (11.3) = 8.5% elong. at R = 10.5 in.

9.5/14 in. (11.3) = 7.7% elong. at R = 9.5

2.7.3. Summary of Damage - 30 ft Bottom Drop

The HONDO runs simulate a cask bottom impact on immovable ground by assigning the 30-ft free fall z-velocity to all nodes, except nodes 1 through 11 on the bottom surface, which are given zero velocity from time point 0 and on. (HONDO model geometry described in Section 2.7.5). From these initial velocity conditions the dyamic response of the cask is determined by the code, and selected displacements, velocities, accelerations, and stresses printed out at specified time intervals.

The computed answers are based on idealized material properties that conservatively substitute the actual material properties within strain and strain-rate ranges experienced in all regions of the cask.

$$V = V_o + a\ t$$

$$S = S_o + V\ t + \frac{1}{2}\ a\ t^2$$

$a = 32 \text{ ft/sec}^2 = 384 \text{ in./sec}^2 \quad V_o = 0 \quad S_o = 0$

$S = 30 \text{ ft} = 360 \text{ in. for } 1/2 \text{ a } t^2 = 360$

or

$$t = \frac{2 \times 350}{384} = \underline{1.3693 \text{ sec}}$$

$V = 0 \ (384) \ (1.3693) = \underline{525.8 \text{ in./sec}}$

Initial z-velocity = -525.8 in./sec for all nodes except nodes 1 - 11.

2.7.4 Materials Data for HONDO Input

The following material characteristics at applicable temperatures are required input:

1. Mass density.

2. Stress as a function of strain up to a permanent set of approximately 0.5% (which correspond to approx. one inch compression of the cask.

3. Yield strength as a function of strain rate.

The stress-strain function is idealized into straight lines and expressed by parameters E, ν, t_o, E_t , and β. A stress-strain curve for the 0.2% Mo-uranium alloy lid shield material was not available from the supplier until after the analysis was made. The idealized curve used in the HONDO input was therefore based on estimates derived from several available sources of information regarding pure uranium and uranium alloys with varying amounts of molybdenum. The idealized curve is conservative in that $\sigma'_y < \sigma_y$. All HONDO runs made produced stresses in the lid shield that were lower than σ'_y (σ'_y = 30,700 psi for 300°F and $\dot{\varepsilon} = 10^{-3}$.

The strain rate sensitivity for the cast 304 stainless steel is based on a 3571 lb/in.^{2} increase in yield strength per decade increase in strain rate (Ref. 2-27). The cask steel temp. is 250°F → 300°F which corresponds to 121°C → 149°C. The actual strain rate sensitivities at these temperatures are probably lower than at room temperature. (Ref. 2-22). The strain rate ($\dot{\varepsilon}$) for a normal tensile test is ~10^{-3}. For strain rates below 10^{-5}

the 304 steel yield strength is assumed constant and equal to the value at $\dot{\varepsilon} = 10^{-5}$.

For the uranium-moly alloys the strain rate sensitivity was assumed similar to the one depicted on Fig. 17, Ref. 2-23 for purge α-uranium-extrapolated downward to $\dot{\varepsilon} = 10^{-6}$. In the range above $\dot{\varepsilon}$ the yield strength is assumed governed by the power equation: (Ref. 2-24, p. 18)

$$t_y = t_o \left[1 + \left(\frac{|\dot{\varepsilon}|}{D} \right)^{1/P} \right]$$

where t_o = the yield strength at $\dot{\varepsilon} = 10^{-6}$ (~zero rate. $\dot{\varepsilon} = 10^{-6}$ in./in./sec corresponds to a doubling of length in 10^6 sec = 278 h, which is a very low rate of strain.)

The "t_o" value read from the idealized stress-strain curve is based on $\dot{\varepsilon} = 10^{-3}$.

Because of uncertainty regarding the validity or the strain rate sensitivity data, the HONDO run will be repeated with strain rate parameters p and D input as zero (gives strain rate insensitive behavior per Ref. 2-24, pg. 71). The model which produces the highest stresses in the lid will be used for analysis of the lid.

The required materials input data are tabulated in Section 2.7.4.

To clarify the results obtained in the HONDO analysis a further discussion of materials data and procedures is provided in Section 2.7.4.

2.7.4.1 Material Identification Nos. 1 & 5

(Cask shells, container shell, inner closure, top member).

304 Stainless Steel ---------→ at $\begin{matrix}250°F\\350°F\end{matrix}$

ASTM A 351 SR CF-8, ASME Code Sect. III Designation: SA-351, CF-8

$\rho = 0.290$ lb/in.^{3}

$g = 980.665$ cm/sec.^{2} -980.665 (0.3937 in./cm) $= 386.0.88$ in./sec

$$\text{Mass density} = \frac{\rho}{g} = \frac{0.290}{368.088} = \underline{0.0007511 \text{ lb/sec}^2/\text{in.}^4}$$

$$E = \frac{\underline{27.4 \times 10^6 \text{ psi}} \text{ @ } 250°F}{\underline{27.1 \times 10^6 \text{ psi}} \text{ @ } 300°F}$$

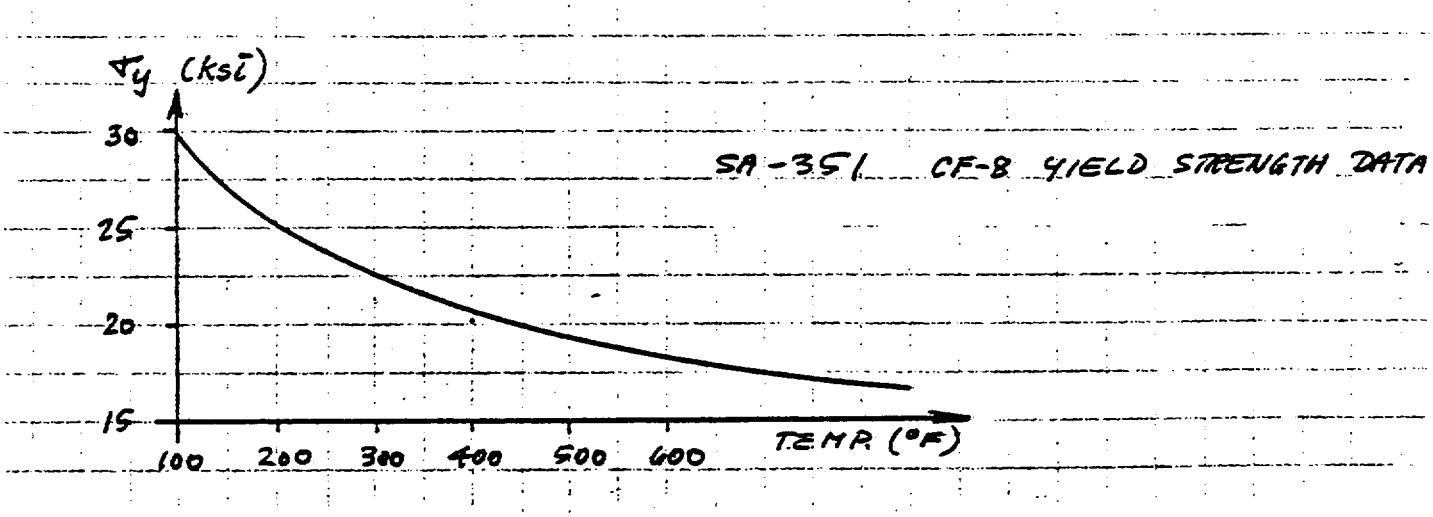

σ_y 250°C = 23.7 ksi

σ_y 300°F = 22.5 ksi

σ_y 400°F = 20.7 ksi

$$\frac{\sigma_{y\ 250°F}}{\sigma_{y\ 400°F}} = \frac{23.7}{20.7} = \underline{1.145}$$

$$\frac{\sigma_{y\ 250°F}}{\sigma_{y\ 400°F}} = \frac{22.5}{20.7} = \underline{1.087}$$

Idealized stress-strain curves are drawn upon Fig. 3.03112 (from Ref. 2-7) below, using E-values and σ_y-ratios from preceding page.

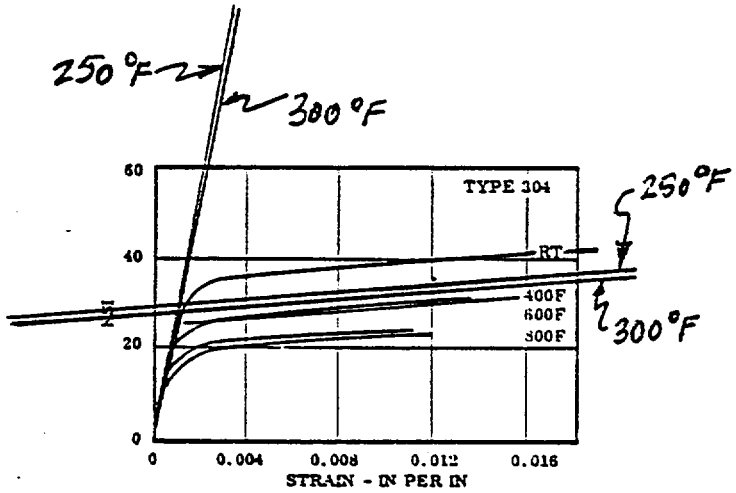

FIG 3.03112 STRESS - STRAIN CURVES AT ROOM AND ELEVATED TEMPERATURES (23)

By scaling graph:

For 250°F (E = 27.4 x 10^6 psi): t_o = 29,500 psi

For 300°F (E = 27.1 x 10^6 psi): t_o = 28,400 psi

Hardening modulus in both cases:

$$E_t = \frac{\Delta\sigma}{\Delta E} = \frac{7368}{0.018} = \underline{409{,}300 \text{ psi}}$$

Strain rate sensitivity: $\Delta\sigma = 3571$ lb/in.^{2} per decade increase in $\dot{\varepsilon}$ for $\dot{\varepsilon} \geq 10^{-5}$. (Ref. 2-27)

$$t_y = t_o = \begin{matrix} \underline{29{,}500 \text{ psi}} \text{ @ } 250°F \\ \underline{28{,}400 \text{ psi}} \text{ @ } 300°F \end{matrix} \quad \text{for } \dot{\varepsilon} = 10^{-3}$$

$$t_y = t_o + [3571]\,[\log_{10}(10^3\,\dot{\varepsilon})] \quad \text{for } \dot{\varepsilon} \geq 10^{-5}$$

2.7.4.2 Material Identification No. 2 (Uranium Shield, Lid)

0.2% Mo Uranium Alloy (Cast) @ 300°F

Density per supplier's data:

$$\rho = \underline{18.81 \text{ g/cm}^3}$$

$$\rho = 18.81 \text{ g/cm}^3 \sim (18.81)\,(0.03613) = \underline{0.67961 \text{ lb/in.}^3}$$

$$\text{Mass density} = \frac{0.67961}{386.088} = \underline{0.0017602 \text{ lb sec}^2/\text{in.}^4}$$

ν = 0.21 compared with ν = 0.25 for pure uranium.

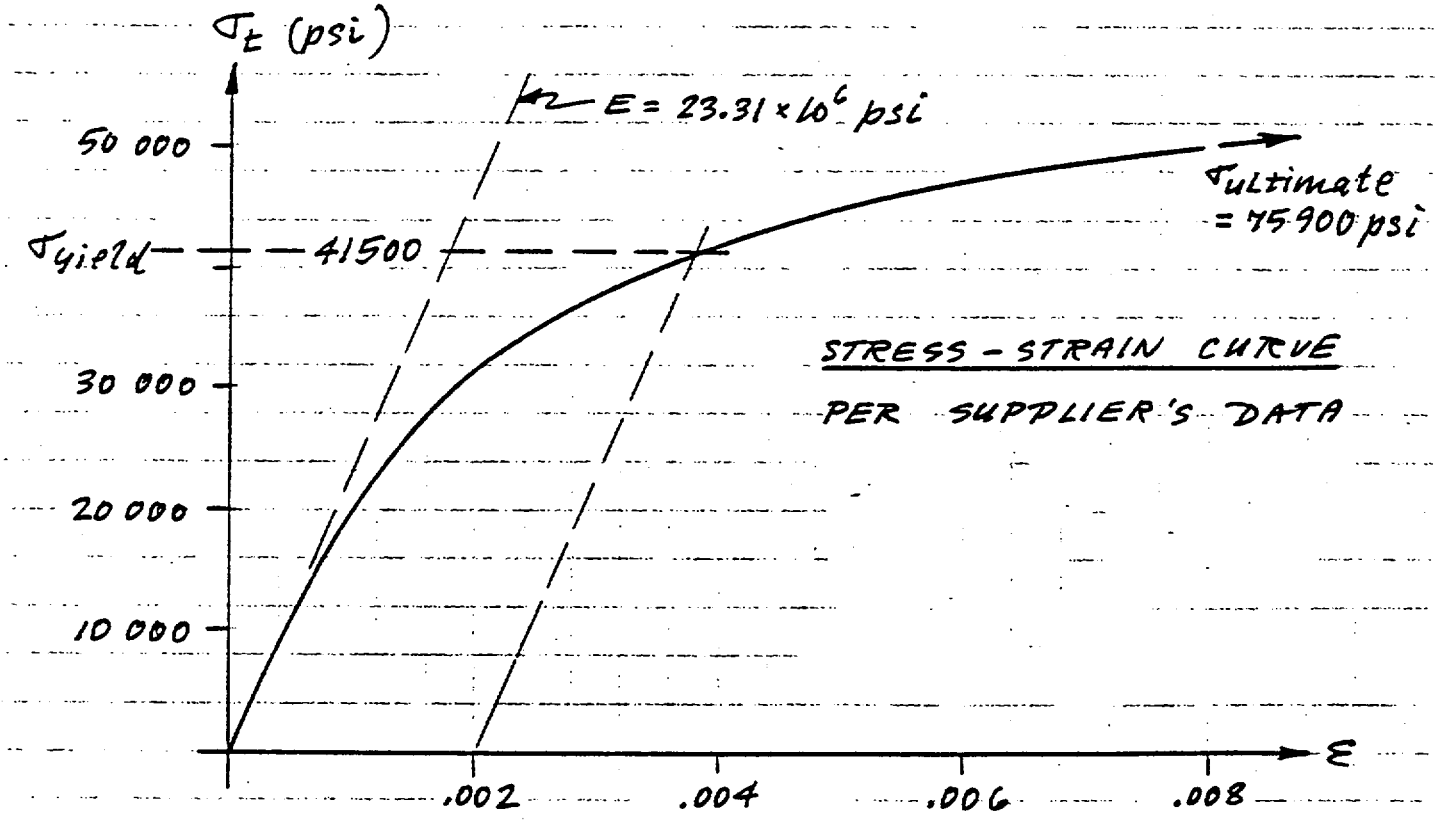

0.2% Mo-uranium alloy (cast) lid shield material @ 70°F in tension.

Strain rate $\dot{\varepsilon} = 10^{-3}$.

Adjustment for 300°F Temperature

Ref. 2-23

70°F ~21°C ~294 K. Read: $E_{70} = 29.0 \times 10^6$ psi

300°F ~149°C = 422 K. Read: $E_{300} = 26.2 \times 10^6$ psi

Ref. 2-23

70°F ~21°C. Read: $\sigma_{yield} = 48$ ksi.

$\sigma_{ult} = 100$ ksi

300°F ~21°C. Read: $\sigma_{yield} = 48$ ksi.

$\sigma_{ult} = 78$ ksi

Adjusted Data:

$$\sigma_y = (41{,}500)\ \frac{42}{48} = \underline{36{,}300 \text{ psi}}$$

$$\sigma_u = (75{,}900)\ \frac{78}{100} = \underline{59{,}200 \text{ psi}}$$

$$E = (23.31 \times 10^6)\ \frac{26.2}{29.0} = \underline{21.1 \times 10^6 \text{ psi}}$$

The stress-strain curve below was constructed on the basis of the adjusted values of σ_y, σ_u, and E.

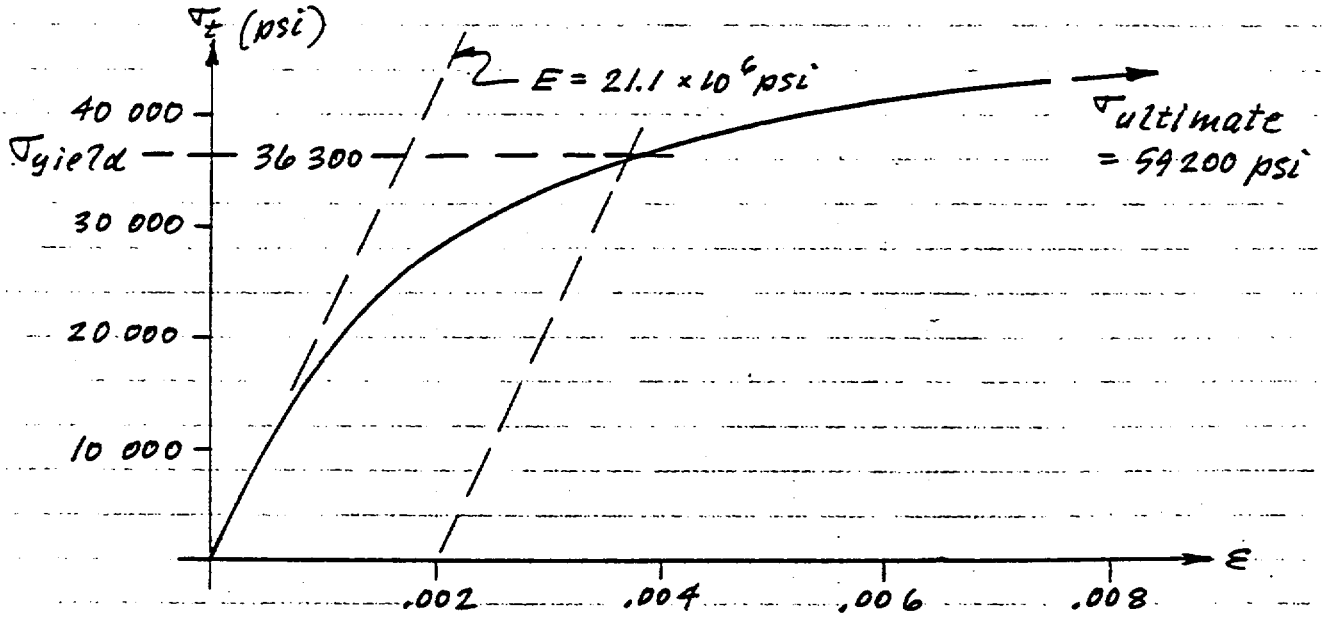

Supplier's Stress-Strain Curve Adjusted for 300°F Temperature

$\dot{\varepsilon} = 10^{-3}$.

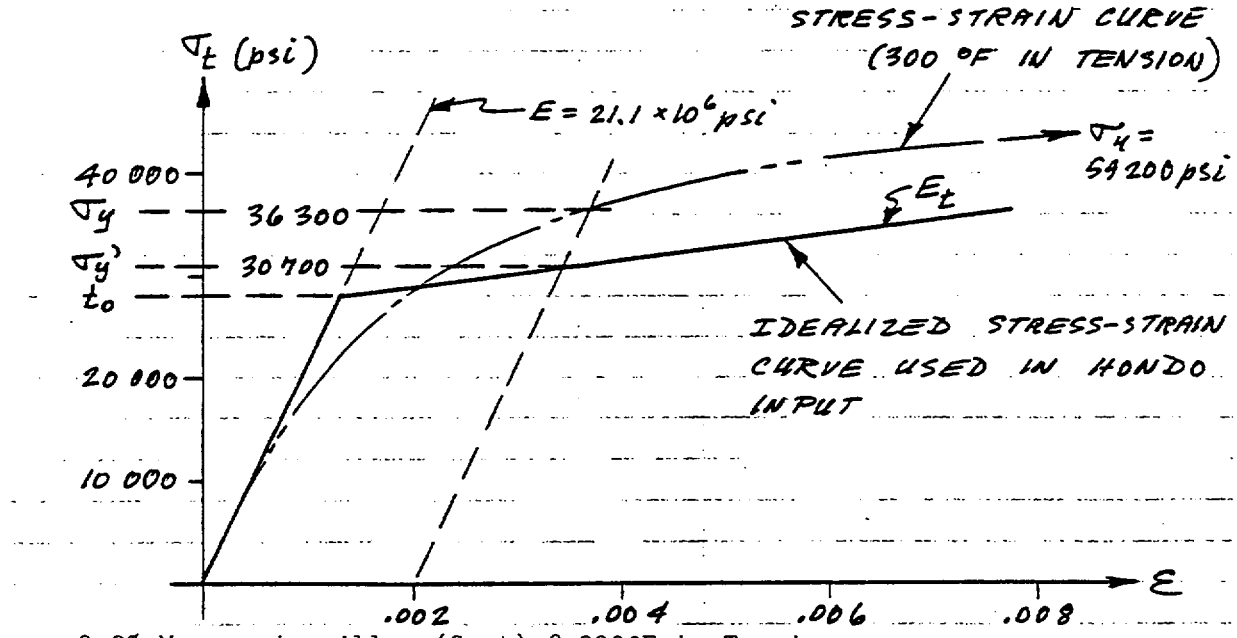

0.2% Mo-uranium Alloy (Cast) @ 300°F in Tension

Strain Rate $\dot{\varepsilon} = 10^{-3}$.

E_t = 1.35 x 10^6 psi

t_o = 28,000 psi

$\sigma'_y = t_o + (E_t)(\varepsilon) = 28{,}000\ (1{,}350{,}000)\ (0.002)$
$= 28{,}000 + 2700 = 30{,}700$ psi

σ'_y = 30,700 psi exceeds stresses experienced in lid.

Slope of E_t line is acceptable for the 30-ft drop analysis since stresses in the lid never reach the idealized static ($\dot{\varepsilon} = 10^{-3}$) yield strength σ'_y.

Strain Rate Sensitivity Constants P&D

Refer to Ref. 2-23 and use $t_o = \sigma$ at $\dot{\varepsilon} = 10^{-6}$ (by extrapolation).

extrapolation).

Analysis of Fig. 17, Ref. 2-23:

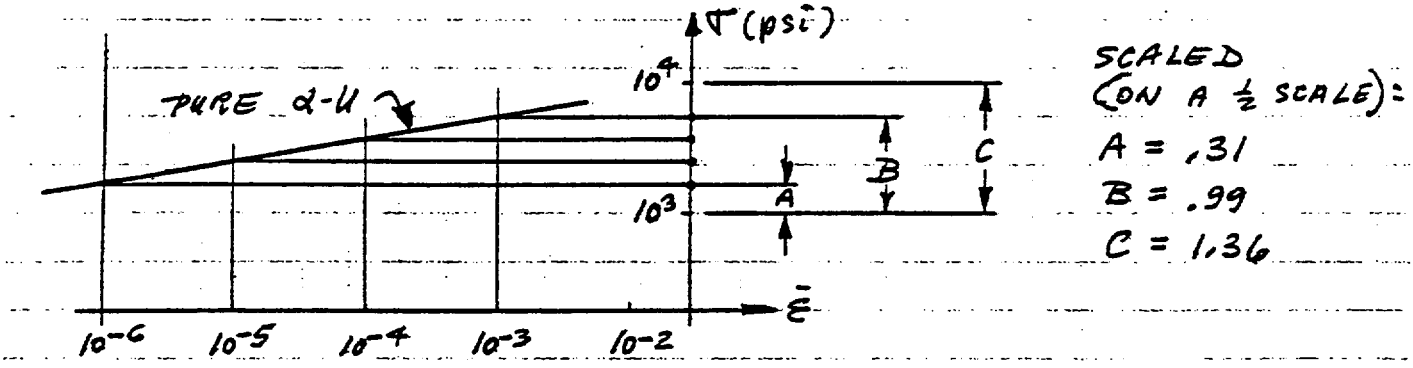

$1/3\ (B-A) = 1/3\ (0.99 - 0.31) = \underline{0.22667}$

$A + 1/3\ (B-A) = 0.31 + 0.22667 = \underline{0.53667}$

$A + 2/3\ (B-A) = 0.31 + 0.45334 = \underline{0.76334}$

$\text{Log } 1.6881 = 0.2274 - (0.2274)\ (1.36) = 0.31 = A$

$\sigma_{10^{-6}} = \underline{1688 \text{ psi}}$

$\text{Log } 2.481 = 0.3946 - (0.3946)(1.36) = 0.53667 = A + 1/3\ (B-A)$

$\sigma_{10^{-5}} = \underline{2481 \text{ psi}}$

$\text{Log } 3.6415 = 0.56128 - (0.56128)(1.36) = 0.76334 = A + 2/3\ (B-A)$

$\sigma_{10^{-4}} = \underline{3642 \text{ psi}}$

$\text{Log } 5.345 = 0.72794 - (0.72794)\ (1.36) = 0.99 = B$

$\sigma_{10^{-3}} = \underline{5345 \text{ psi}}$

Power law (Ref. 2-24):

$$t_y = t_o\left[1 + \left(\frac{|\dot{\varepsilon}|}{D}\right)^{1/p}\right] \text{ or } |\dot{\varepsilon}| = D\left(\frac{t_y}{t_o} - 1\right)^p$$

$$\text{for } |\dot{\varepsilon}| > 10^{-6}$$

Taking $t_o = t_y$ for $\dot{\varepsilon} = 10^{-6}$: $t_o = 1688$ psi

$$(1): \quad 10^{-5} = D\left(\frac{2481}{1688} - 1\right)^{p}$$

$$(2): \quad 10^{-4} = D\left(\frac{3642}{1688} - 1\right)^{p}$$

$$(3): \quad 10^{-3} = D\left(\frac{5345}{1688} - 1\right)^{p}$$

$$\frac{(1)}{(2)} \quad 10^{-1} = \left(\frac{\frac{2481}{1688} - 1}{\frac{3642}{1688} - 1}\right)^{p} = \left(\frac{0.4698}{1.1576}\right)^{p} = (0.4058)^{p}$$

$$-1 = p \log (0.4058)$$

$$p = \frac{-1}{-0.3917} = \underline{2.553}$$

$$(1): \quad 10^{-5} = D\left(\frac{2481}{1688} - 1\right)^{2.553}$$

$$\frac{10^{-5}}{D} = (0.4698)^{2.553} = 0.1453$$

$$D = \frac{10^{-5}}{0.1453} = \underline{6.882 \times 10^{-5}}$$

$$\frac{(2)}{(3)} \quad 10^{-1} = \left(\frac{\frac{3642}{1688} - 1}{\frac{5345}{1688} - 1} \right)^{p} = \left(\frac{1.1576}{2.1665} \right)^{p} = (0.5343)^{p}$$

$$-1 = p \log (0.5343)$$

$$p = \frac{-1}{-0.2722} = \underline{3.6738}$$

(2): $10^{-4} = D\,(1.576)^{3.6738}$

$$\frac{10^{-4}}{D} = (1.576)^{3.6738} = 1.7110$$

$$D = \frac{10^{-4}}{1.7110} = \underline{5.8412 \times 10^{-5}}$$

For HONDO analysis use average values:

$$p = 1/2\,[2.553 + 3.6738] = \underline{3.113}$$

$$D = 1/2\,[6.882 + 5.8412]\,10^{-5} = \underline{6.362 \times 10^{-5}}$$

For 0.2% Mo-uranium alloy @300°F: idealized

$$t_y = 28{,}000 \text{ psi for } \dot{\varepsilon} = 10^{-3}$$

$$|\dot{\varepsilon}| = D \left[\frac{t_y}{t_o} - 1 \right]^{p}$$

$$10^{-3}\ [6.362 \times 10^{-5}] \left[\frac{23{,}000}{t_o} - 1\right]^{3.113}$$

$$15.718 = \left[\frac{28{,}000}{t_o} - 1\right]^{3.113} = x^{3.113}$$

$$\text{Log } 15.718 = 3.113 \text{ Log } x = 1.1964$$

$$\text{Log } x = \frac{1.1964}{3.113} = 0.3843$$

$$x = \frac{28{,}000}{t_o} - 1 = 2.4228$$

$$\frac{28{,}000}{t_o} = 3.4228 \qquad t_o = \frac{28{,}000}{3.4228} = \underline{8180 \text{ ksi}}$$

$$t_y = t_o \left[1 + \left(\frac{\dot{\varepsilon}}{D}\right)^{1/p}\right]$$

$$\dot{\varepsilon} = 10^{-5} : t_y = (8180) \left[1 + \left(\frac{10^{-5}}{6.362 \times 10^{-5}}\right)^{1/3.11}\right] = (8180)\ [1.552]$$

$$= \underline{12{,}695 \text{ psi}}$$

$$\dot{\varepsilon} = 10^{-4} : t_y = (8180) \left[1 + \left(\frac{10^{-4}}{6.362 \times 10^{-5}}\right)^{1/3.113}\right] = (8180)\ [2.156]$$

$$= \underline{17.640 \text{ psi}}$$

$$\dot{\varepsilon} = 10^{-3} : t_y = (8180)\left[1 + \left(\frac{10^{-3}}{6.362 \times 10^{-5}}\right)^{1/3.113}\right] = (8180)\,[3.423]$$

$$= \underline{27{,}800 \text{ psi}}$$

$$\dot{\varepsilon} = 10^{-2} : t_y = (8180)\left[1 + \left(\frac{10^{-2}}{6.362 \times 10^{-5}}\right)^{1/3.113}\right] = (8180)\,[3.423]$$

$$= \underline{49{,}707 \text{ psi}}$$

2.7.4.3 Material Identification No. 3 (Uranium Shield, Cylinder)

0.2% Mo Uranium Alloy (Cast) @250°F

Densities per Ref. 2-25,

Pure Cast Uranium : $\rho = 18.9$ g/cm³

2% Mo-Uranium Alloy: $\rho = 18.4$ g/cm³

0.2% Mo-Uranium Alloy: $\rho = 18.9 - 1/10\,(18.9 - 18.4) = \underline{18.85 \text{ g/cm}^3}$

$\rho = 18.85 \text{ g/cm}^3 - (18.85)(0.3613) = \underline{0.68105 \text{ lb/in.}^3}$

$$\text{Mass density} = \frac{0.68105}{386.088} = \underline{0.0017640 \text{ lb.sec}^2 \text{ in.}^4}$$

For Poisson's ratio use: $\nu = 0.21$

Stress-Strain Data

The cask items of this material are primarily subject to compression loading. The stress-strain constants will therefore be based on the compression curve in Fig. 2-6. The average curve from Ref. 2-23, which is for pure uranium at room temperature, has been adjusted for 0.2% Mo addition and 250°F temperature and shown together with E and E_t lines for strain range of up to 0.5% permanent set.

Ref. 2-25 $E = [25 - 1/10\ (25 - 21)] \times 10^6$

$s\ 2 = 24.6 \times 10^6$ psi

For 0.2% Mo-uranium alloy at room temperature.

Reduction of E for 250°F temperature:

For 70°F ~21°C ~294 K. Read: $E_{70} = 29.0 \times 10^6$ psi

For 250°F ~121°C ~394 K. Read: $E_{250} = 26.8 \times 10^6$ psi

$$E = [24.6 \times 10^6] \frac{26.8}{29.0} = \underline{22.73 \times 10^6 \text{ psi}}$$

Reduction of σ_{yield} for 250°F temperature:

70°F ~21°C. Read: $\sigma_{yield} = 48$ ksi

250°F ~121°C. Read: $\sigma_{yield} = 43$ ksi

$$\text{Factor} = \frac{43}{48} = \underline{0.8958}$$

Increase of σ_{yield} for 0.2% Mo addition:

Pure uranium: $\sigma_{yield} = 25$ ksi

0.2% Mo-uranium alloy: $\sigma_{yield} = 55$ ksi

0.2% Mo-uraniium alloy: $\sigma_{yield} = 25 + 1/10\ (55-25)$ =28 ksi

$$\text{Factor} = \frac{28}{25} = 1.12$$

Total Adadjustment factor = (0.8958)(1.12) = 1.0033

By scaling and adjusting points on the curve in Section 2.7.4.2, the following points are arrived at:

$$\varepsilon = 0.002 \text{ permanent set} = \sigma = \sigma_{yield} = (73{,}000)\ (1.0033)$$
$$= 73{,}241 \text{ psi}$$

$$\varepsilon = 0.005 \text{ permanent set} = \sigma = (82{,}105)\ (1.0033)$$
$$= 82{,}376 \text{ psi}$$

Using E = 22.73 x 10^6 psi together with the two stress values above, the stress-strain curve detail in Section 2.7.4.3 was drawn.

HONDO input values are scaled from this graph:

t_o = 64,200 psi

E_t = 3.15 x 10^6 psi

t_o for the strain rate sensitive case is determined from equation;

$$t_y = t_o \left[1 + \left(\frac{|\dot{\varepsilon}|}{D} \right)^{1/p} \right]$$

$$64{,}000 = t_o \left[1 + \left(\frac{10^{-3}}{6.362 \times 10^{-5}} \right)^{1/3.113} \right]$$

$= t_o [1 + 2.4228]$

$t_o = \underline{18,756 \text{ psi}}$

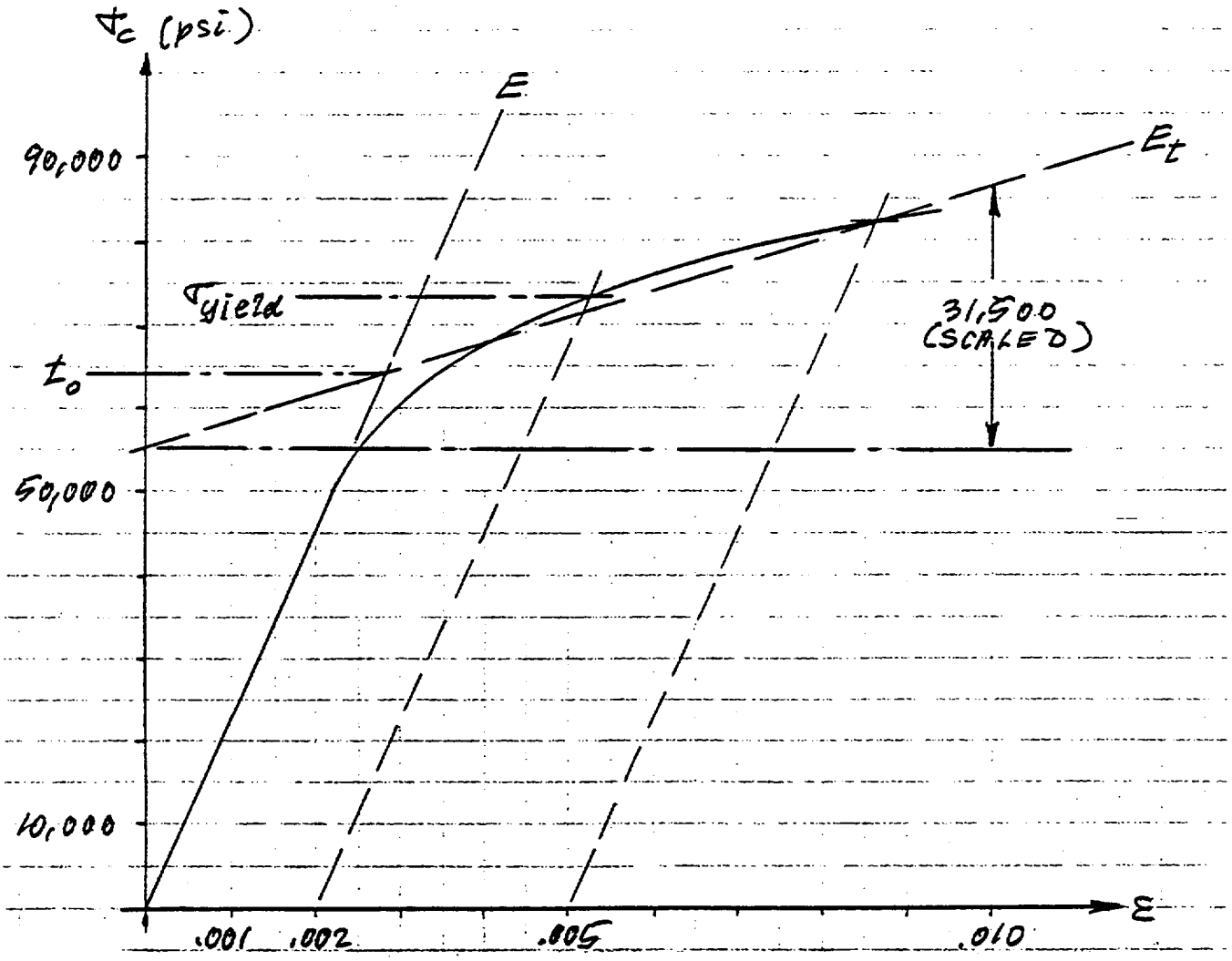

Figure 2-6

Detail of Stress-Strain Curve for 0.2% Mo-Uranium Alloy (Cast) @250°F in compression.

$E = 22.73 \times 10^6$ psi

σ_{yield} = 73,241 psi

By scaling graph:

t_o = 64,200 psi

$$E_t = \frac{\sigma}{\varepsilon} = \frac{31,500}{0.01} = 3.15 \times 10^6 \text{ psi}$$

2.7.4.4 Material Identification No. 4 (Inner Closure Top Membrane)

Identical to material identification No. 5 except for the use of an arbitrary small E value. This was done in order to simulate the weight effect of the lid membrane without taking advantage of any stiffness that in the solution could unrealistically benefit the uranium shield.

Material Identification No. 6 (Top Head of Cask)

4340 Low Alloy Steel. Heat treated to minimum 150,000 psi yield @300°F. Composition = 0.4C, 1.8 Ni, 0.8 Cr, 0.25 Mo.

150 ksi yield @300°F requires an F_{tu} = approximately 175 psi at room temperature (Ref. 2-7).

ρ = 0.285 lb/in.^{3}

$$\text{Mass density} = \frac{\rho}{g} = \frac{0.285}{386.088} = 0.0007382 \text{ lb/sec}^2/\text{in.}^4$$

E = 29.0 x 10^6 psi @300°F.

Stress-Strain Data

The 0.002 yield point for 175 ksi material will be ~165 ksi.

By comparison with low alloy steel SA-533 (1/2 Mo):

$$\sigma_{yield} = \begin{matrix} 82.5 \text{ ksi } @100°F \\ 76.0 \text{ ksi } @300°F \end{matrix}$$

$$4340 \text{ yield point } @300°F = \frac{76.0}{82.5}(165)$$

$$= 152 \text{ ksi } \sim 150 \quad \text{o.k.}$$

Although the curve is flat at room temperature, there will be some slope at 300°F.

$$E = \frac{1}{2}\frac{54{,}000}{0.01221} = \underline{2.22 \times 10^6 \text{ psi}}$$

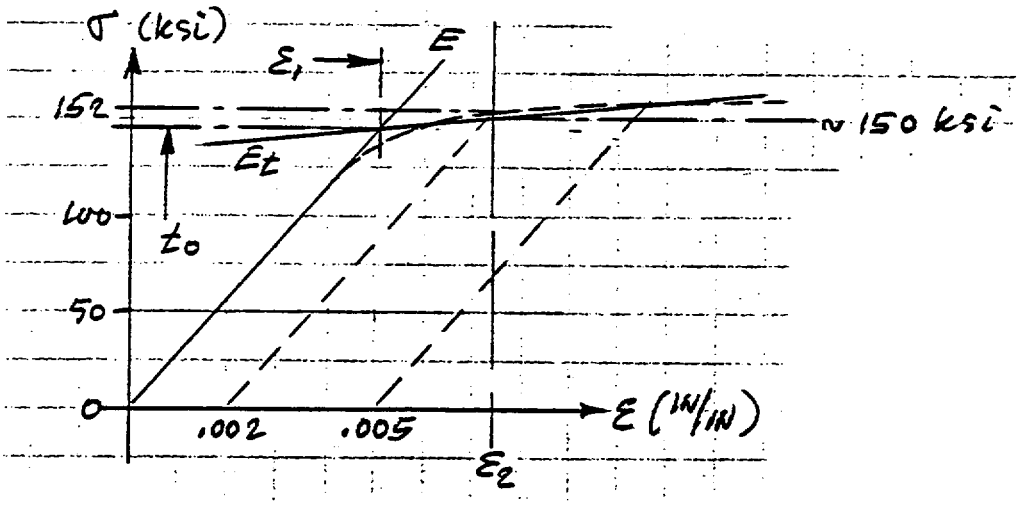

* Stresses in the bulkhead never reached t_o in any of the HONDO runs. Consequently, the E_t value had no effect on the computer answers.

$$\varepsilon_2 = 0.002 + \frac{\sigma}{E} = 0.002 + \frac{152{,}000}{29.0 \times 10^6}$$

$$= 0.002 + 0.00524 = \underline{0.00724}$$

$$t_o = E\,\varepsilon_1 = \underline{29.0 \times 10^6\ \varepsilon_1}$$

$$150{,}000 = t + (\varepsilon_\tau - \varepsilon_r)\,E_t = t_o + (0.00724 - \varepsilon_1)\,(2.22 \times 10^6)$$

or

$$150{,}000 = t_o + \left(0.00724 - \frac{t_o}{29.0 \times 10^6}\right)(2.22 \times 10^6)$$

$$150{,}000 = t_o + 16{,}076 - 0.07655\ t_o$$

$$t_o = \underline{145{,}000\ \text{psi}}$$

4340 Low Alloy Steel

Strain Rate Sensitivity is minimal for 4340 material @300°F (Ref. 2-22).

Materials Data from Ref. 2-7:

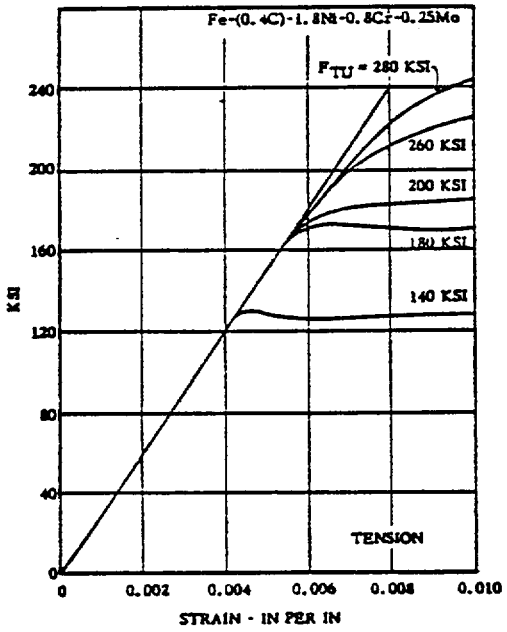

FIG. 3.02111 TYPICAL STRESS-STRAIN CURVES FOR VARIOUS STRENGTH LEVELS (31) (35)

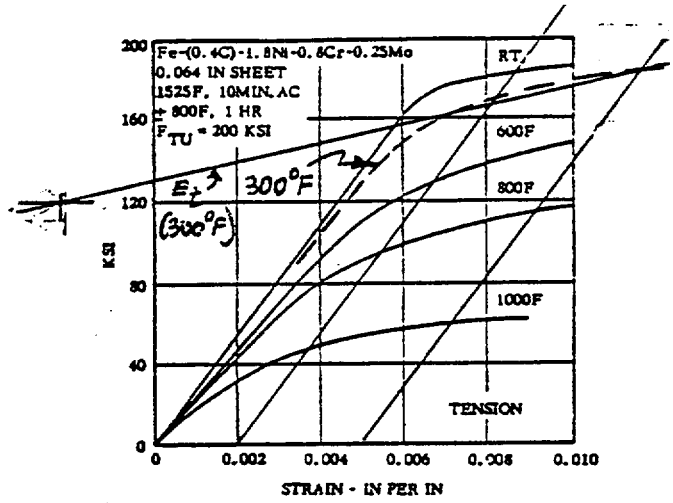

FIG. 3.03111 STRESS-STRAIN CURVES AT ROOM AND ELEVATED TEMPERATURES FOR SHEET HEAT TREATED TO F_{TU} = 200 KSI (20, p. 15)

CODE 1206
PAGE 6

Fe
0.4 C
1.8 Ni
0.8 Cr
0.25 Mo

43404337

CODE 1206
PAGE 13

FIG. 3.03111 = 300°F DATA & .002 & .005 ELASTIC LINES ADDED.

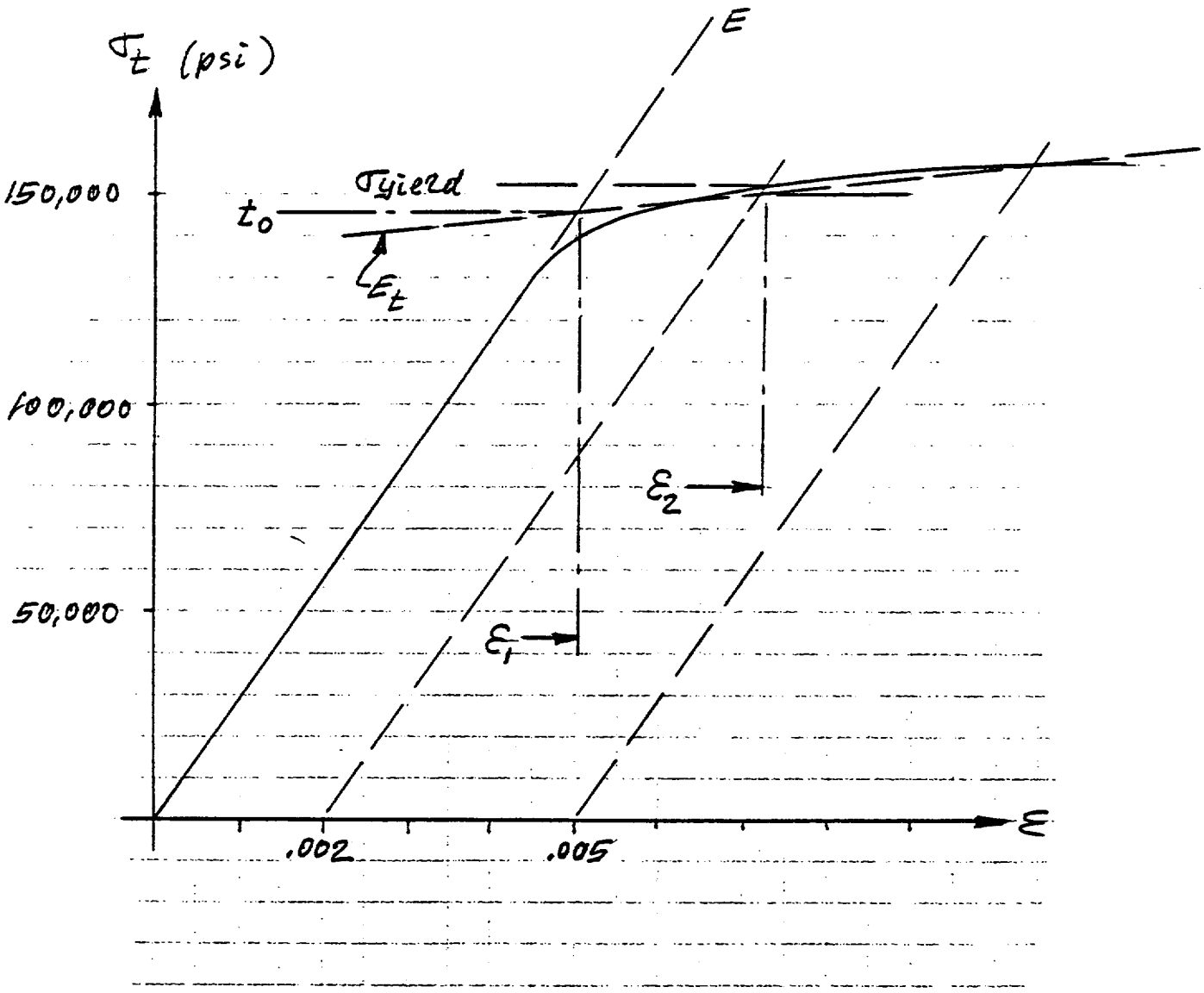

DETAIL OF STRESS-STRAIN CURVE FOR 4340 LOW ALLOY STEEL (F_{tu} = 175 ksi) @ 300 °F

t_o = 145 000 psi

E_t = 2.22 × 10^6 psi

TABLE 2-6

SUMMARY OF MATERIALS DATA FOR HONDO INPUT

Item	Mat'l Ident. No.	Mat'l	Temp. (°F)	Mass Density ($\frac{lb\ sec^2}{in.^4}$)	E (10^6 psi)	ν	t_o (psi) Strain Rate Sensitive Case ($\dot{\varepsilon} = 10^{-6}$)	t_o (psi) Strain Rate Insensitive Case ($\dot{\varepsilon} = 10^{-3}$)	E_t (10^6 psi)	p	D x 10^5	Notes
Cask shells container shell	1	304 SS cast	250	0.0007511	27.4	0.3	29,500	29,500	0.4093	←Note 3→		9
Uranium shield, lid	2	0.2% Mo-U alloy cast	300	0.0017602	21.1	0.21	8,180	28,000	1.35	3.113	6.362	4 5 6
Uranium shield, cylinder	3	0.2% Mo-U alloy cast	250	0.0017640	22.73	0.21	18,756	64,200	3.15	3.113	6.362	4 7
Primary closure, top membrane	4	304 SS (low E)	300	0.0007511	Aribtrary	0.3	28,400	28,400	0.4093	←Note 3→		5 9
Prim. closure plate, top end of cask shells	5	304 SS	300	0.0007511	27.1	0.3	28,400	28,400	0.4093	←Note 3→		5 9
Top head of cask	6	4340 low alloy steel $F_{tW_{ksi}} = 175$	300	0.0007382	29.0	0.3	Note 8	145,000	2.22	←Note 8→		5 6 9

NOTES:
1. Symbols per Ref. 2-24.
2. β = 1.0 for all materials.
3. 304 SS = $t_v = t_o + [3571][\log_{10}]\ (10^3\ \dot{\varepsilon})]$ for $\dot{\varepsilon} \geq 10^{-5}$ in strain rate sensitive case.
4. Strain rate sensitivity governed by power law (Ref. 2-24 for materials No. 2 and 3.
5. Top end of cask is insulated by plywood. Design temp. = 300°F.
6. Stress-strain constraints bsaed on tensile data.
7. Stress-strain constants based on compression data.
8. Strain rate sensitivity is negligible for material No. 6 @ 300°F (Ref. 2-22).
9. Stress-strain functions for this material are similar for tension and compression within range considered (permanent set ≤ 0.5%).

2.7.5 Cask Model for HONDO Analysis. Figure 2-7 on the following pages describes the computer model with node and element numbers which were produced by a mesh generation program.

TABLE 2-7

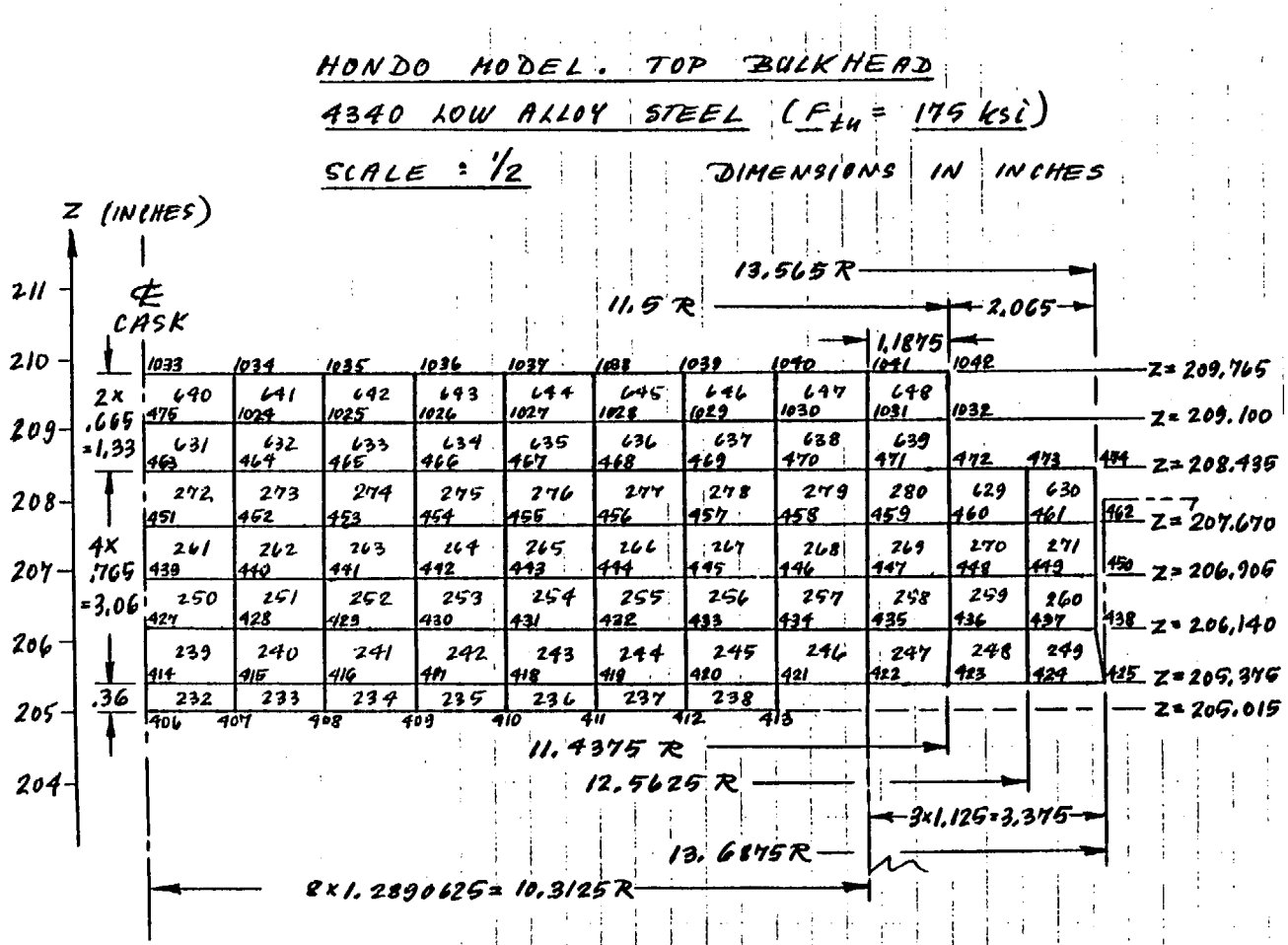

TABLE 2-8
BOTTOM 30-FT DROP HONDO MODEL
ELEMENT MATERIALS SUMMARY

Element From	Element To	Item	Material	Type (Identification)
1	206	Cask shells	304 SS @250°F	1
207	231	Top end of cask shells	304 SS @300°F	5
232	280	Bulkhead top end	4340 low alloy steel	6
281	302	Primary closure plate	304SS @300°F	5
303	358	Uranium shield, lid	0.2% Mo-U alloy	2
359	370	Primary closure, top membrane	304 SS (Low E)	4
371	464	Container shell	304 SS @250°F	1
465	474	Container shell, top end	304 SS @300°F	5
475	628	Uranium shield, cylinder	0.2% Mo-U alloy	3
629	648	Bulkhead top end	4340 low alloy steel	6

Figure 2-7.

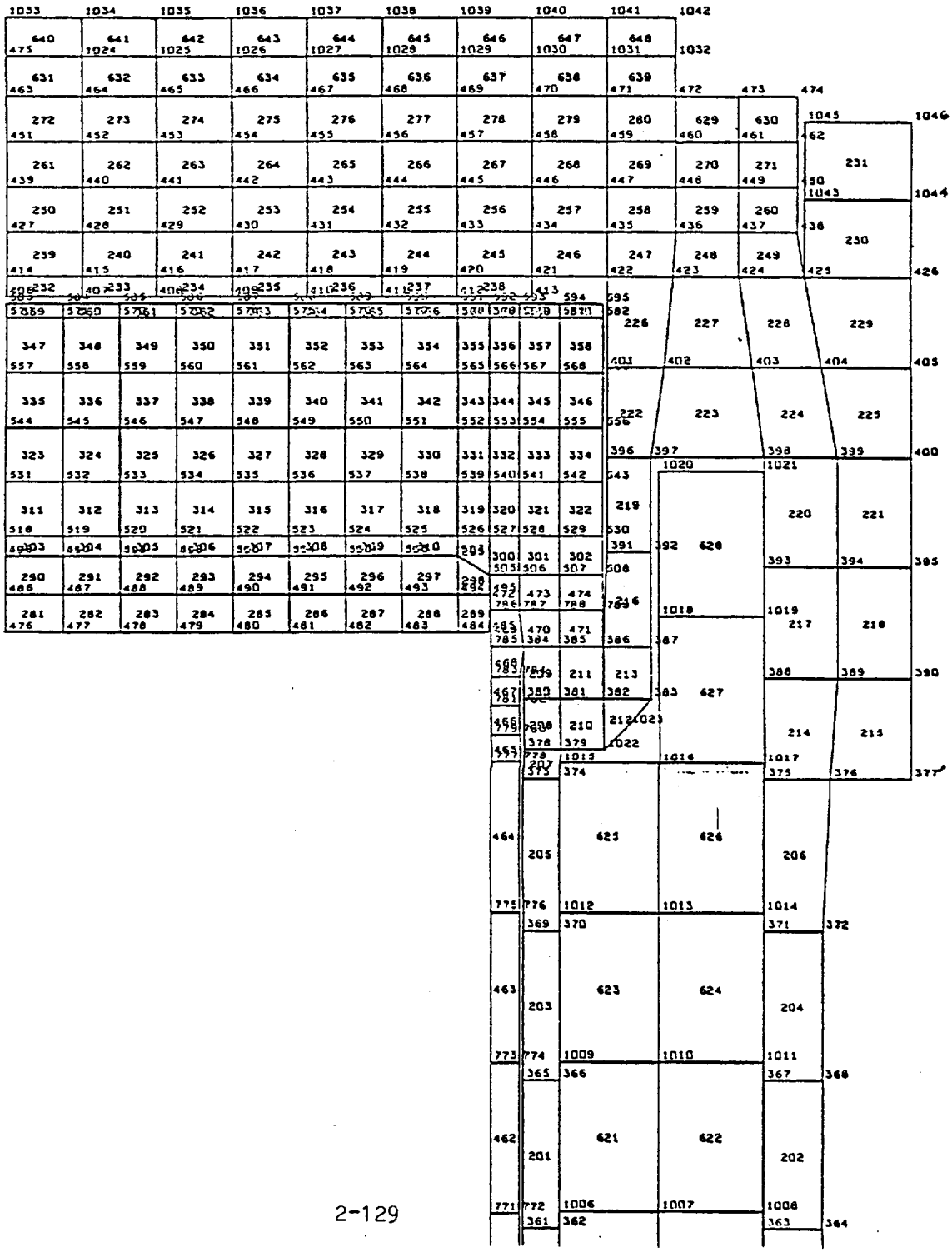

Figure 2-7 cont.

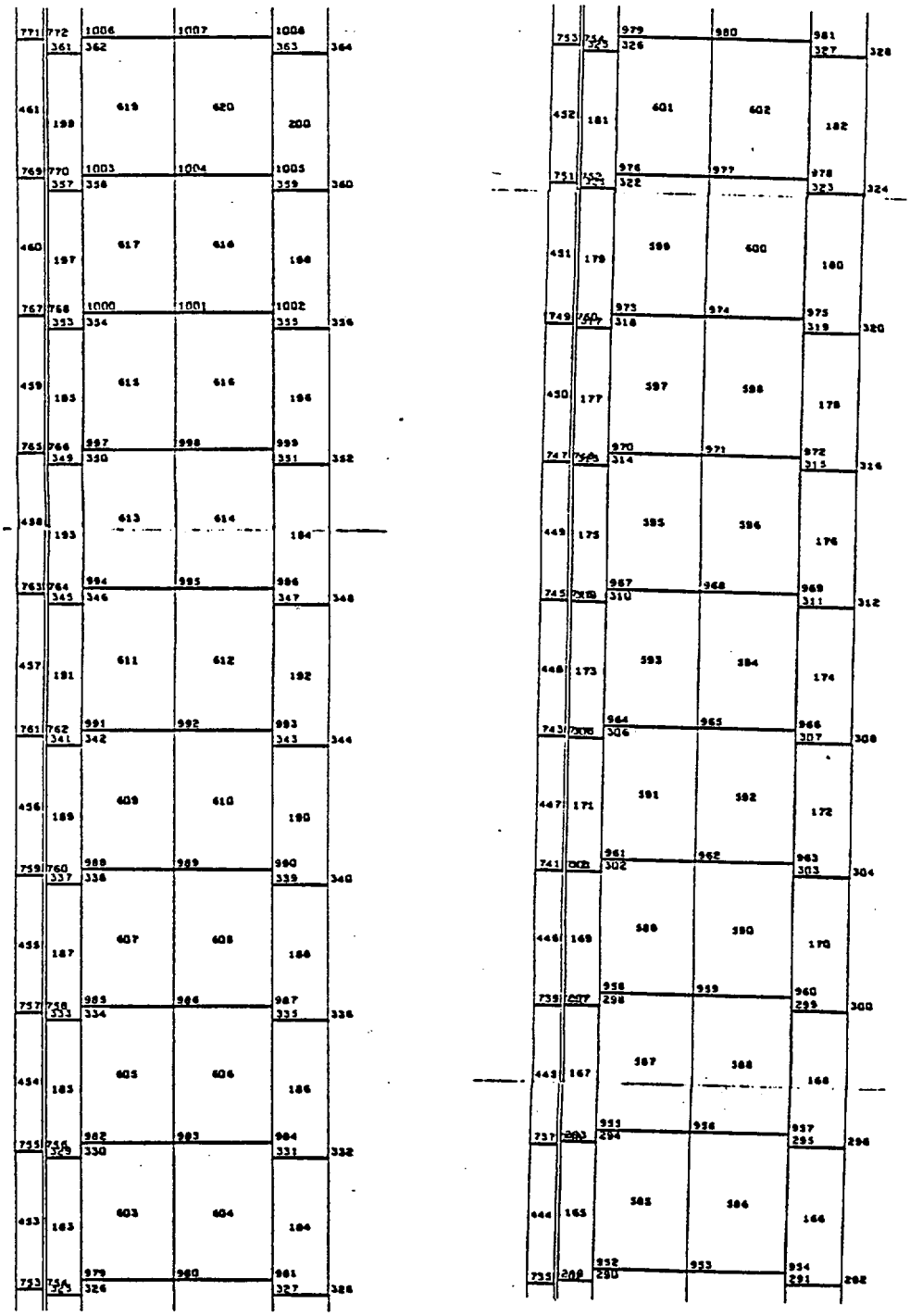

Figure 2-7 cont.

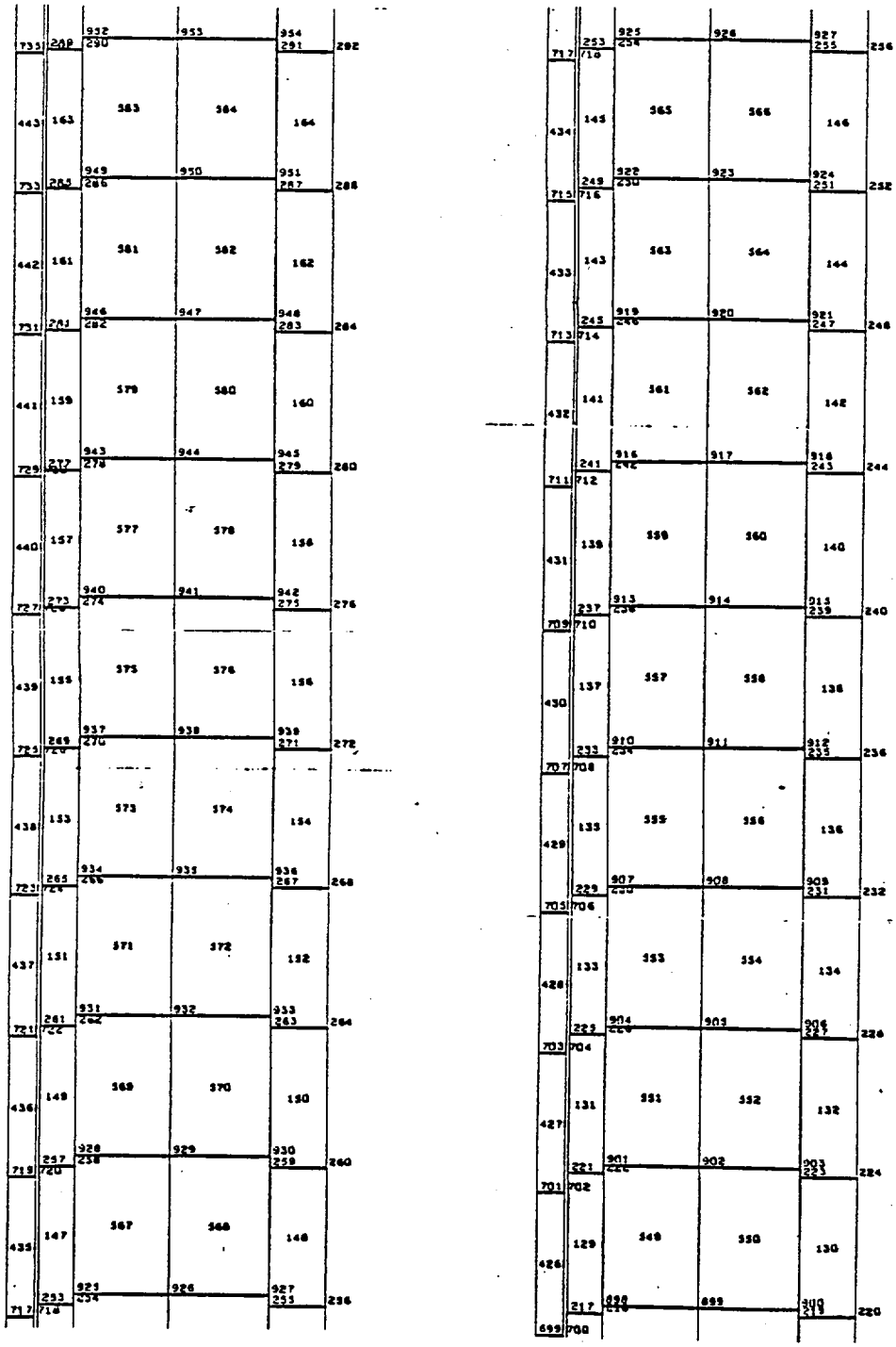

Figure 2-7 cont.

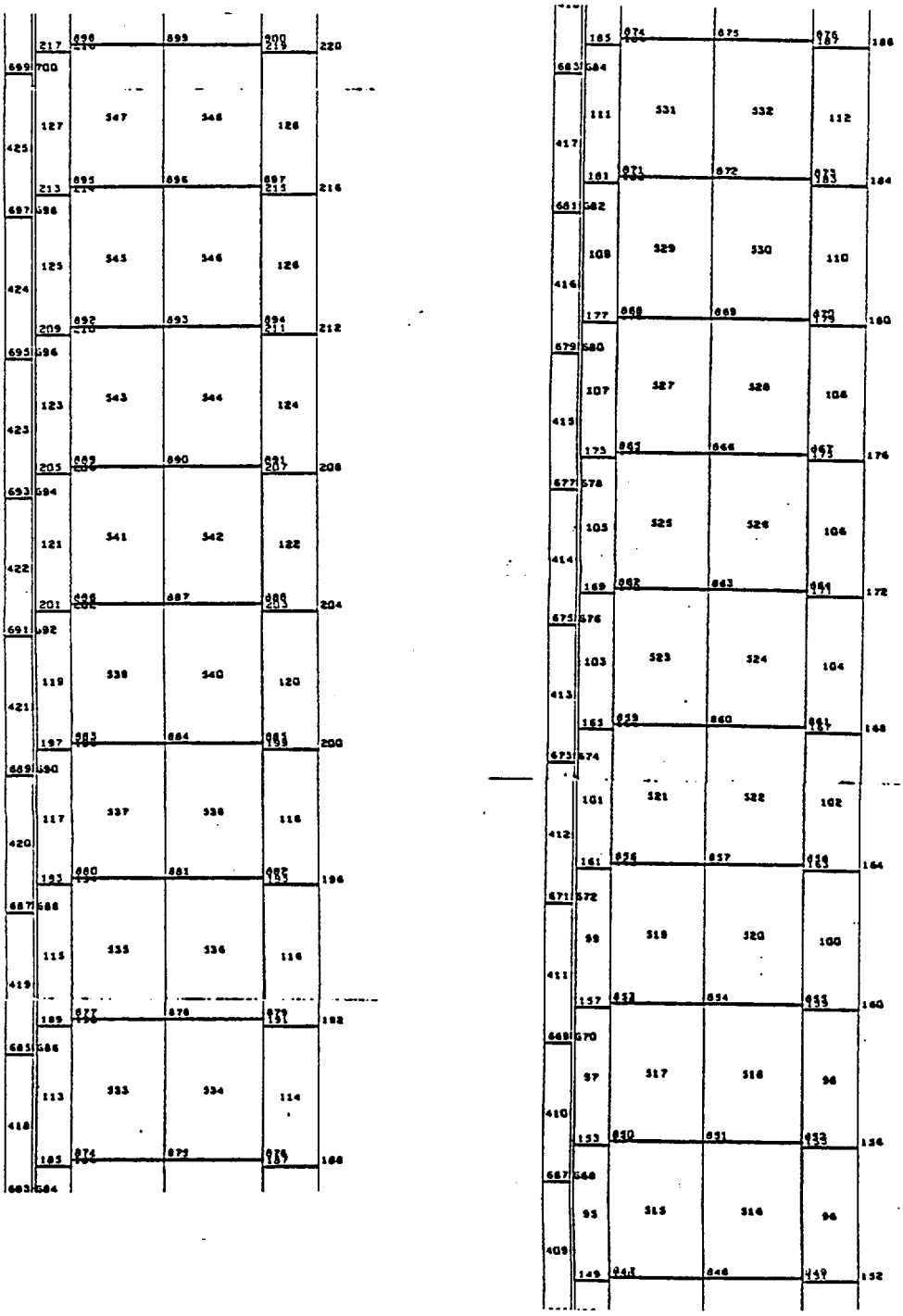

Figure 2-7 cont.

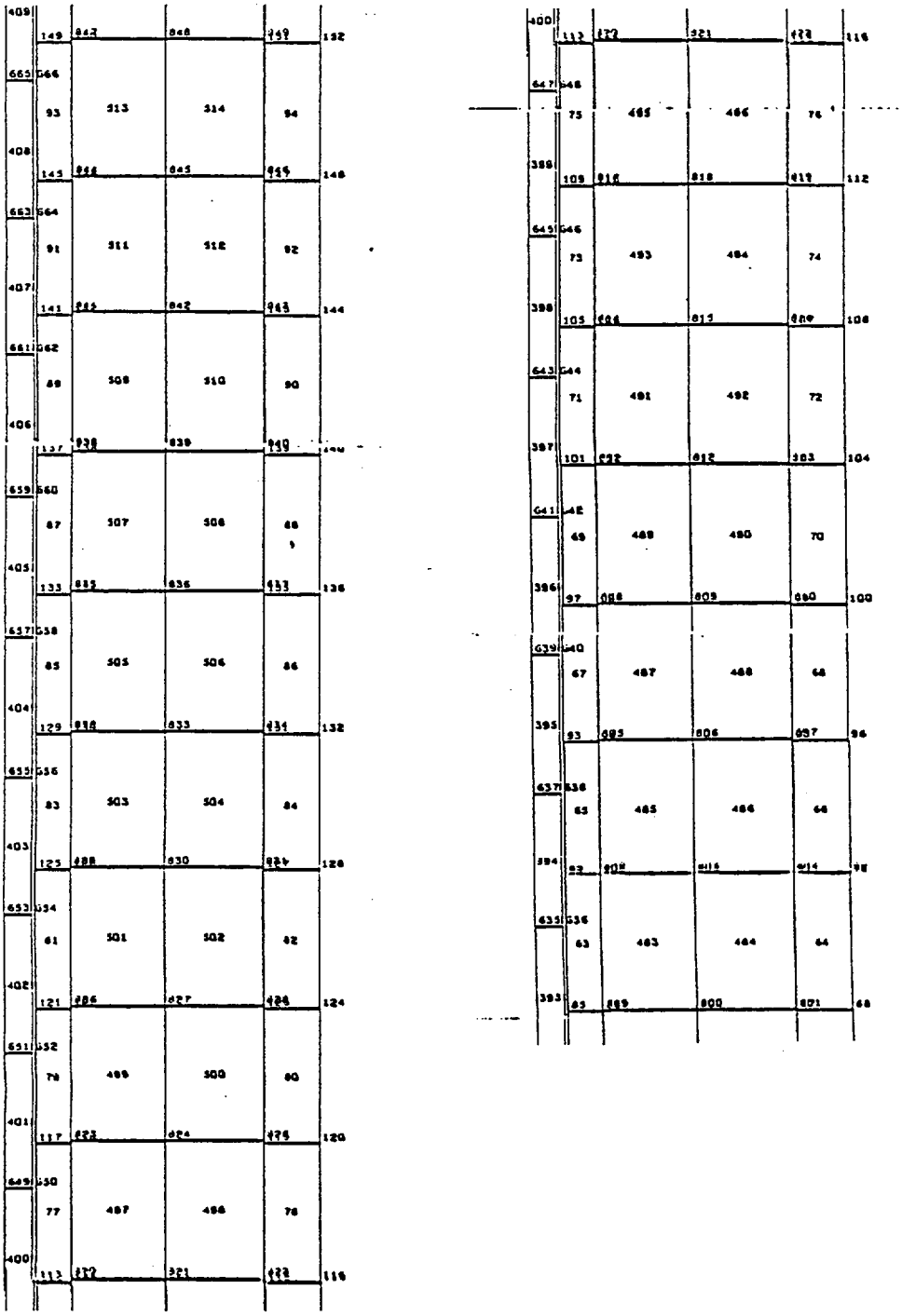

Figure 2-7 cont.

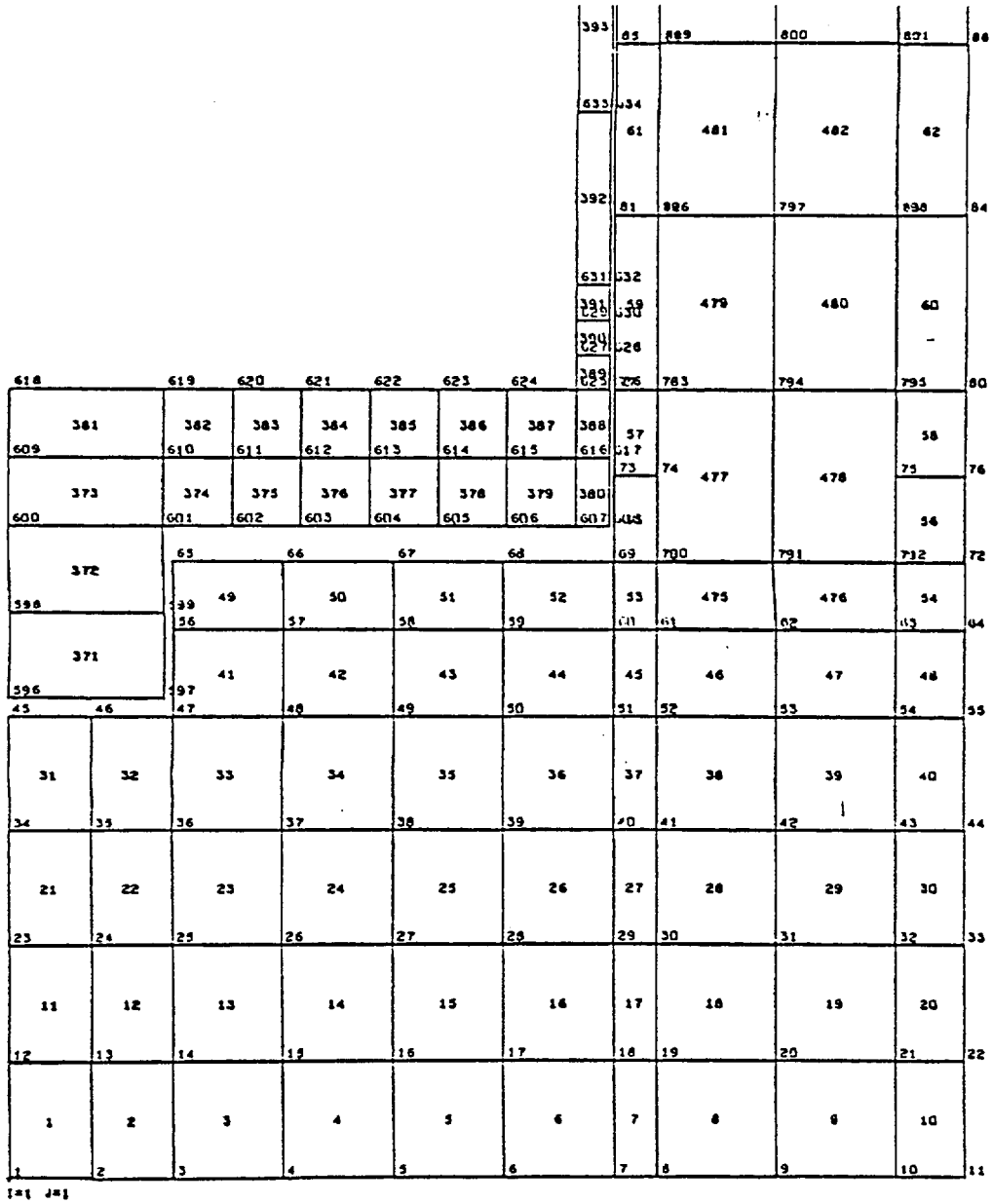

2.7.6 Conclusions of HONDO Analysis

2.7.6.1. Summary of HONDO Analysis

The two HONDO runs made (for strain rate sensitive and strain rate insensitive material behavior) were based on an assumed perfectly vertical bottom impact after a 30-ft drop.

Any impact at an angle with the vertical sufficiently small to prevent the cask from falling on its side after the initial contact (that is with the projected C.G. being within the bottom support circle) will be very similar to the perfectly vertical case. In fact, an impact at a slight angle will probably result in more energy absorption through plastic flow [in compression with no tendency to cracking] of the impacted corner and consequently a lower G-loading of the container lid structure. The perfectly vertical case analyzed should therefore conservatively cover all impacts with the projected C.G. within the bottom support circle.

A drop at a larger angle with the vertical will be less severe on the initial impact because part of the fall energy is being converted into rotation of the cask. The eventual side impact of the cask would be less severe than a perfect side impact after a 30-ft drop. In conclusion the perfectly vertical impact and the perfectly horizontal impact cases will conservatively cover any case in between.

The following computer generated plots are presented on the following pages:

1. Computer model with node and element numbers (result of a mesh generation program).

2. Plots from time of impact of selected stresses, displacements, and displacement gradients (L + ΔL/L) vs. time for the strain rate sensitive and strain rate insensitive case (HONDO plot).

It is evident from the plots that absolute values of all critical stresses are maximum for the strain rate sensitive case. Absolute values of all critical displacements are maximum for the strain rate insensitive case.

Vertical displacements of top bulkhead lower surface and container lid upper surface vs. time are virtually identical. Similarly, the bottom surface of the uranium shield in the container lid and the top surface of the lid itself are moving at the same rate. Thus, there appears to be no problem of interference among these parts by closing of the initial gaps between them.

The maximum absolute principal stresses in the top end of the cask have been extracted from the HONDO output and listed below. As expected some yielding will take place in the cylindrical stainless steel portion of the cask and container shells. However, stresses in the container lid and bulkhead are below the yield strengths of the materials at 300°F. Distortion of the structure supporting the seals should therefore be negligible, assuring that no leakage past the seals develops as a result of the drop.

TABLE 2-9
MAXIMUM ABSOLUTE STRESS SUMMARY PER C.P.O.
(STRAIN RATE SENSITIVE CASE) (RUN NO. BOT-12)

Component	Element No.	Time (10^{-4} sec)	Predominant Stress Type(s)	Max. or Min. Principal Stress (psi)	Yield Strength at Temp. (psi)
4340 Stl Bulkhead	232(Bot. CL)	12.0	Radial & Hoop	38,970	150,000 (300°F)
0.2% Mo-U Alloy Shield, Lid	347 (Top CL)	13.5	Radial & Hoop	-29,030	36,300
	303 (Bot. CL)	13.5	Radial & Hoop	28,850	(300°F)
Top End of Container	205 (Inner Cyl.)	12.0	Axial Compr.	-53,140	*30,300 (250°F)
Top End of Container	468 Cylinder Below Flange	19.0	Axial Tens.	**50,990	*29,200 (300°F)
Container Lid Housing	281 (Bot. CL)	13.0	Rad & Hoop	27,860	*29,200 (300°F)

*$\sigma_y \sim t_o + E_t\ (0.002) = 29{,}500 + (409{,}300)(0.002) = \underline{30{,}300\ \text{psi}}$ @250°F

$\sigma_y \sim t_o + E_t\ (0.002) = 28{,}400 + (409{,}300)(0.002) = \underline{29{,}200\ \text{psi}}$ @300°F

**Ultimate tensile strength = 64,300 psi at 300°F
(0.90 (UTS) = (0.90) (64,300) = 57,870 psi

Bolts

The 1/2-in. bolts for the container lid and the 1-1/4 in. bolts for the cask cover head are designed for side and drop cases, and are not critical for the bottom drop conditions, where the lids are being forced by inertia downward toward the seals.

blank page

Drop Conditions at Low Temperature (-40°F)

Protection against brittle fracture at temperatures down to -40°F is provided through the selection of proper materials for the structural parts of the alternate closure system.

The container lid housing (304 stainless steel SA-240) with its bolts (high alloy steel per ATM 5735), and the outer lid bolts (SA-453, Grade 660) are all of austenitic stainless steel material for which no impact testing is required (see Ref. 2-2).

For the outer lid HY-140(T) material typical data from Ref. 2-7 indicate an energy absorption of at least 15 ft lb at -40°F.

The 0.2% Mo-uranium alloy lid shield material has been impact tested and found to exhibit acceptable toughness at -40°F. Documentation of the charpy V-notch testing of this and other alloys of depleted uranium is provided in Ref. 2-21.

Figure 2-8

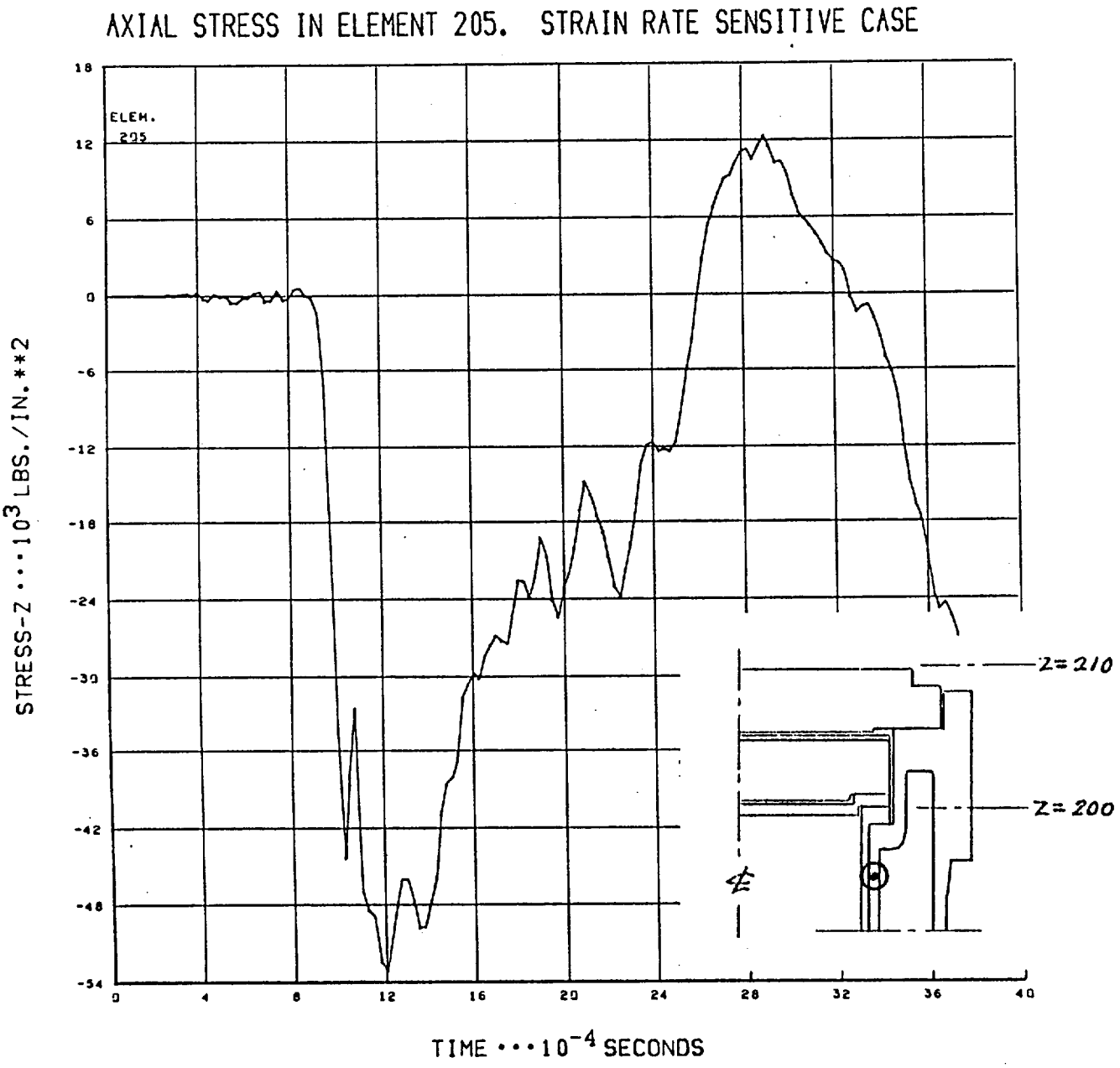
AXIAL STRESS IN ELEMENT 205. STRAIN RATE SENSITIVE CASE
ELEM. 205
STRESS-Z ···10³ LBS./IN.**2
TIME ···10⁻⁴ SECONDS
Z=210
Z=200
REF. HONDO RUN NO. BOT-12.

Figure 2-9

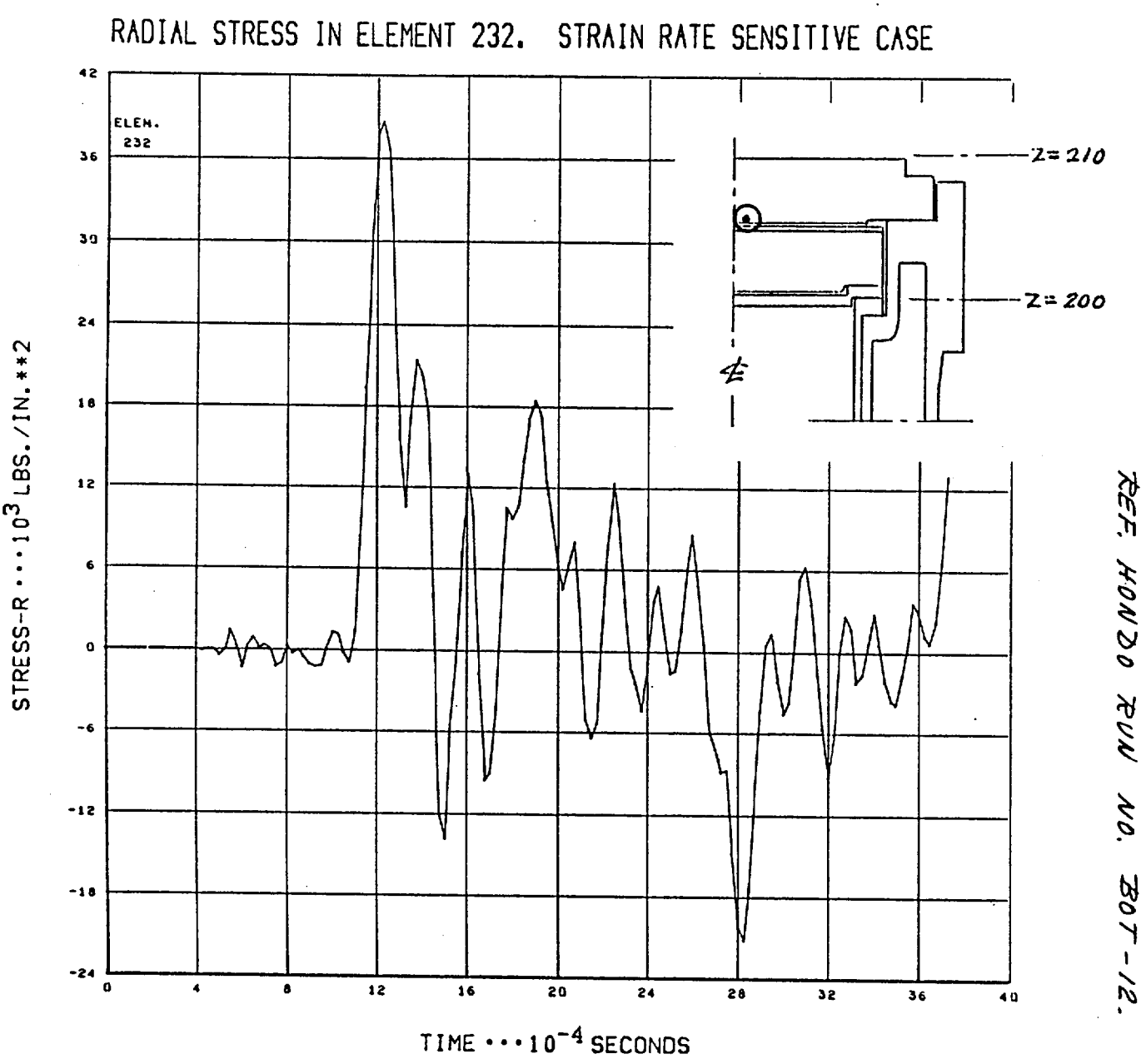
RADIAL STRESS IN ELEMENT 232. STRAIN RATE SENSITIVE CASE
ELEM. 232
Z= 210
Z= 200
STRESS-R ...10^3 LBS./IN.**2
TIME ...10^-4 SECONDS
42
36
30
24
18
12
6
0
-6
-12
-18
-24
0
4
8
12
16
20
24
28
32
36
40
REF. HONDO RUN NO. BOT-12.

Figure 2-10

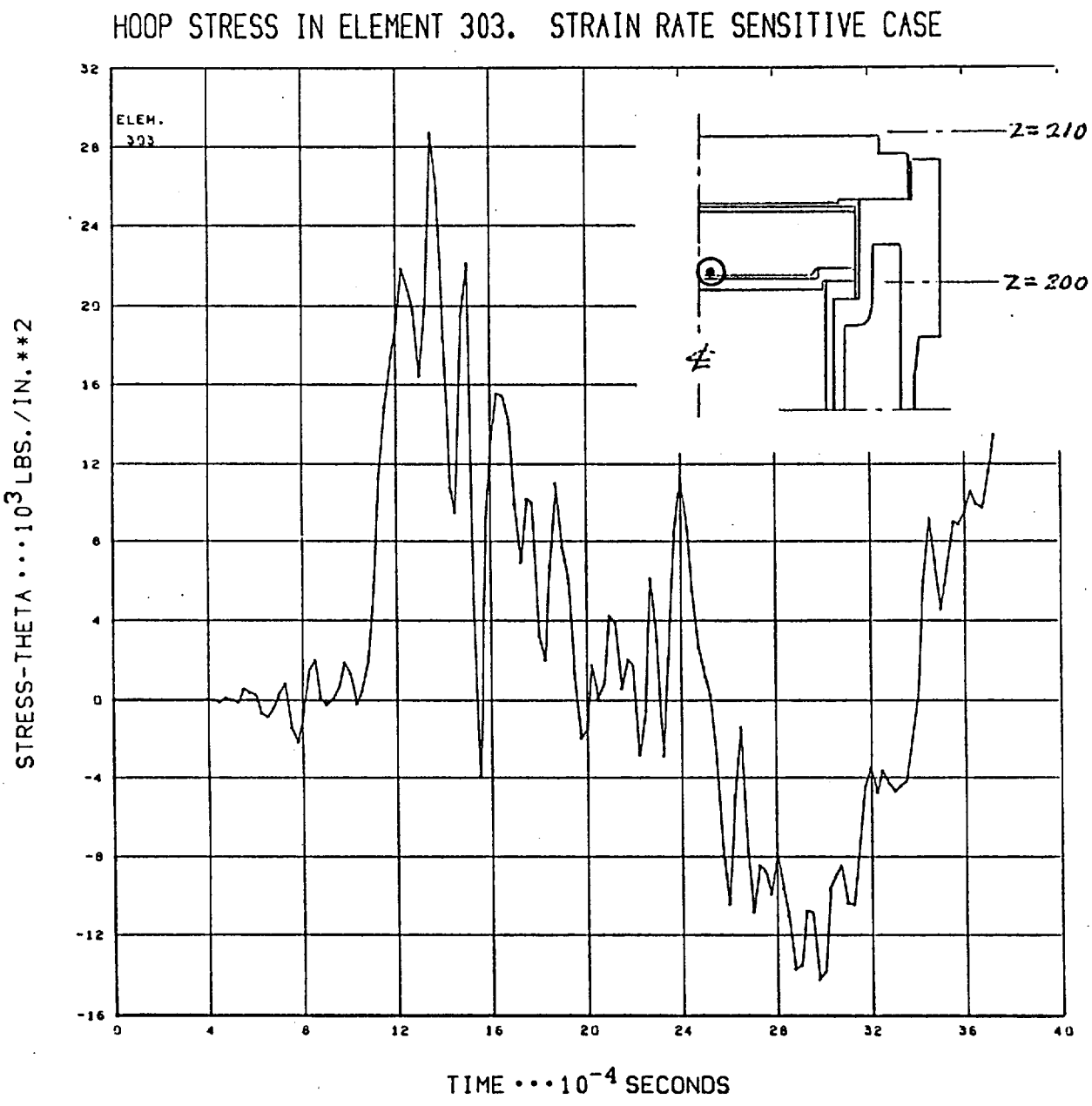

REF. HONDO RUN NO. BOT-12.

Figure 2-11

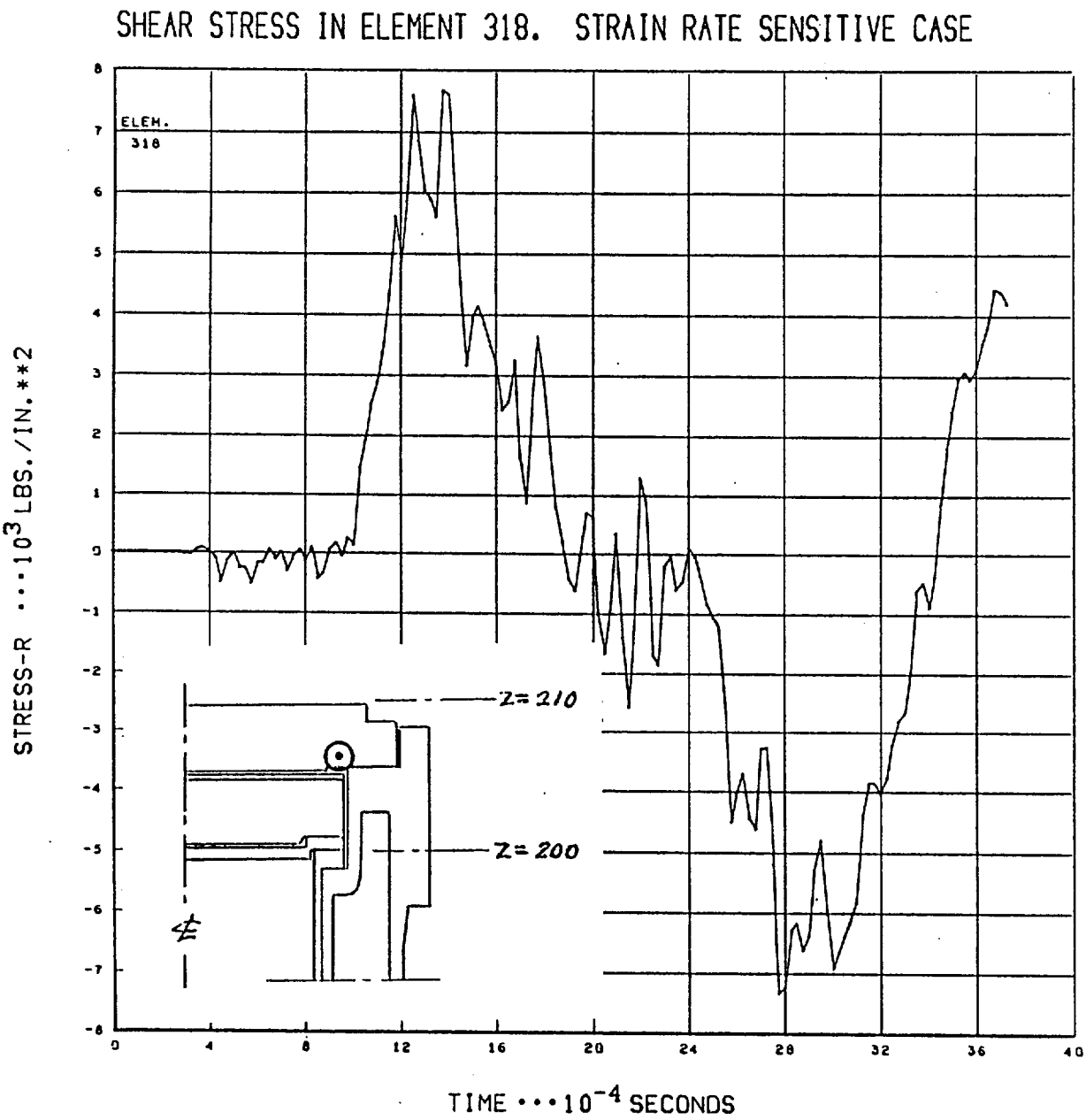

REF. HONDO RUN NO. BOT-12.

Figure 2-12

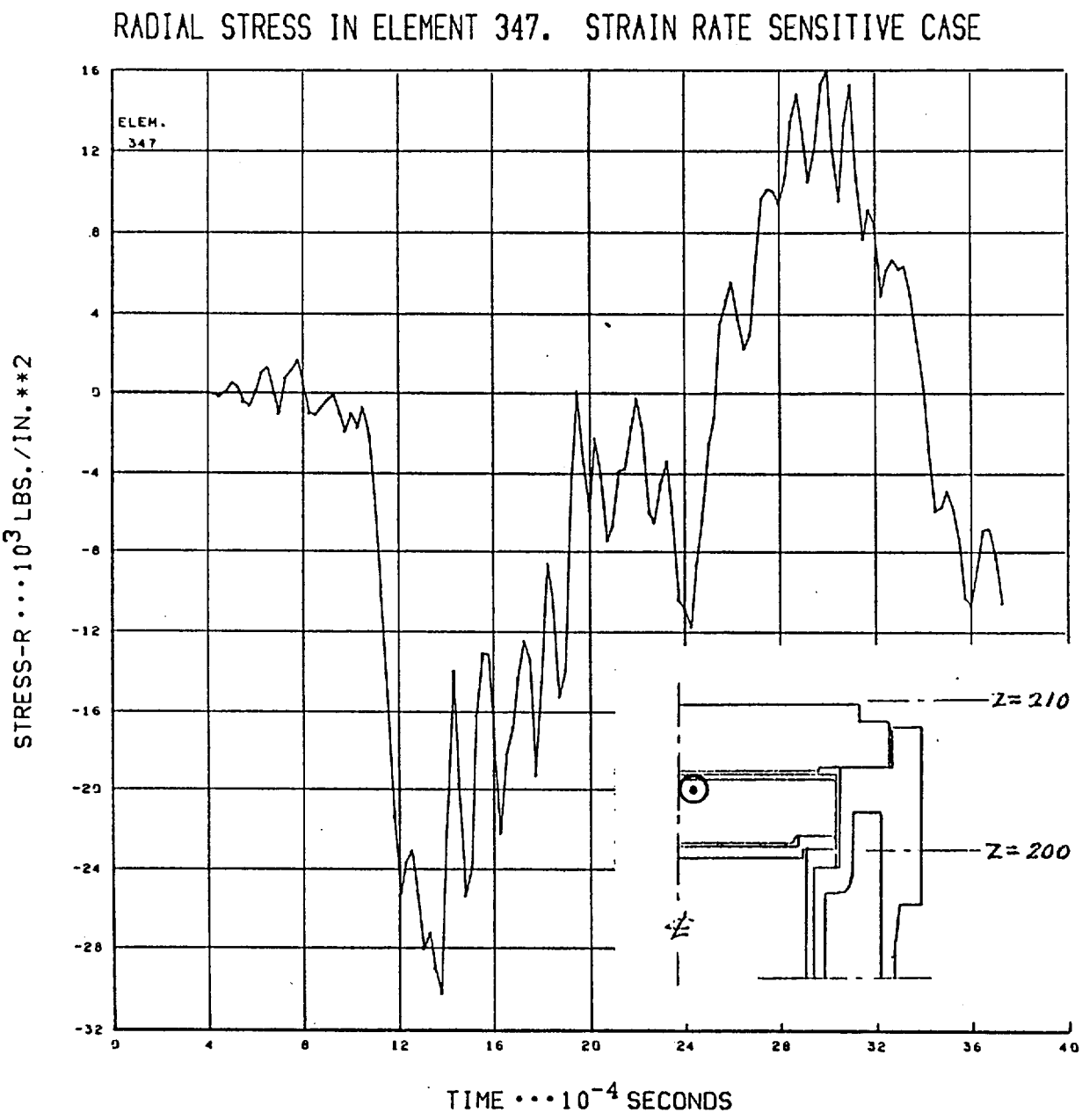

REF. HONDO RUN NO. BOT-12.

Figure 2-13

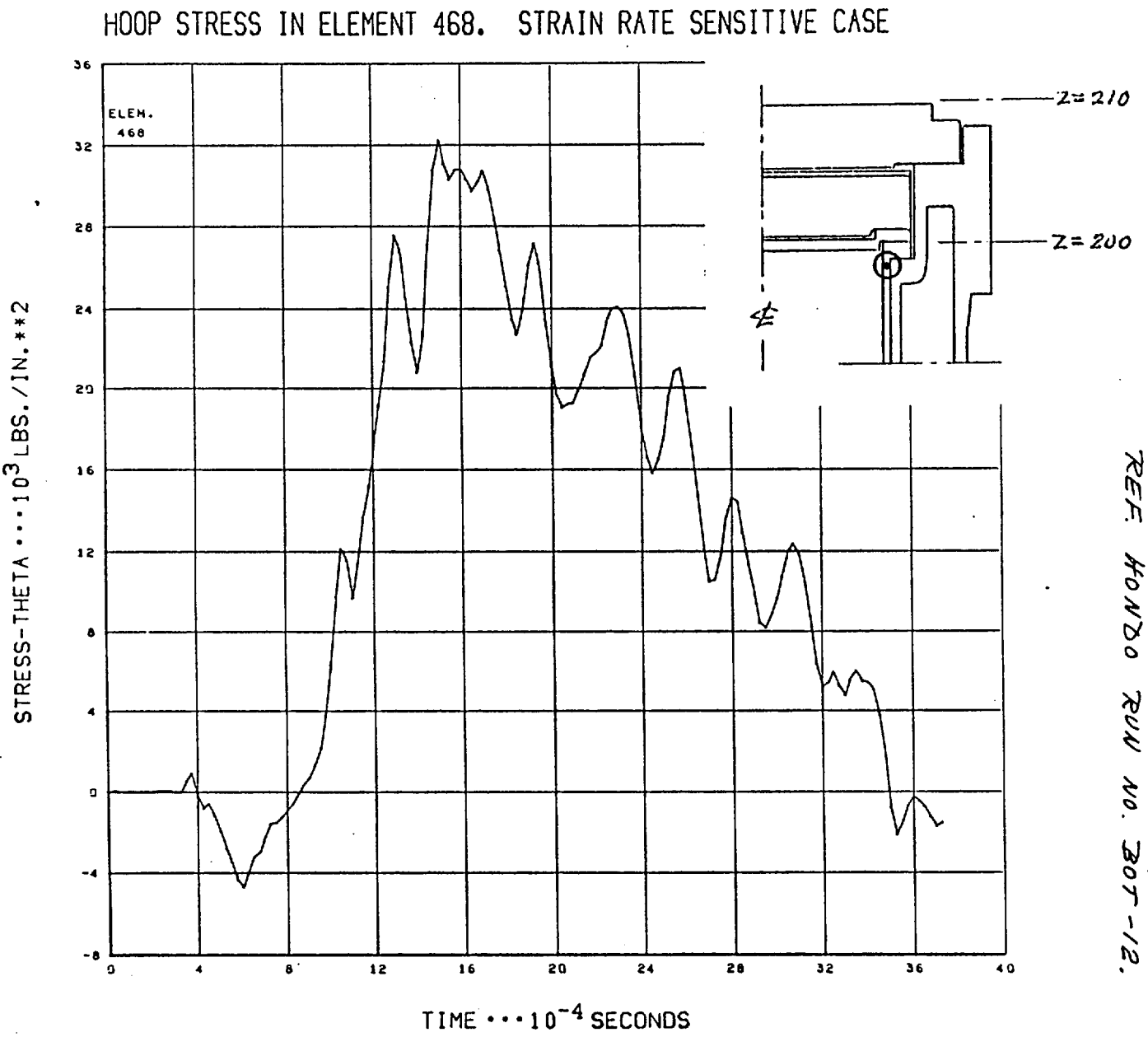
HOOP STRESS IN ELEMENT 468. STRAIN RATE SENSITIVE CASE
ELEM. 468
Z= 210
Z= 200
STRESS-THETA ···10^3 LBS./IN.**2
TIME ···10^-4 SECONDS
36
32
28
24
20
16
12
8
4
0
-4
-8
0
4
8
12
16
20
24
28
32
36
40
REF. HONDO RUN NO. BOT-12.

Figure 2-14

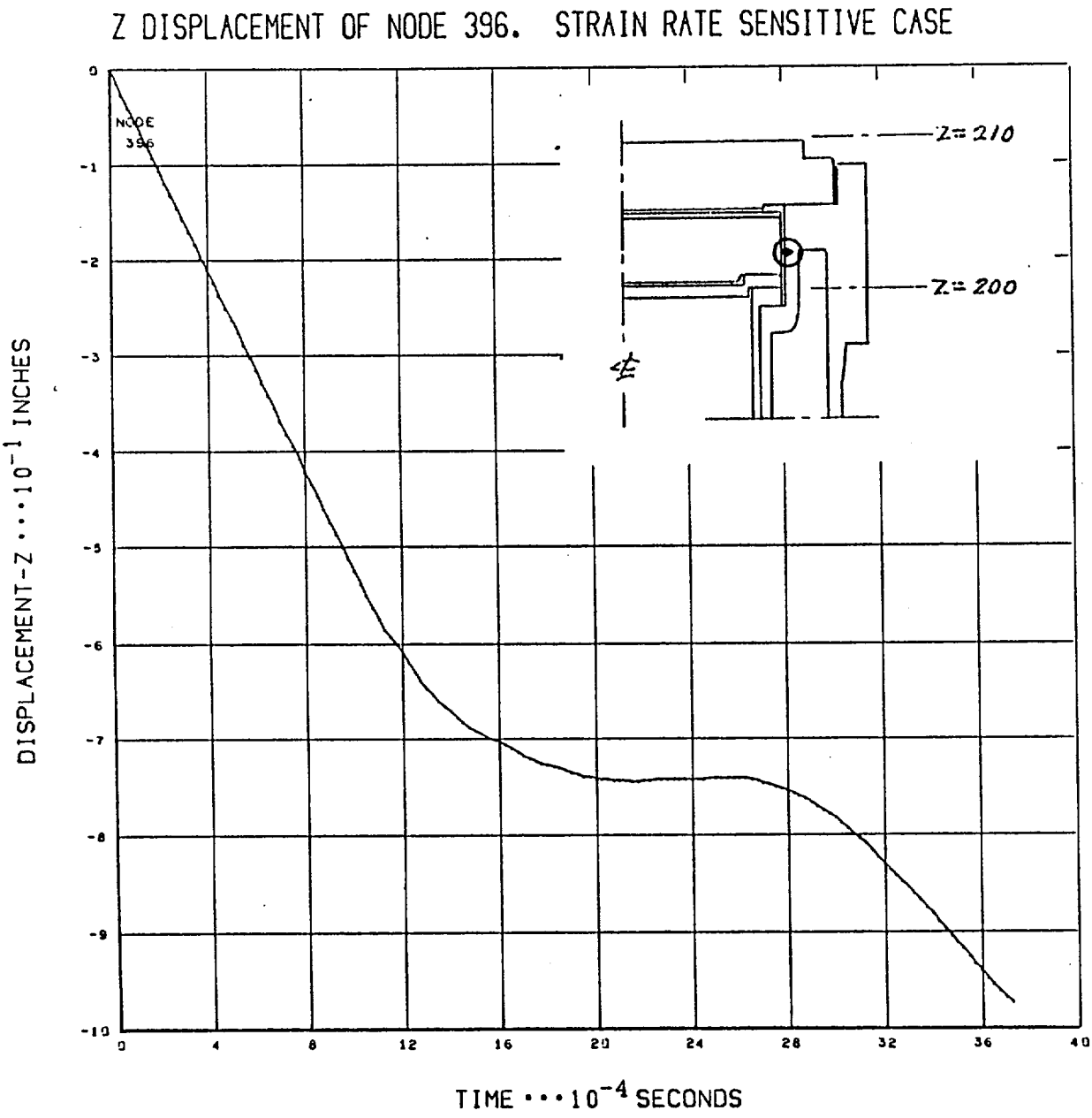

REF. HONDO RUN NO. BOT-12.

Figure 2-15

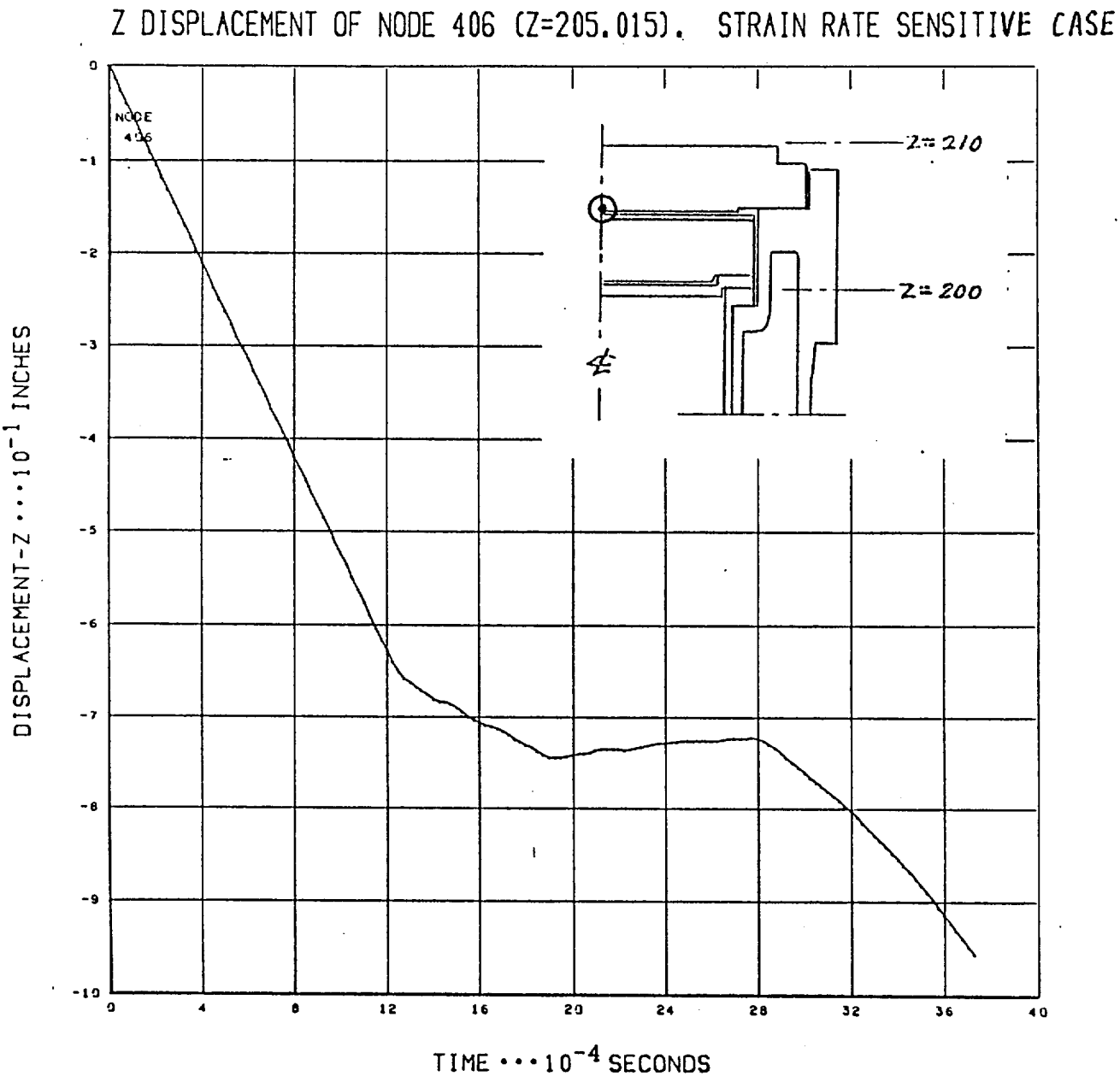

REF. HONDO RUN NO. B07-12.

Figure 2-16

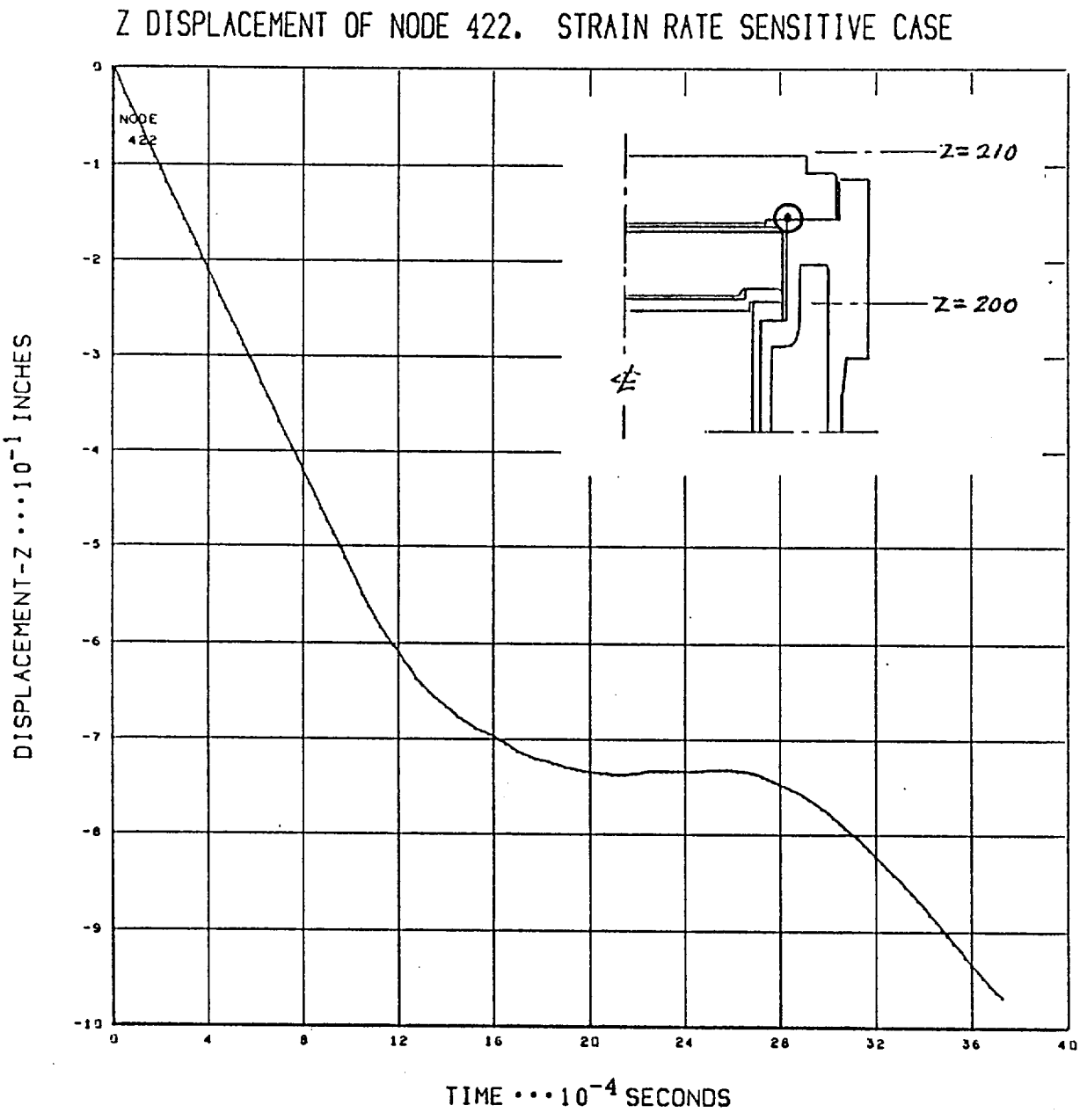

REF. HONDO RUN NO. BOT-12.

Figure 2-17

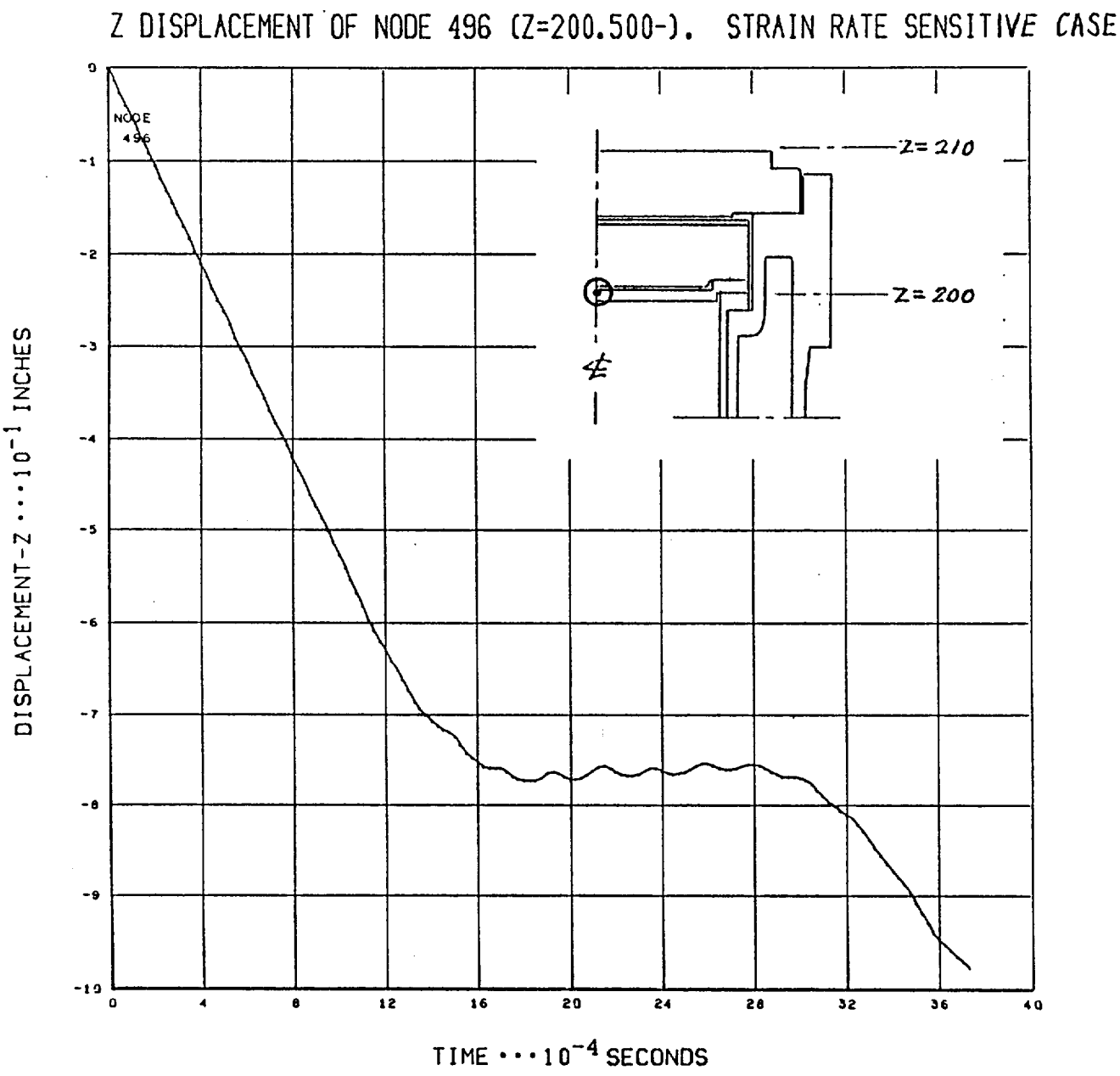

REF. HONDO RUN NO. BOT-12.

Figure 2-18

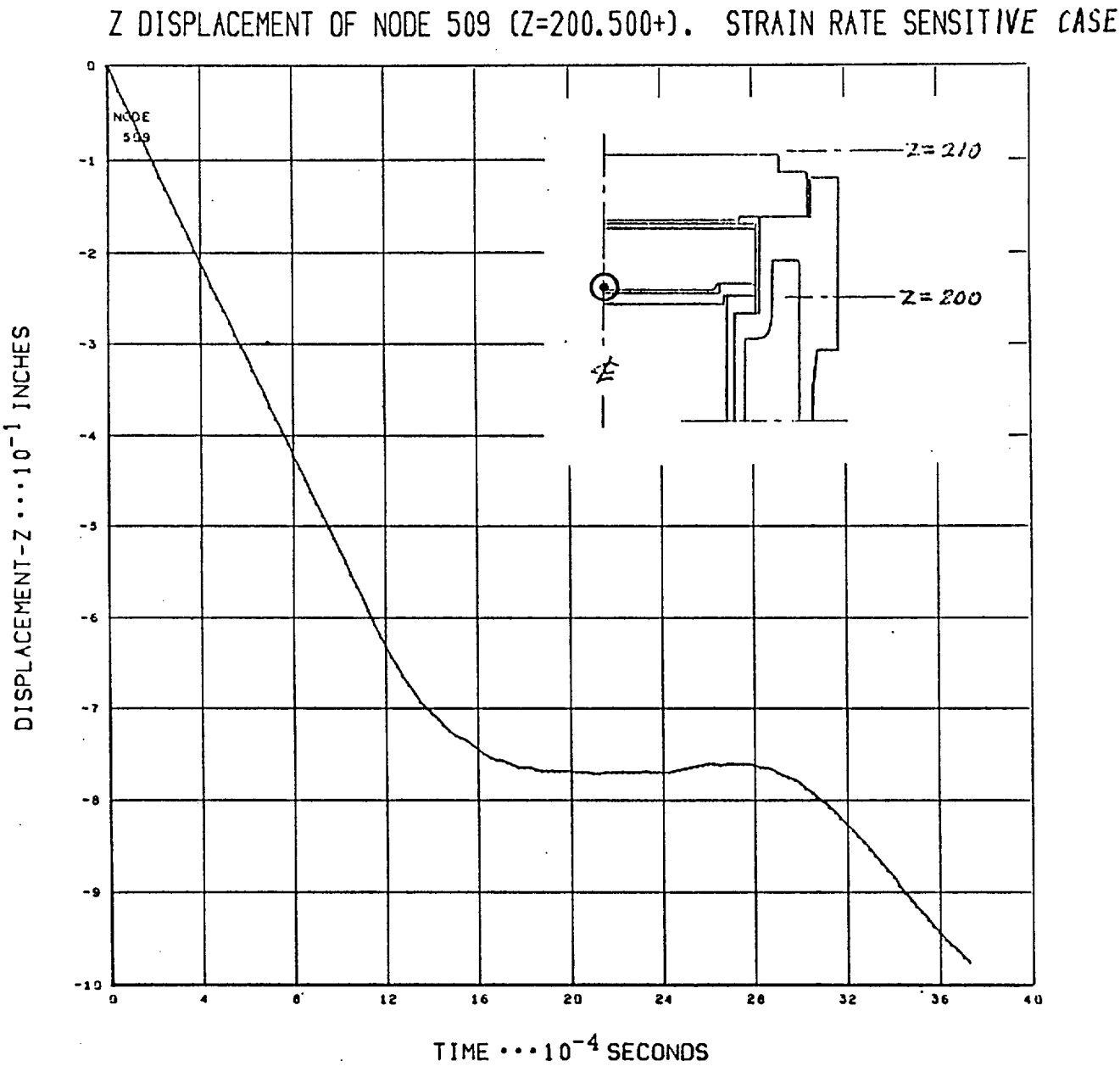

REF. HONDO RUN NO. BOT-12.

Figure 2-19

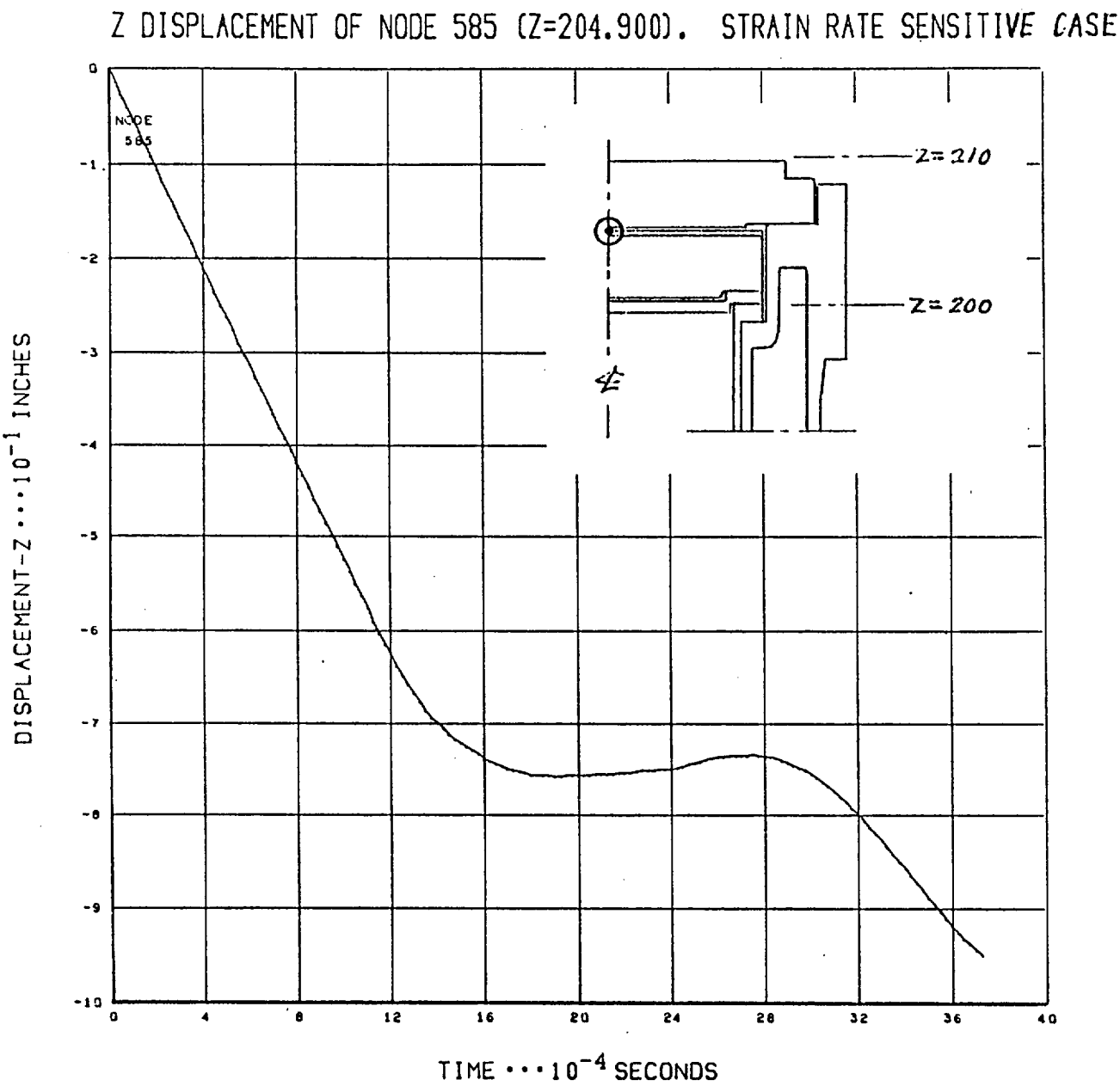

REF. HONDO RUN NO. BOT-12.

Figure 2-20

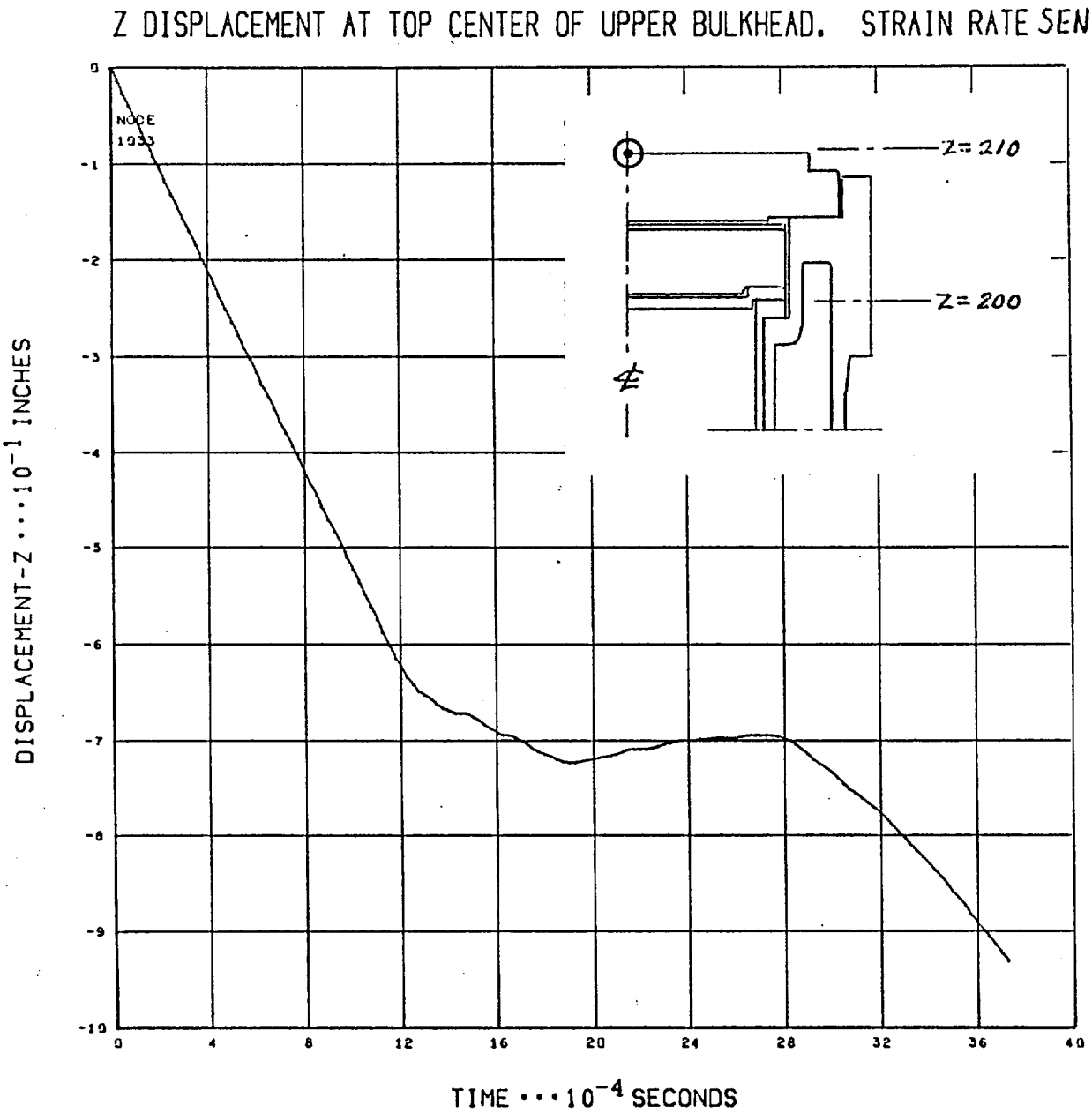

REF. HONDO RUN NO. BOT-12.

Figure 2-21

AXIAL DISPLACEMENT GRADIENT IN ELEMENT 205. STRAIN RATE SENSITIVE CASE

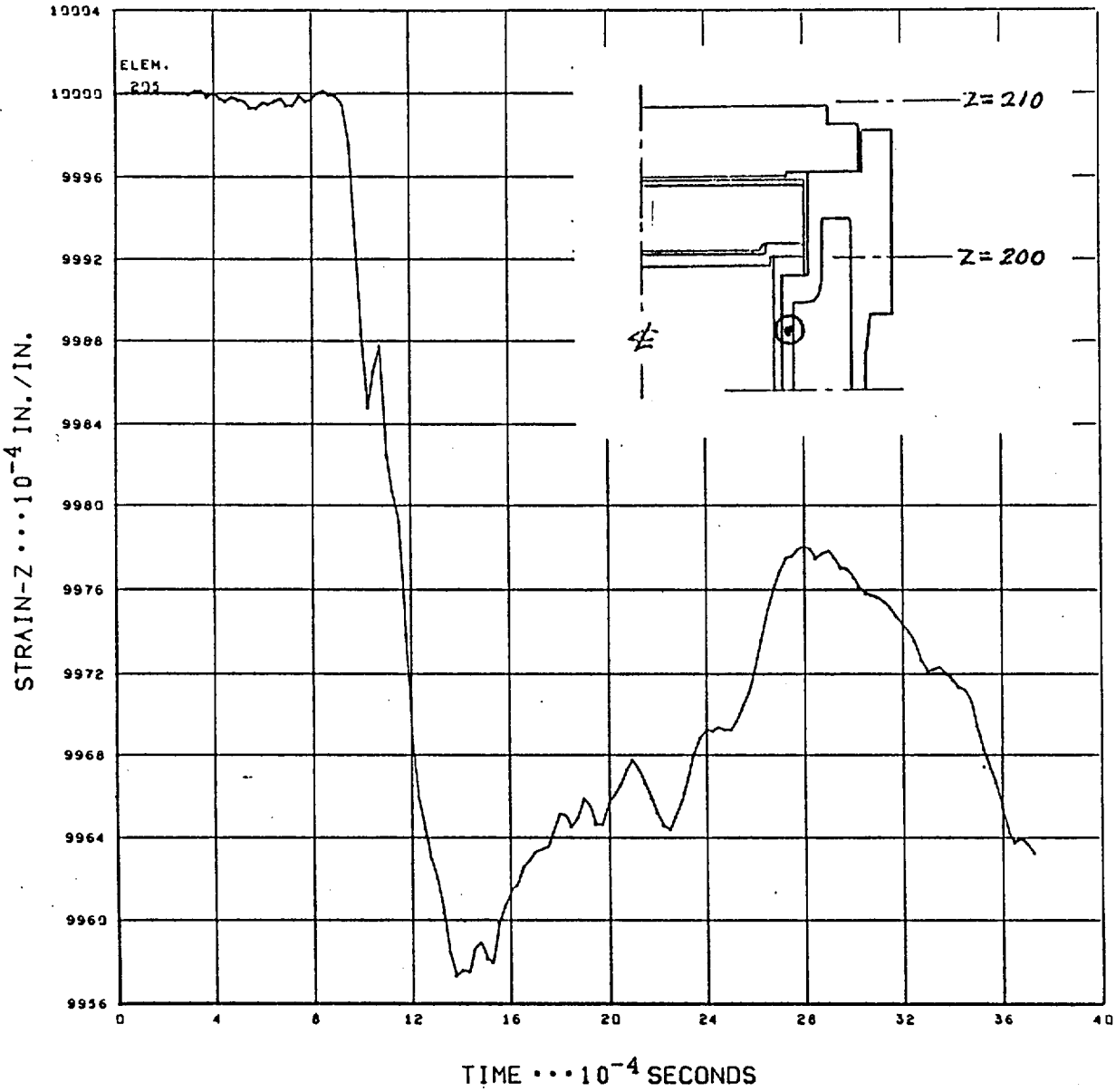

REF. HONDO RUN NO. BOT-12.

F 2-22

AXIAL STRESS IN ELEMENT 205. STRAIN RATE INSENSITIVE CASE

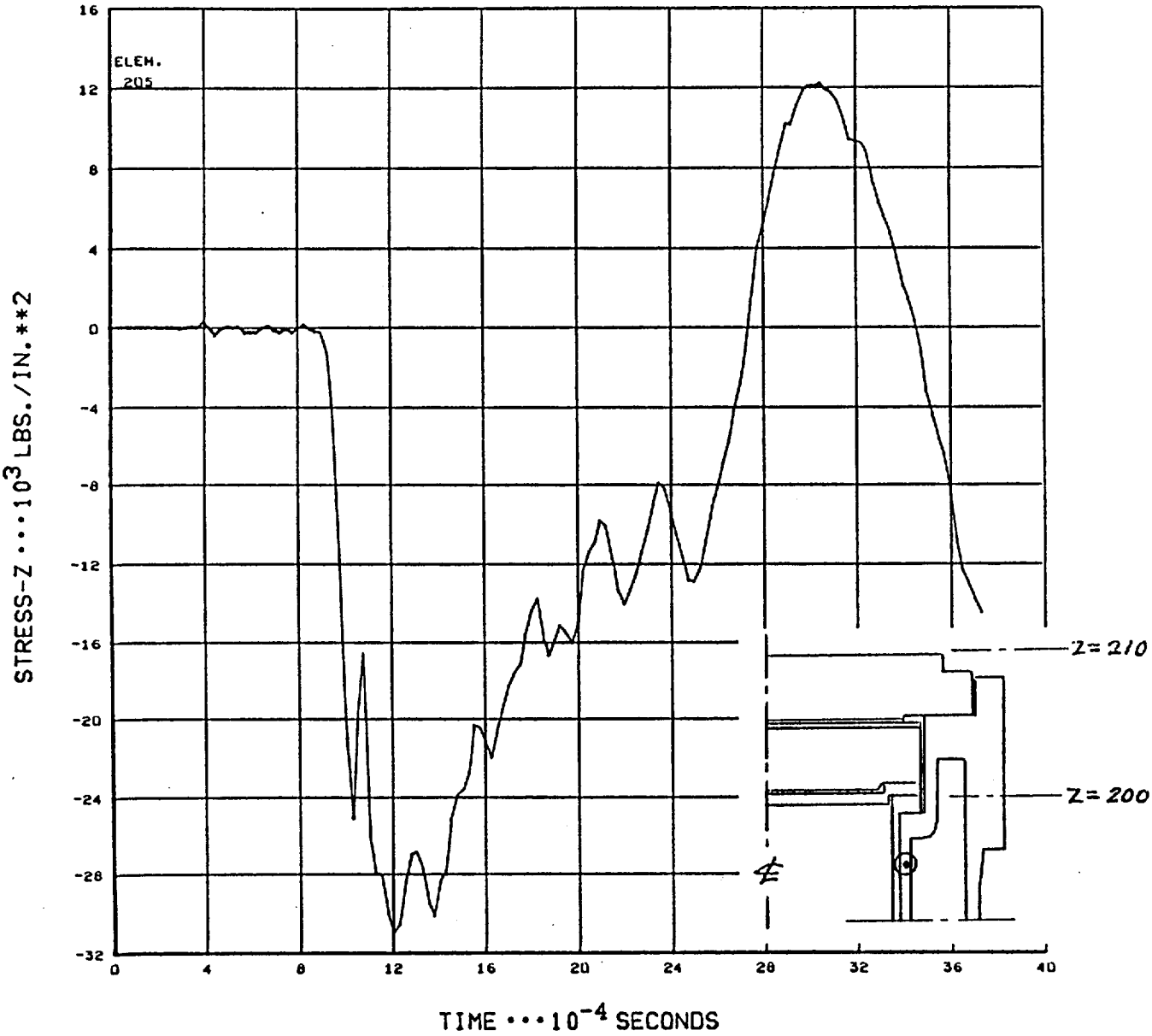

Figure 2-23

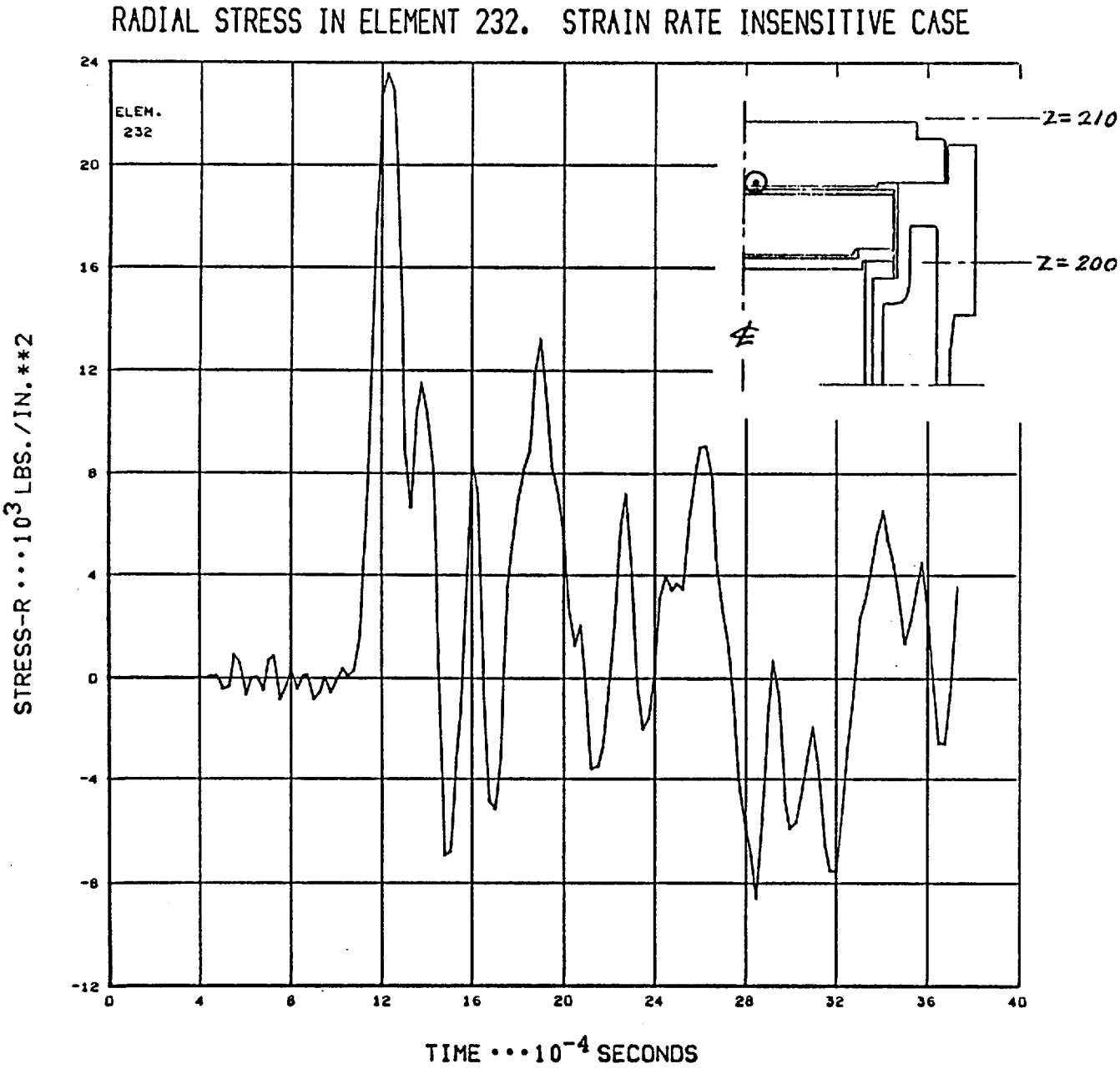
RADIAL STRESS IN ELEMENT 232. STRAIN RATE INSENSITIVE CASE
ELEM. 232
Z= 210
Z= 200
STRESS-R •••10^3 LBS./IN.**2
TIME •••10^-4 SECONDS
24
20
16
12
8
4
0
-4
-8
-12
0
4
8
12
16
20
24
28
32
36
40

Figure 2-24

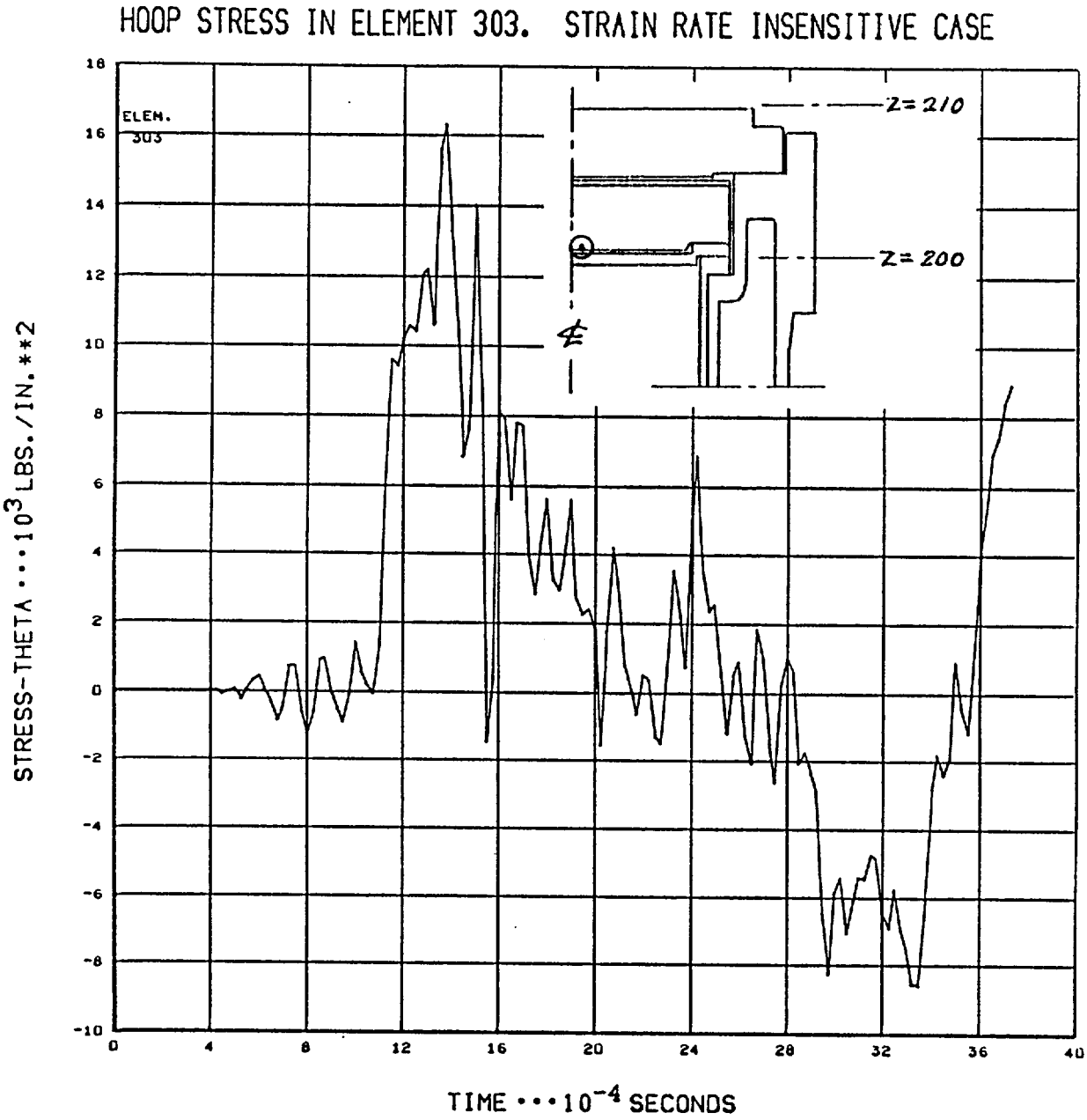
HOOP STRESS IN ELEMENT 303. STRAIN RATE INSENSITIVE CASE
ELEM. 303
Z= 210
Z= 200
STRESS-THETA •••10^3 LBS./IN.**2
TIME •••10^-4 SECONDS
18
16
14
12
10
8
6
4
2
0
-2
-4
-6
-8
-10
0
4
8
12
16
20
24
28
32
36
40

Figure 2-25

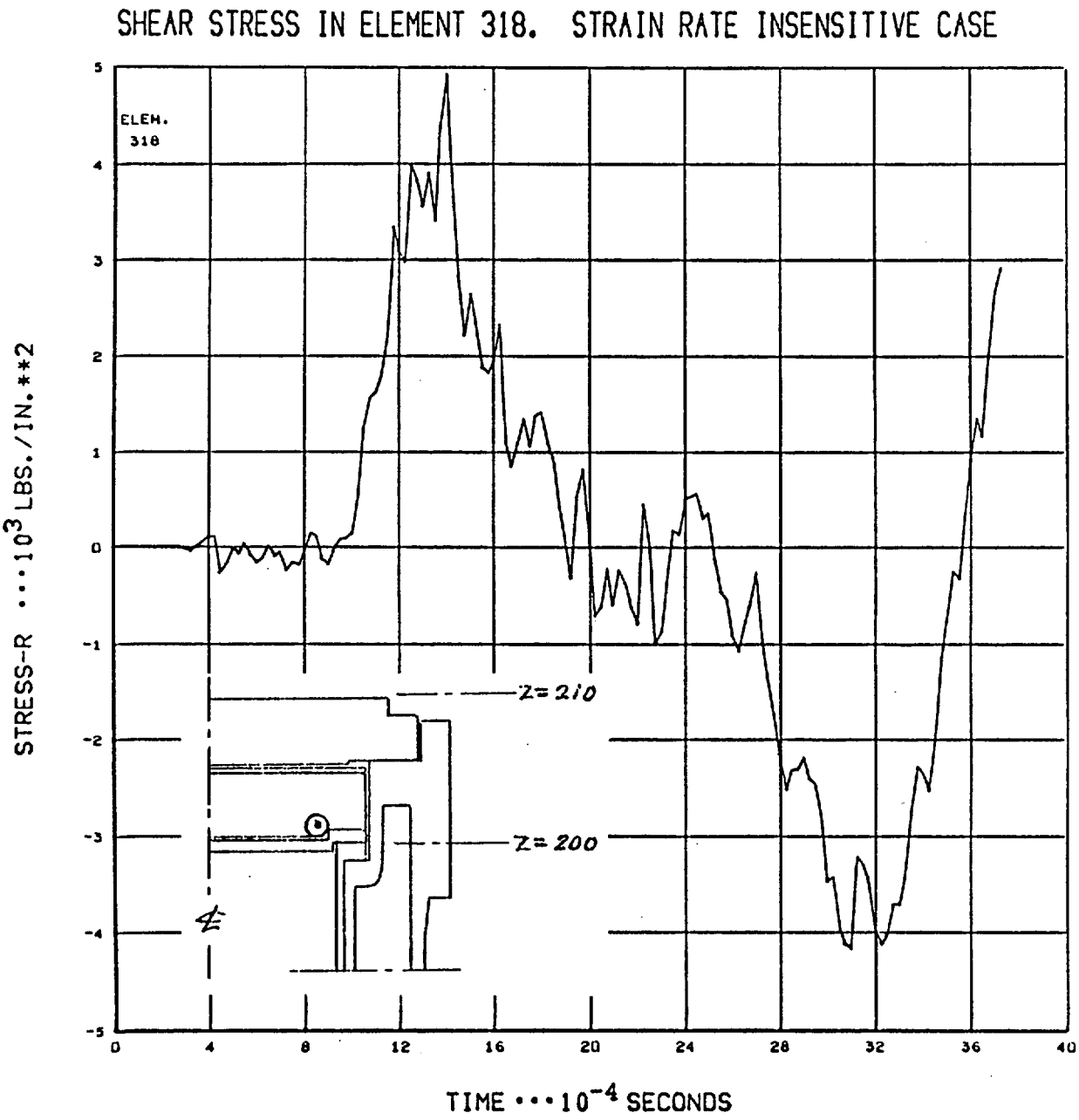
SHEAR STRESS IN ELEMENT 318. STRAIN RATE INSENSITIVE CASE
ELEM. 318
STRESS-R •••10³ LBS./IN.**2
TIME •••10⁻⁴ SECONDS
Z= 210
Z= 200
5
4
3
2
1
0
-1
-2
-3
-4
-5
0
4
8
12
16
20
24
28
32
36
40

Figure 2-26

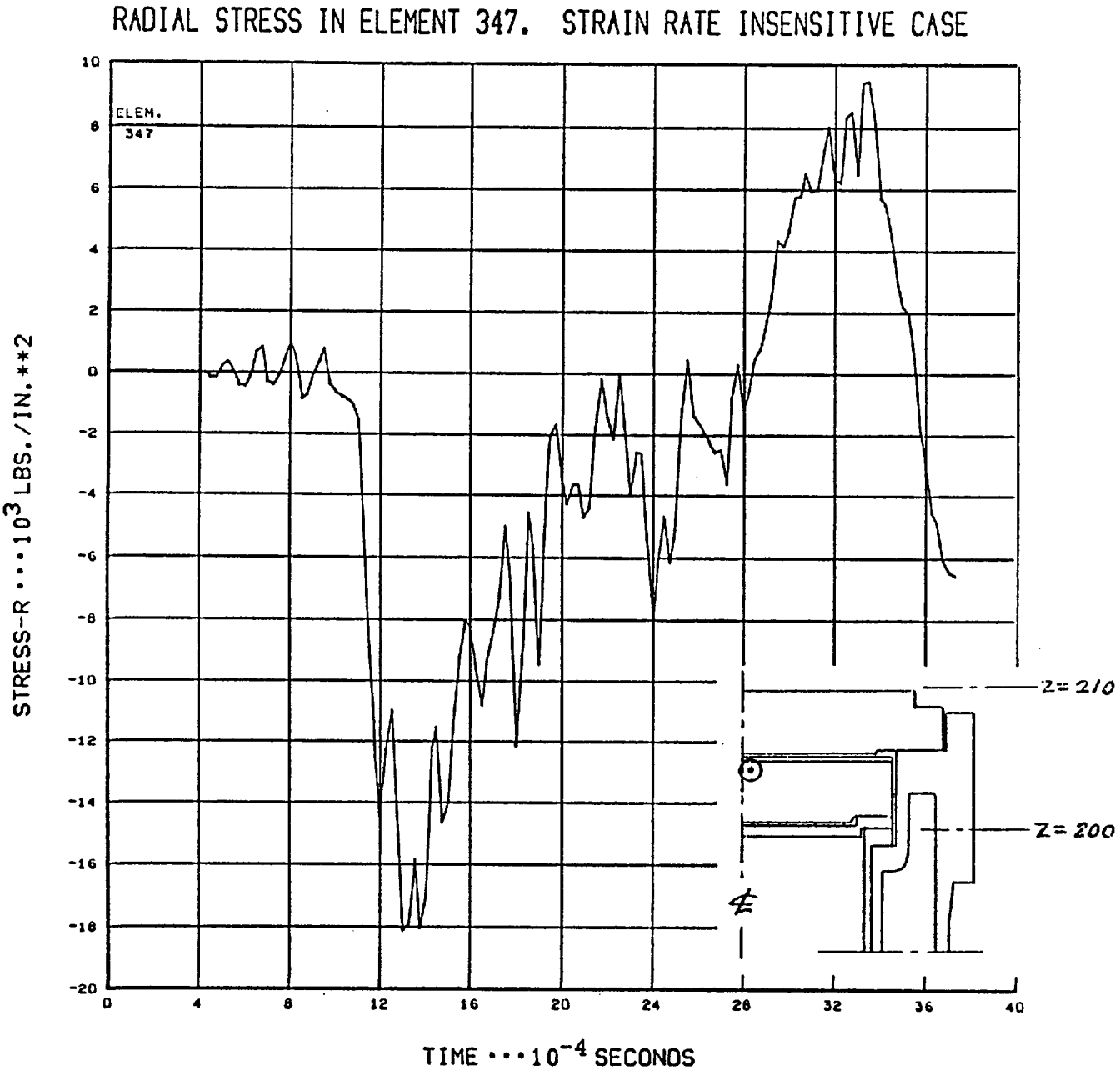
RADIAL STRESS IN ELEMENT 347. STRAIN RATE INSENSITIVE CASE
ELEM.
347
STRESS-R •••10^3 LBS./IN.**2
TIME •••10^-4 SECONDS
Z= 210
Z= 200
10
8
6
4
2
0
-2
-4
-6
-8
-10
-12
-14
-16
-18
-20
0
4
8
12
16
20
24
28
32
36
40

Figure 2-27

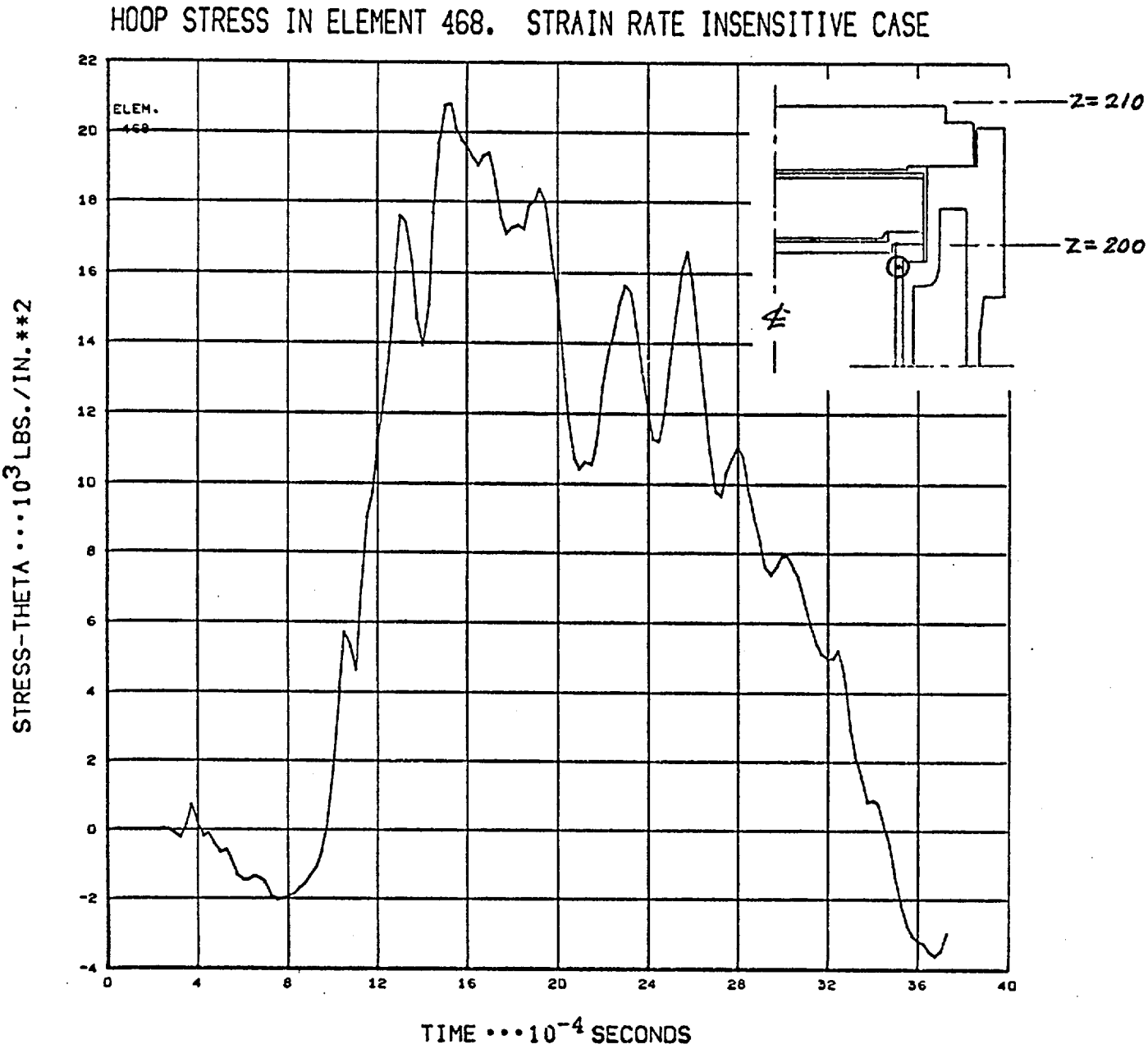
HOOP STRESS IN ELEMENT 468. STRAIN RATE INSENSITIVE CASE
ELEM. 468
STRESS-THETA •••10^3 LBS./IN.**2
TIME •••10^{-4} SECONDS
Z= 210
Z= 200
22
20
18
16
14
12
10
8
6
4
2
0
-2
-4
0
4
8
12
16
20
24
28
32
36
40

Figure 2-28

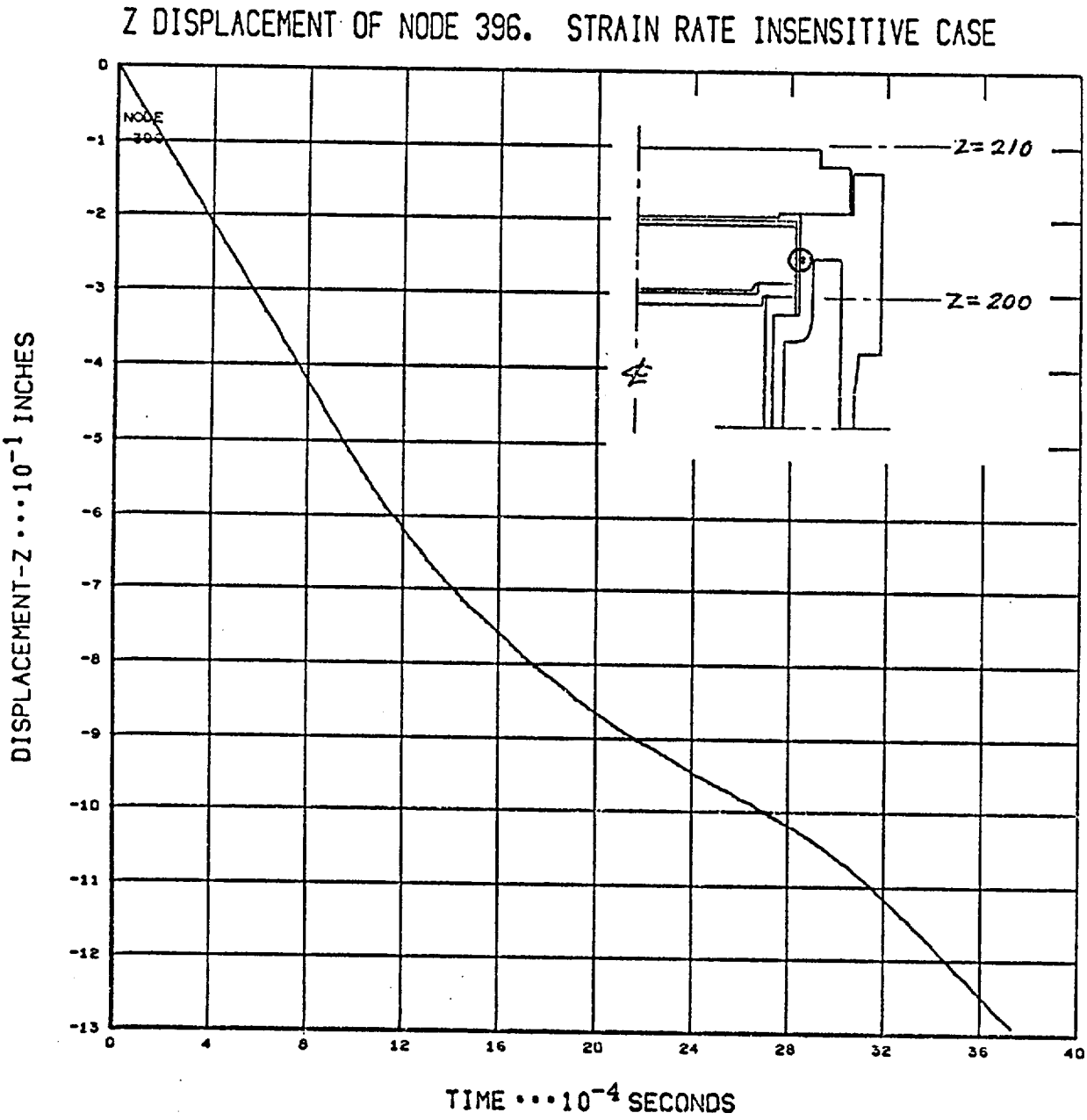
Z DISPLACEMENT OF NODE 396. STRAIN RATE INSENSITIVE CASE
NODE 396
Z= 210
Z= 200
DISPLACEMENT-Z ...10⁻¹ INCHES
TIME ...10⁻⁴ SECONDS
0
-1
-2
-3
-4
-5
-6
-7
-8
-9
-10
-11
-12
-13
0
4
8
12
16
20
24
28
32
36
40

Figure 2-29

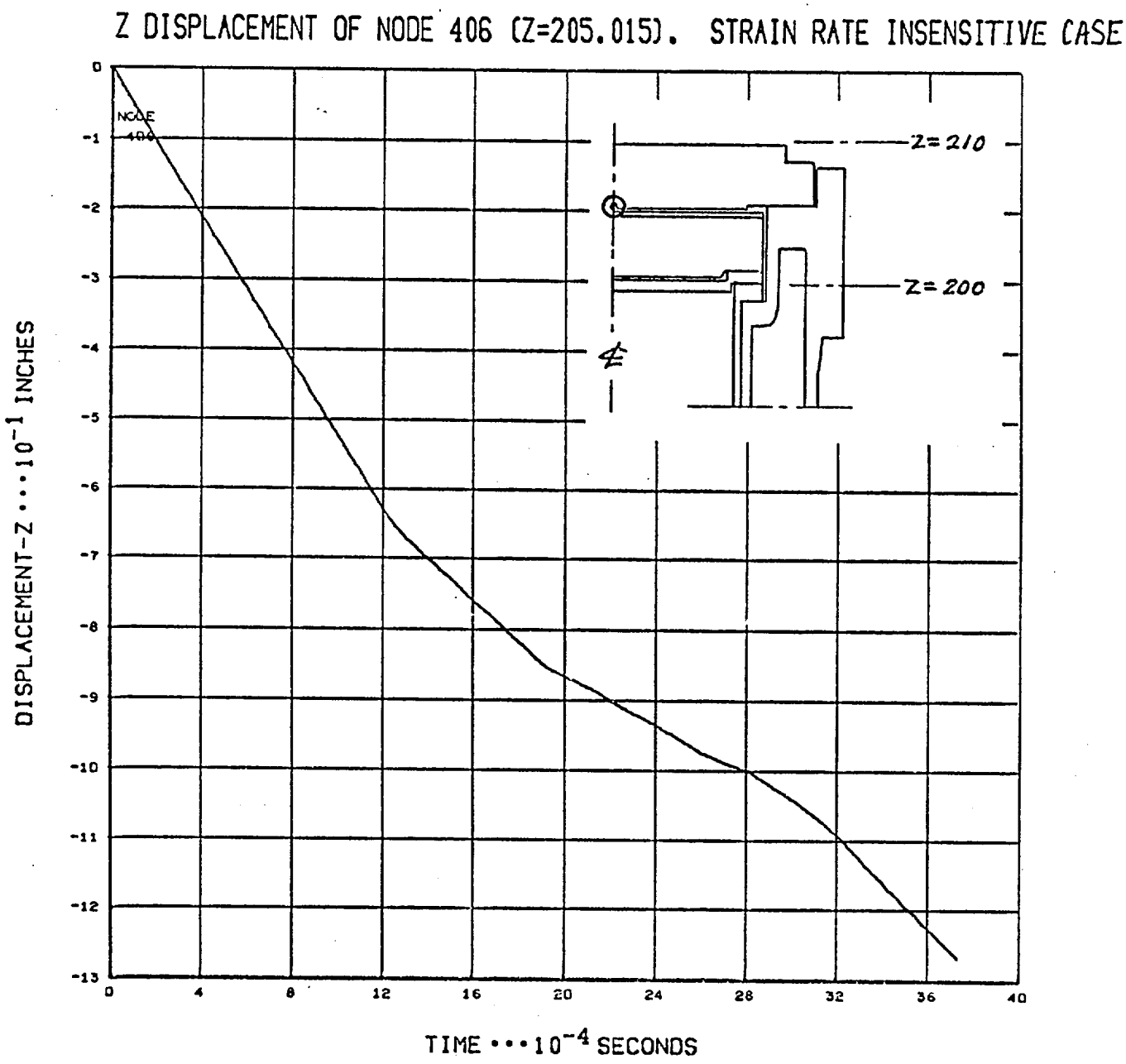
Z DISPLACEMENT OF NODE 406 (Z=205.015). STRAIN RATE INSENSITIVE CASE
NODE 406
Z=210
Z=200
DISPLACEMENT-Z •••10⁻¹ INCHES
TIME •••10⁻⁴ SECONDS
0
-1
-2
-3
-4
-5
-6
-7
-8
-9
-10
-11
-12
-13
0
4
8
12
16
20
24
28
32
36
40

Figure 2-30

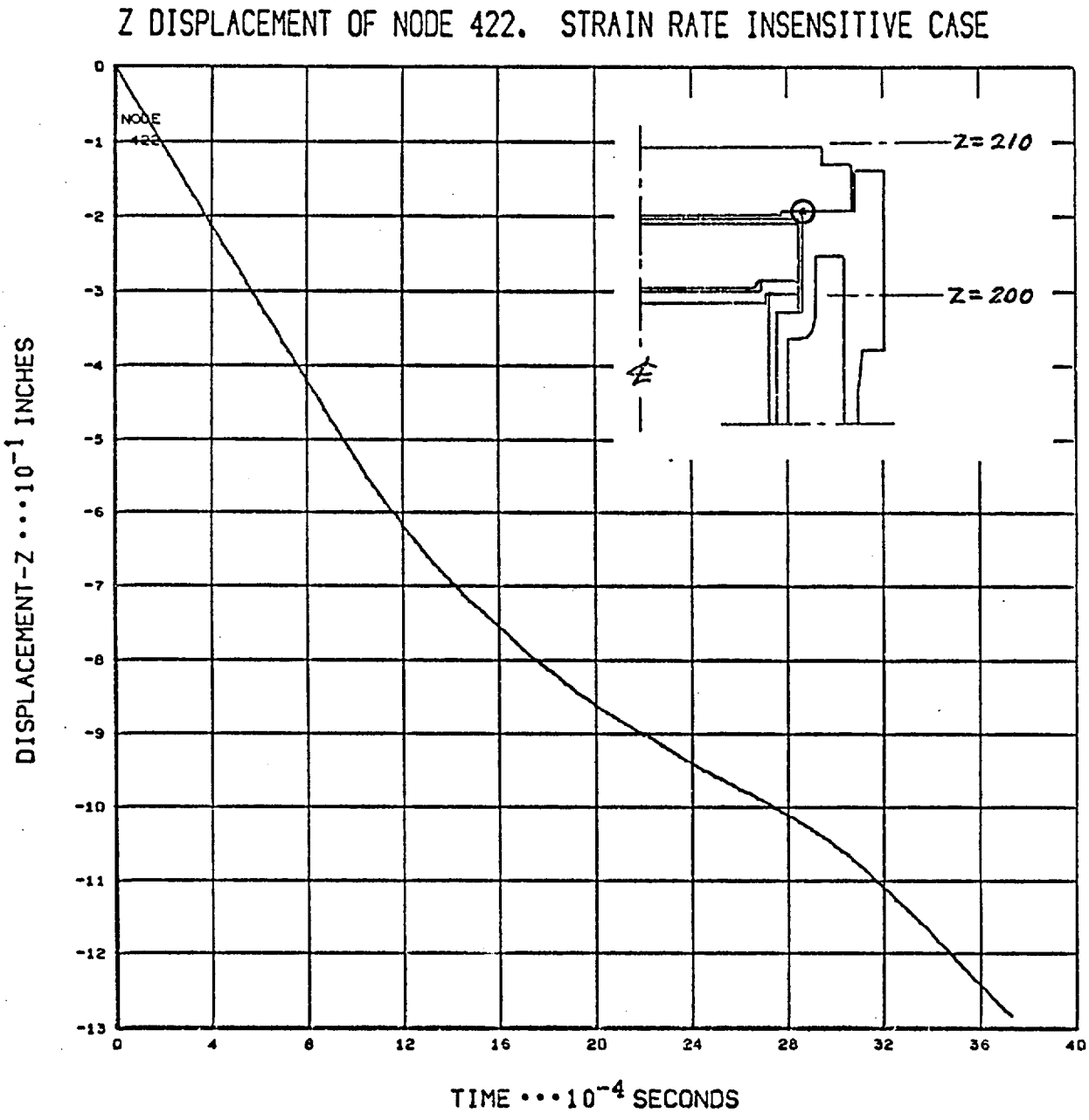
Z DISPLACEMENT OF NODE 422. STRAIN RATE INSENSITIVE CASE
NODE 422
Z=210
Z=200
DISPLACEMENT-Z •••10⁻¹ INCHES
0
-1
-2
-3
-4
-5
-6
-7
-8
-9
-10
-11
-12
-13
0
4
8
12
16
20
24
28
32
36
40
TIME •••10⁻⁴ SECONDS

Figure 2-31

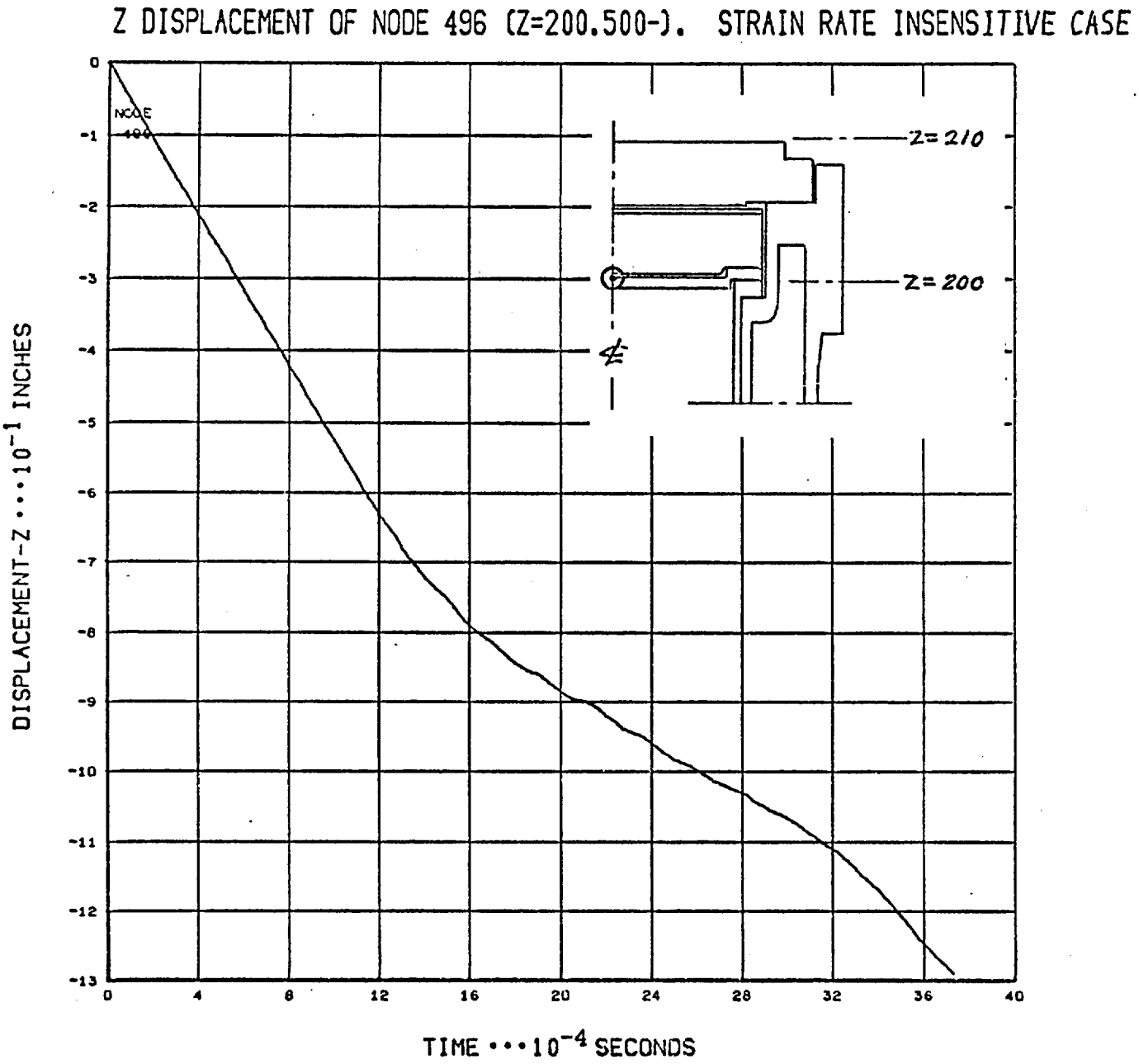
Z DISPLACEMENT OF NODE 496 (Z=200.500-). STRAIN RATE INSENSITIVE CASE
NODE 496
Z=210
Z=200
DISPLACEMENT-Z •••10^{-1} INCHES
TIME •••10^{-4} SECONDS
0
-1
-2
-3
-4
-5
-6
-7
-8
-9
-10
-11
-12
-13
0
4
8
12
16
20
24
28
32
36
40

Figure 2-32

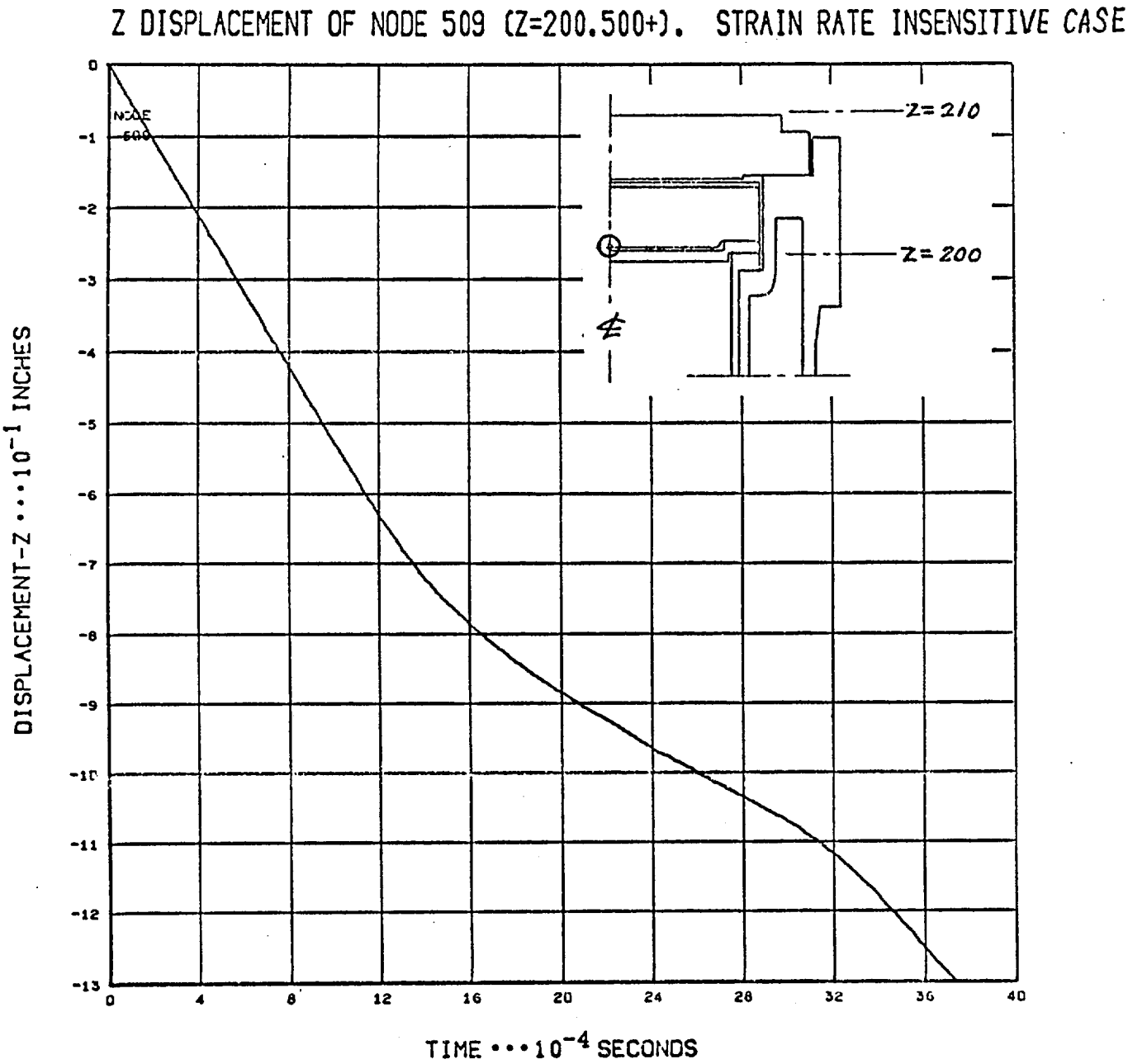
Z DISPLACEMENT OF NODE 509 (Z=200.500+). STRAIN RATE INSENSITIVE CASE
NODE 509
Z=210
Z=200
DISPLACEMENT-Z •••10⁻¹ INCHES
TIME •••10⁻⁴ SECONDS
0
-1
-2
-3
-4
-5
-6
-7
-8
-9
-10
-11
-12
-13
0
4
8
12
16
20
24
28
32
36
40

Figure 2-33

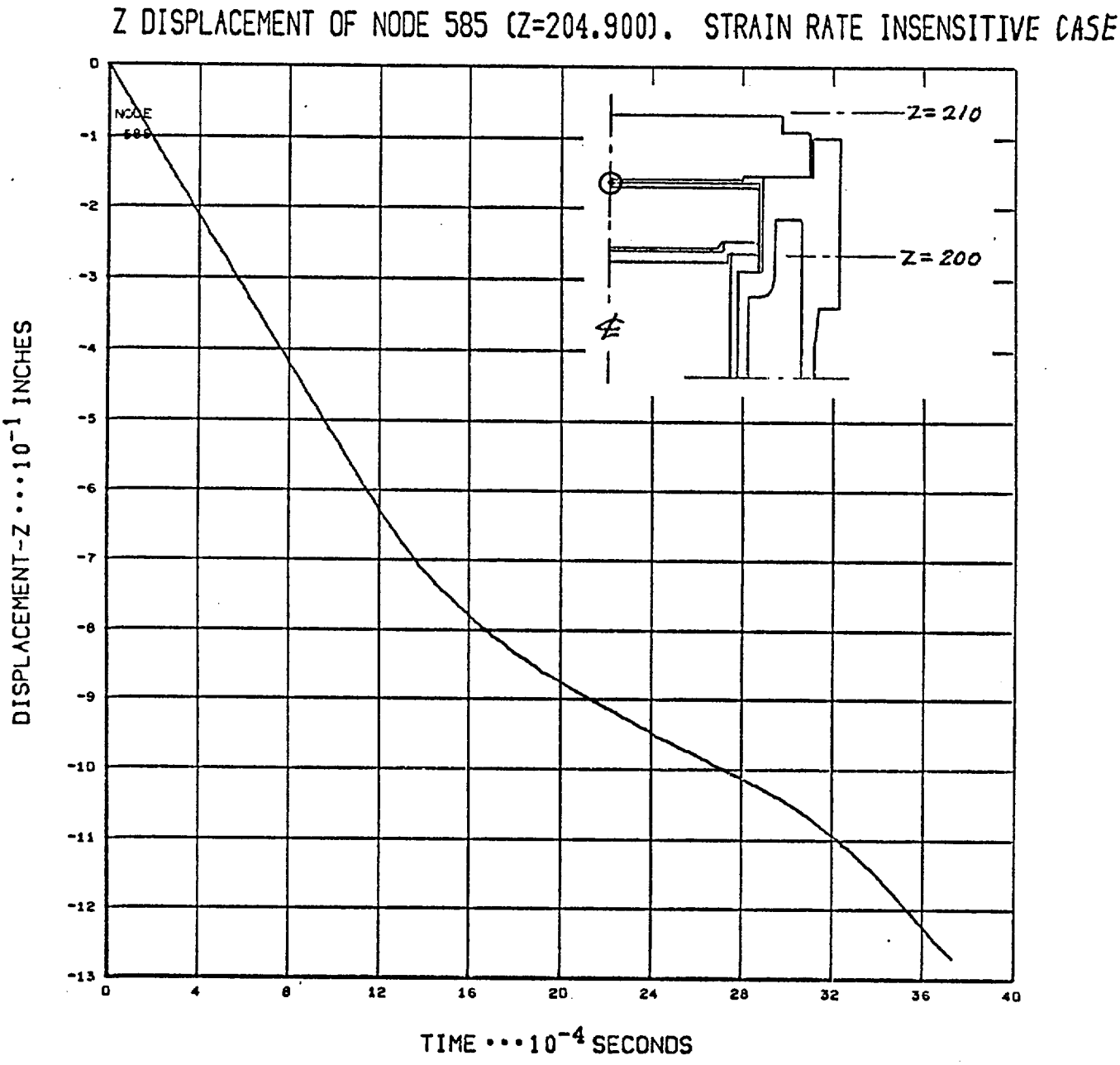
Z DISPLACEMENT OF NODE 585 (Z=204.900). STRAIN RATE INSENSITIVE CASE
NODE 585
Z= 210
Z= 200
DISPLACEMENT-Z ···10⁻¹ INCHES
TIME ···10⁻⁴ SECONDS
0
-1
-2
-3
-4
-5
-6
-7
-8
-9
-10
-11
-12
-13
0
4
8
12
16
20
24
28
32
36
40

Figure 2-34

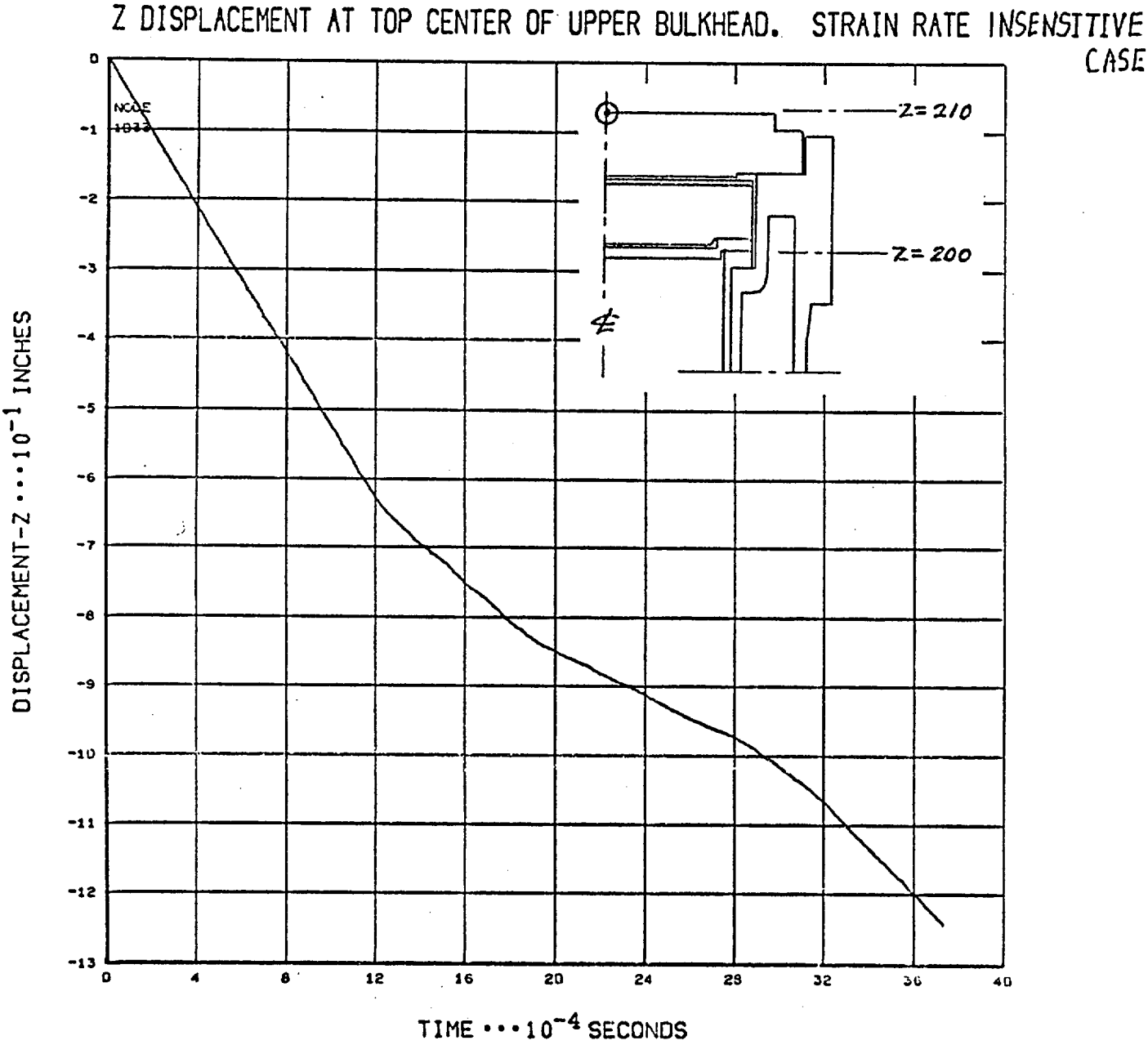
Z DISPLACEMENT AT TOP CENTER OF UPPER BULKHEAD. STRAIN RATE INSENSITIVE CASE
Z=210
Z=200
DISPLACEMENT-Z ···10⁻¹ INCHES
TIME ···10⁻⁴ SECONDS
0
-1
-2
-3
-4
-5
-6
-7
-8
-9
-10
-11
-12
-13
0
4
8
12
16
20
24
28
32
36
40

Figure 2-35

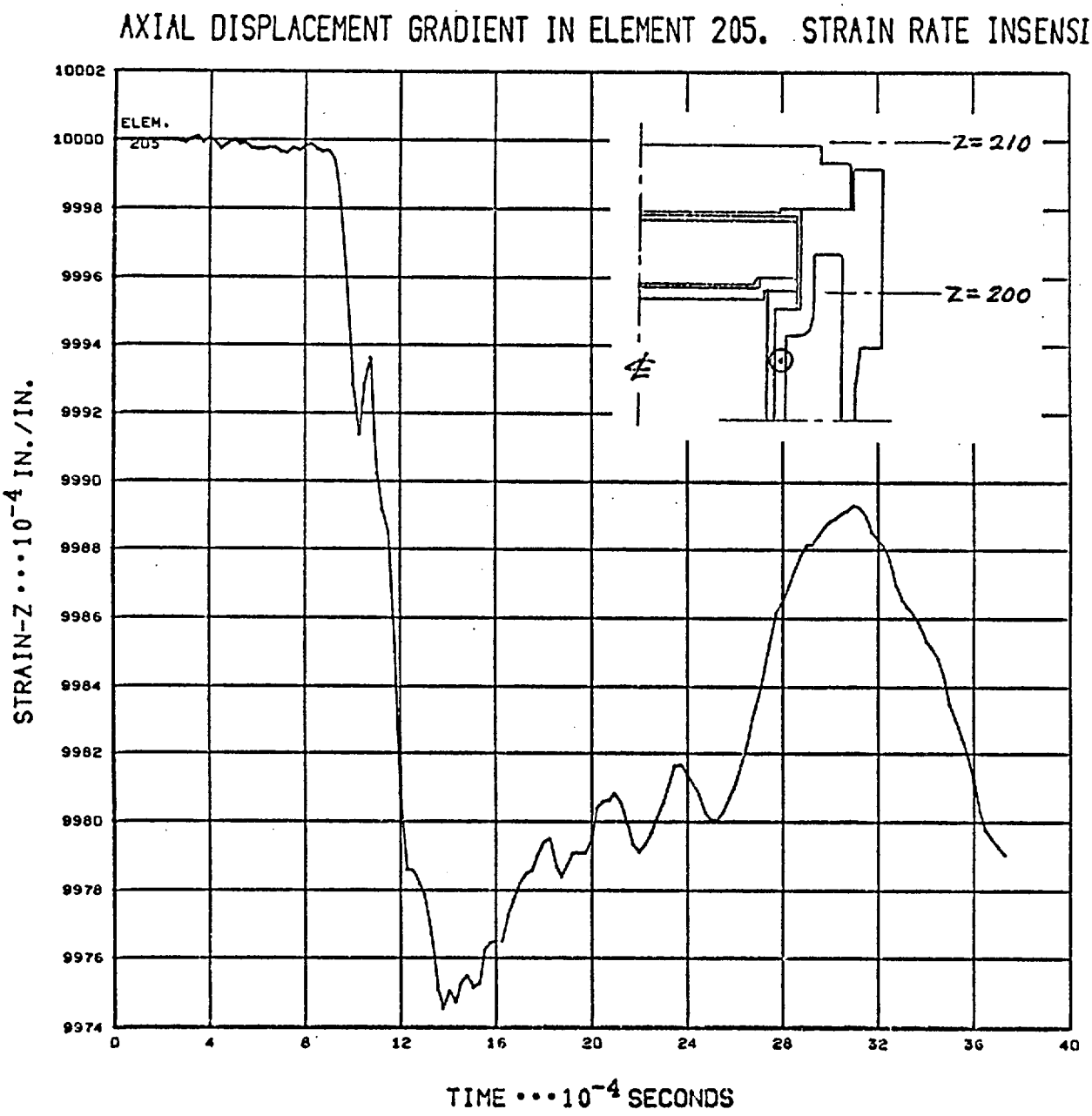
AXIAL DISPLACEMENT GRADIENT IN ELEMENT 205. STRAIN RATE INSENSITIVE CASE
ELEM. 205
Z=210
Z=200
STRAIN-Z •••10⁻⁴ IN./IN.
TIME •••10⁻⁴ SECONDS
10002
10000
9998
9996
9994
9992
9990
9988
9986
9984
9982
9980
9978
9976
9974
0
4
8
12
16
20
24
28
32
36
40

2.7.6.2 Discussion of HONDO Analysis

As stated in Section 2.7.6.1, the critical stresses are maximum for the strain rate sensitive case. For comparison with the stress summary in Section 2.7.6.1, Table 2-10 is provided for the strain rate insensitive case HONDO run.

Z-displacements depicted on Figures 2-14 through 2-20 and Figures 2-28 through 2-34 vary between approximately 0.7 in. and 1.3 in. for the time span considered.

Corresponding range of elongation based on a cask length of ~200 in.:

$$\frac{0.7}{200} < \varepsilon < \frac{1.3}{200}$$

or

$$0.35\% < \varepsilon < 0.65\%$$

which corresponds well to the 0.5% range used for construction of stress-strain diagrams in the materials data for HONDO input Section 2.7.4.

Materials

In order to clarify the validity of the materials data used, an additional HONDO run was made in December 1978 (Run No. BOT-08). The model for this run is identical to the original strain rate sensitive case model (Run No. BOT-02) with the exception of the lid uranium shield, for which strain rate insensitive behavior was input.

TABLE 2-10
MAX. ABSOLUTE STRESS SUMMARY PER C.P.O.
(STRAIN RATE SENSITIVE CASE. (RUN NO. BOT-03)

Component	Element No.	Time (10^{-4} sec.)	Predominant Stress Type(s)	Max. or Min. Principal Stress (psi)	Yield Strength at Temp. (psi)
4340 Stl. Bulkhead	232 (Bot. CL)	12.5	Rad & Hoop	23,520	150,000 (300°F)
0.2% Mo-U Alloy Shield, Lid	347 (Top CL)	13.0	Rad & Hoop	-18,110	36,300
	303 (Bot. CL)	13.5	Rad & Hoop	15,650	(300°F)
Top end of Cask	205 (Inner Cyl.)	12.0	Axial Compr.	-30,980	30,300 (250°F)
Top End of Container	468 Cylinder Below Flange	23.0	Axial Tens.	30,830	29,200 (300°F)
Container Lid Housing	281 (Bot. CL)	13.0	Rad & Hoop	18,260	29,200 (300°F)

As expected the stress and strain histories of all points outside of the lid are virtually identical for the two models. For the critical points (top and bottom centerline) of the lid shield results from Run No. BOT-08 are summarized in Table 2-11 (compare with Table 2-10).

TABLE 2-11
MAXIMUM ABSOLUTE STRESS SUMMARY PER C.P.O (RUN NO. BOT-08)
(STRAIN RATE SENSITIVE CASE, EXCEPT FOR LID SHIELD)

Component	Element No.	Time (10^{-4} sec.)	Predominant Stress Type(s)	Max. or Min. Principal Stress (psi)	Yield Strength at Temp. (psi)
0.2% Mo-U Alloy Shield Lid	347 (Top CL)	13.0	Rad & Hoop	-28,930	36,300 (300°F)
	303 (Bot CL)	13.5	Rad & Hoop	29,660	

Plots of the hoop stress in element 303 and the radial stress in element 347 vs. time for Run No. BOT-08 are shown on Figure 2-24 and 2-26 (compare with Figures 2-10 and 2-12.)

It is seen that for all three enveloping models (strain rate insensitive case, strain rate sensitive case, and strain rate sensitive with insensitive shield case) the maximum absolute stress in the uranium alloy lid shield will be below static ($\dot{\varepsilon} = 10^{3}$) yield strength at 300°F.

Run BOT-08 vertical displacements of bulkhead and lid are virtually identical to those depicted on Figures 2-15 and 2-19. The comments in Section 2.7.6.1 regarding possible interference are therefore still applicable.

For the strain rate sensitive case depicted on Figure 2-10 for elem. 303 there may theoretically be some plastic strain in the shield since a yield strength of 8180 psi is assumed at an extreme low strain rate of 10^{-6}. However, as shown below by a conservative calculation, the amount of plastic strain will be negligible.

For $\sigma \leq 8180$ psi: elastic strain regardless of strain rate.

Time span during which 8180 psi $< \sigma <$ 26,190 psi: $T = 6 \times 10^{-4}$ sec (Ref.: Figure 2-10 and Section 2.7.6.1).

Plastic strain may occur during this time span, provided the strain rate $\dot{\varepsilon} < 10^{-3}$.

If $\dot{\varepsilon}$ exceeds 10^{-3} the material will not yield at stresses below 28,000 psi (Ref. Table 2-5).

$$\text{Total plastic strain } \varepsilon = \int_{T_1}^{T_2} (\dot{\varepsilon})\, dT$$

where T_1 = time when σ first exceeds 8180 psi,
T_2 = time when σ drops below 8180 psi, and
$\dot{\varepsilon}$ = strain rate.

Consequently, for $\dot{\varepsilon} < 10^{-3}$:

$$\varepsilon < (10^{-3}) \int_{T_1}^{T_2} dt = (10^{-3})\,(T)$$

$$= (10^{-3})\,(6 \times 10^{-4}) = \underline{6 \times 10^{-7} \text{ in./in.}}$$

$$\sim 6 \times 10^{-5}\% = \underline{0.00006\%}$$

This amount of plastic strain is minute compared with the tested failure strain of the material and will not affect the integrity of the shield.

Properties input for the uranium shield, cylinder, material (material identication No. 3) are irrelevant for the analysis of the top head and lid of the cask. This is because the uranium cylinder is slip-fitted between the inner and outer container shells, and there is a 0.15 in. gap between the top of the shield and the stainless steel cavity containing it. The pressure wave from the ground impact will therefore travel through the stainless steel shells (Material No. 1) unaffected by the uranium shield. In other words: the HONDO stress-strain history of the cask closure system would have been the same regardless of what properties had been input for material no. 3.

The principal tension stress of 50,990 psi shown for element 468 in Table 2-8 is according to the computer output derived from the following stress components:

σ_r = -4,530 psi (radial stress)
σ_z = -50,850 psi (axial tension stress)
σ_T = -26,120 psi (hoop tension stress)
τ = 2,741 psi (shear stress)

Clearly the maximum principal stress in element 468 is oriented very close to the axial direction of the cask.

Ultimate tensile strength of material no. 1 is 70,000 psi min. at room temperature. According to the "International Nickel Company Stainless Steel Data Book, Sect. 2, Bulletin A (1963 Edition)," pg. 9, the

nominal UTS varies from 78,000 psi @70°F to 55,000 psi @1000°F. Conservatively assuming a linear variation even at the lower end of the range from 70°F to 1000°F this corresponds to 78,000 - 55,000/1000 - 70 = 24.73 psi/°F. UTS at 300°F = 70,000 - (300-70)(24.73) = 70,000 - 5700 = 64,300 psi.

2.7.7 Evaluation of FSV-1 Configurations F and G

2.7.7.1 DISCUSSION

The complete structural evaluation of Model FSV-1 in Configurations E, F and G is presented in other parts of Section 2.0. This evaluation is applicable to Configurations F and G when used for the transport of irradiated hardware.

2.7.7.2 Evaluation

The 12-in. thick closure plug for the burial canister provides supplemental shielding for both the normal conditions of transport and the hypothetical accident conditions. During the normal conditions of transport, there are no forces which would move this closure plug from its installed position. The hypothetical accident condition most likely to apply forces tending to move the closure plug is the 30-ft drop onto an essentially unyielding surface. Neither a drop on the impact limiter nor a drop on the side would apply forces which would move the closure plug from its installed position. The drop from 30 ft onto the bottom end of the cask could apply a deceleration force of up to 905 times the force of gravity (905 g). The burial canister rests on the bottom of the cask cavity and the closure plug is supported on a shoulder at the open end of burial canister as shown on GADR-55-2-12 and GADR-55-2-13. As a result of the drop, the closure plug, which weighs 654 lb, will apply a force of 592,000 lb to the

burial canister. The shoulder contact area between the burial canister and the closure plug is 11.2 in.^{2} and the burial canister wall has an area of 12.4 in.^{2} Therefore, the stress at the shoulder is:

$$\frac{592,000}{11.2} = 52,857 \text{ lb/in.}^2$$

and in the wall is:

$$\frac{592,000}{12.4} = 47,742 \text{ lb/in.}^2$$

The carbon steels used for these components of the burial canister have yield strengths of 30,000 to 35,000 lb/in.^{2} and ultimate strengths of 55,000 to 60,000 lb/in.^{2}. As a result of these stresses which are above yield for the materials involved, there will be some deformation until the available energy is expended. This deformation will be contained within the cask cavity and thus the displaced position of the closure plug will be such that its shielding effectiveness will be maintained.

The base plate of the burial canister as shown on GADR 55-2-12 and GADR 55-2-13 also provides supplemental shielding for both the normal conditions of transport and the hypothetical accident conditions. Only during the 30-ft drop onto the closure end of the cask would there be forces which would tend to move the base plate from its installed location. Because of the plywood impact limiter, the axial decelerating will not exceed 107 times the force of gravity (107 g). As a result of this deceleration, the base plate which weighs 165 lb, will apply a force of 17,655 lb to the burial canister wall. This wall has an area of 12.4 in.^{2} and the stress in the wall will be:

$$\frac{17,655}{12.4} = \underline{1,424} \text{ lb/in.}^2$$

This stress is well below the 30,000 to 35,000 lb/in.^{2} yield strength of the material and, therefore, the base plate will remain in place and provide the necessary shielding.

2.8 APPENDIX

2.8.1. Discussion

In an effort to obtain a preliminary indication of the ductility properties of uranium at subzero temperatures, a series of drop test was scheduled and conducted at National Lead Company's Albany branch. Samples of unalloyed depleted uranium were tested along with various samples of low alloys to serve as a basis for comparison.

Various diameters of as cast depleted uranium round bar were used; however, each round bar was cut to length such that the length to diameter ratio was 8 to 1 - this being approximately the same as the L/D ratio of the depleted uranium in Model FSV-1 in Configurations E, F and G.

Most drops were conducted from a height of 29 feet, 3 inches onto essentially unyielding surfaces of either steel or concrete. Two samples, also from a height of 29 feet 3 inches, were dropped on a sharp edged fulcrum. Temperature at the top of drop of all samples ranged between -55°F to -60°F.

Results of these preliminary drop test indicated that the unalloyed depleted uranium exhibited good ductility properties at low temperatures. Furthermore, it wasn't until the third 29 feet 3 inches drop of a test specimen that ductility failure occurred. A 1-3/16" diam by 9-1/2 inch long unalloyed depleted uranium round bar was dropped on a concrete impact surface with no visible failure resulting. The same test specimen was then dropped from the same height of 29 feet 3 inches and at the same temperature of -60°F on a steel plate. This time a slight bend in the bar was noted. On the third test, the specimen was dropped on the sharp edge of a steel

angle. Along with a greater bend in the bar, it was noted that a small crack developed opposite the side of impact.

2.8.2 Results

See Table 2-12 on following page for the results of these tests.

2.8.3 Low Temperature 1/8 Scale Uranium Shell Impact Tests

2.8.3.1 Purpose of Tests

Experimental knowledge is required of the effects of impact loads as used in casks with uranium shielding and having relatively large L/D ratios. The experimental test specimen was subjected to several puncture tests to determine the amount of deformation and to observe the surface condition of the uranium in the impacted areas.

TABLE 2-12
RESULTS

Test No.	Specimen Drop No.	Material (As-Cast)	Diameter (in.)	Attitude at Impact	Impacting Surface	Test Results
1	1	U-2% Mo	1-1/4	Horizontal	Concrete	No failure
2	1	Unalloyed	1-3/16	Horizontal	Concrete	No failure
3	1	Unalloyed	1-3/16	Horizontal	Concrete	No failure
4	1	U-1% Mo, 1% Nb	0.6	Horizontal	Concrete	No failure
5	1	U-1% Mo, 1% W	0.6	45° Corner Drop	Concrete	No failure
6	1	U-1% Nb, 1% W	0.6	45° Corner Drop	Concrete	No failure
7	1	U-1% Ta, 1% W	0.6	Horizontal	Concrete	No failure
8	1	Unalloyed	0.6	Horizontal	Concrete	No failure
9	1	Unalloyed	0.6	Horizontal	Concrete	No failure
10	2	Unalloyed	1-3/16	Horizontal	Stl Plate	Slight Bend
11	2	Unalloyed	1-3/16	Horizontal	Stl Plate	Slight Bend
12	2	U-2% Mo	1-1/4	Horizontal	Stl Plate	No failure
13	2	U-1% Mo, 1% W	0.6	Horizontal	Stl Plate	No failure
14	2	Unalloyed	0.6	Horizontal	Stl Plate	Slight Bend
15	3	Unalloyed	1-3/16	Horizontal	90° Corner	Bent & Cracked
16	3	Unalloyed	1-3/16	Slight Angle Corner Drop	90° Corner	Bent

Test Conditions

Height of drop	29'3"
Temperature of specimens	-55°F to -60°F
Material Condition	As cast
Material Configuration	Round bars, L/D = 8:1

2.8.3.2 Material Used

An as cast 0.2% - 0.3% molybdenum-uranium cylindrical shell, 1/8 the size of the actual shielding in the shipping cask, was used for this series of tests.

Comparative dimensions and weights:

	1/8 Scale Cylindrical Shell	Full Size Uranium Shielding
Outside diameter	3-1/4"	26"
Inside diameter	2-3/8"	19"
Length	24-3/8"	194"
Weight	64 lb	32,800 lb

2.8.3.3 Test Procedures

Tests were conducted using the indoor drop test facilities of NLC, Wilmington branch.

An iron-constantan thermocouple was attached to the outer surface of the uranium cylindrical shell. The thermocouple extension leads were connected to a calibrated pyrometer indicator.

The test specimen was then submerged in a solution of acetone and dry-ice until it reached a temperature of approximately -60°F. With the thermocouple still attached, the uranium was connected to a quick release mechanism which, in turn, was attached to an overhead crane. The entire assembly was moved over the impact area which consisted of a 3/4 inch wide carbon steel fulcrum 4 inch deep and 12 inch long welded to a 12 inch x 12 inch x 3/4 inch carbon steel base plate. This weldment was resting on a steel anvil pad supported by a concrete foundation. With the use of a scaled line and plumb bob, the test specimen was raised to a height of 40

inches over the fulcrum. Its long axis was positioned level and perpendicular to the long axis of the fulcrum so that the center of gravity of the shell would impact against the fulcrum.

When the pyrometer indicator measured a surface temperature of -40°F the solenoid on the release mechanism was actuated, pulled a release pin and allowed the test specimen to free fall on the fulcrum.

This same test was conducted at 60 inches, 80 inches, 100 inches and 120 inches. Measurements were taken after each test of the outside diameter, inside diameter, length and angle of bend.

2.8.3.4 Results

Results of all free fall fulcrum tests proved negative. The test specimen experienced no dimensional changes or deformations.

The 120 inches drop test had a rebound after impact of 31-1/4 inches above the fulcrum--the test specimen remained level during the rebound. Although no damage occurred to the uranium, the 3/4 inch fulcrum received an indentation approximately 1/4 inch deep.

2.8.4. Uranium Weld Joint Study

2.8.4.1 Discussion

Successful completion of side puncture tests on a uranium casting scale model has prompted a review of impact condition analyses and has also allowed consideration of a type of joint for the uranium sections which permits a greatly reduced depth of welding.

The previous calculations for side wall puncture assumed the onset of plastic hinge deformation at 30,000 psi, and required that 83% of the kinetic energy of the 40 in. drop had to be absorbed by this mechanism. The new drop tests proved that more than double this height of drop did not produce any measurable permanent set. Obviously, justification of this performance requires that the calculated instantaneous peak bending stresses be allowed to reach for higher values and still be elastic.

The effects of this new performance are now investigated in regard to accident conditions, and include the behavior of the redesigned joints under such loadings.

According to the tests, separately reported, a drop height of 120 in., with a rebound of 31-1/4 in., can be credited, conservatively, with kinetic energy proportional only to a drop of 120 - 31-1/4 = 88-3/4 in. This means that energy 2.22 times the specified 40 in. drop was successful absorbed elastically.

2.8.4.2 Puncture Side Wall - 88-3/4 in. drop analysis.

The stainless steel outer shell, as the member directly exposed to penetration by the steel piston, is not critical. The piston merely cuts partly into the wall, due to the back-up effects of the uranium cylinder.

The uranium cylinder (as tested) is taken as a model, but calculations are now made on a full size cylinder analyzed as a separate body in an elastic drop up to 88-3/4 in.

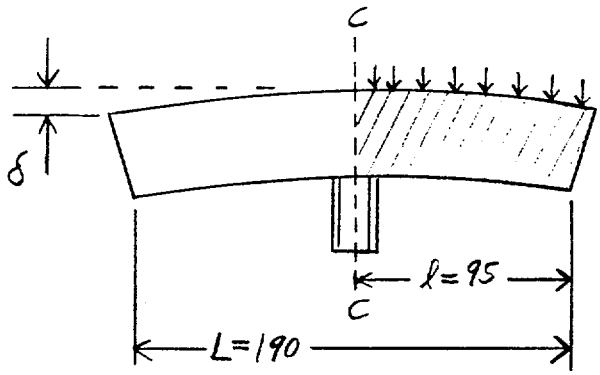

Consider 1G Load on Cantilever

D = 26 in., d = 19 in.

ℓ = 95 in., L = 190 in.

Vol. = (531-284) in.^{2} (190 in.) = 46,930 in.^{3} total

Wt = 46,930 (0.683) = 32,000 lb total

I = 0.0491 ($26^4 - 19^4$) = 16,041 in.^{4}

Z = 16,041/13 = 1235 in.^{3}

$$M_c = \frac{w\ell}{2} = \frac{32{,}000}{2}\ \frac{95}{2} = 760{,}000 \text{ in. lb}$$

$$\delta = \frac{w\ell^3}{8EI} = \frac{16{,}000\ (95)^3}{8(29)\ 10^6\ (16{,}041)} = 0.0369 \text{ in.}$$

$$S_b = \frac{M_c}{Z} = \frac{760{,}000}{1235} = 615 \text{ psi}$$

From Marks Handbook, sixth edition, page 5-44:

$$U_{cantilever} = \frac{n^2}{m} \left(\frac{K}{c}\right)^2 \frac{S^2 V}{2E} \text{ for uniform load}$$

$n = 2 \quad m = 8 \quad K = \text{rad. gyr.} = \frac{\sqrt{D^2 + d^2}}{4}$ for tube section

$c = D/2$

$$\therefore U_{cant.} = \frac{(2)^2}{8} \frac{4}{16} \frac{(D^2 + d^2)}{D^2} \frac{S^2 V}{2E} = \frac{D^2 + d^2}{16D^2} \frac{S^2 V}{E} \text{ for 1/2 beam lgth.}$$

$$U_B = \frac{D^2 + d^2}{8D^2} \frac{S^2 V}{E} \text{ for full length beam as above}$$

$$= \frac{26^2 + 19^2}{8 \times 26^2} \frac{S^2 (46{,}930)}{29\ (10^6)} = \frac{674 + 361}{8\ (676)} S^2 \frac{1615}{10^6} = \frac{310}{10^6} S^2$$

Now S = 615 psi for 1G load

$$U_B = \frac{310\ (615)^2}{10^6} = 117 \text{ in. lb} \quad \text{Note: } U_B \alpha S^2 \alpha (G's)^2$$

Line	G's	S psi	δ in.	$(G's)^2$	U_B in. lb	Height Drop
1	1	615.	0.00369	1	117	
2	50	30,750	0.1845	2500	292,500	
3	104.5	64,300	0.386	10,920	1,280,000	40
4	156.	96,000	0.575	24,280	2,840,000	88-75

The stress of 96,000 psi is reached "instantaneously" and only at the top mid point of the beam. This peak is quite consistent with nominal properties of unalloyed cast uranium. Static compression, stress-strain curves for cast, unalloyed depleted uranium are shown in Figure 2-36.

The specification is limited to the values of Line 3. The joints are actually at positions B and the moment and stress is reduced to 4/9.

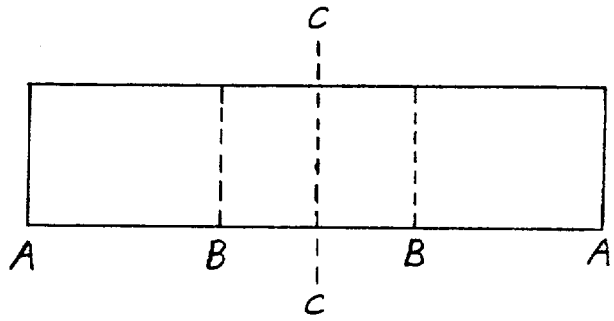

$$\frac{M_B}{M} = \frac{(2/3\ Wt)(2/3\ell)}{(Wt)(\ell)} = 4/9 \quad \therefore S_B = \frac{4}{9} S_B = \frac{4}{9} (64,300)$$

$$= \underline{28,600 \text{ psi}}$$

2.8.4.3 Results

Since the "solid" cylinder of the tests (equivalent to full depth penetration weld) has withstood at its midsection 96,000 psi, it would be theoretically possible to reduce the depth of an outside weld for position B so that Z for the weld area is only

$$Z_{B2} = \frac{28,600}{96,000} 1235 = \underline{368}$$

Figure 2-36.

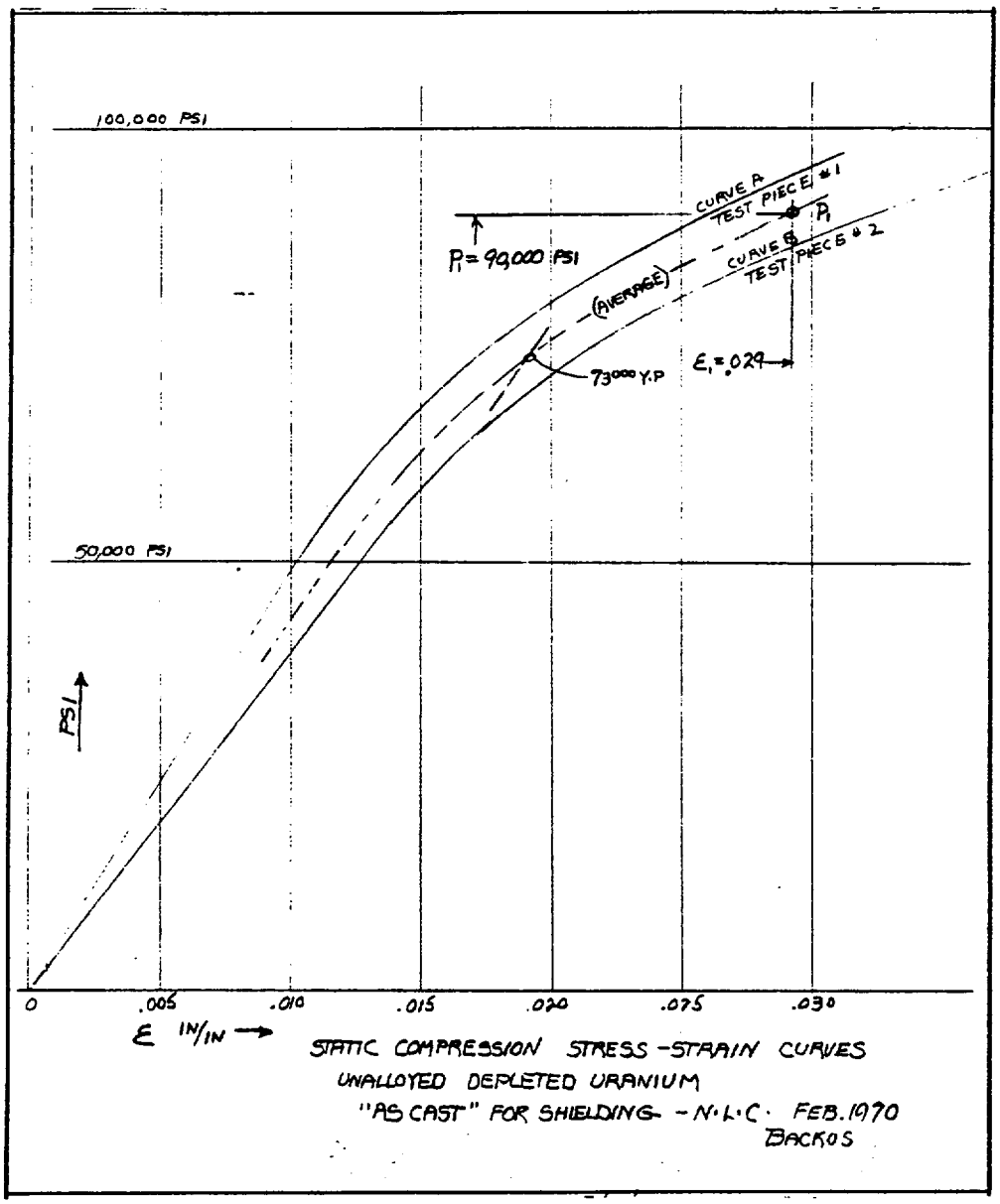
100,000 PSI
50,000 PSI
PSI
P_1 = 99,000 PSI
CURVE A
TEST PIECE #1
P_1
(AVERAGE)
CURVE B
TEST PIECE #2
73000 Y.P
E_1 = .029
0
.005
.010
.015
.020
.025
.030
E IN/IN
STATIC COMPRESSION STRESS-STRAIN CURVES
UNALLOYED DEPLETED URANIUM
"AS CAST" FOR SHIELDING - N.L.C. FEB. 1970
BACKUS

to find the i.d. which corresponds to this Z value, let

$$Z_{B2} = 368 = \frac{0.098}{26}(26^4 - d^4) = 0.00378\,[457{,}000 - d^4]$$

$$d^4 = \frac{1725 - 368}{0.00378} = 359{,}000$$

$$d = 24.5 \text{ in.} \quad \therefore\ t = \frac{26 - 24.5}{2} = \underline{3/4\text{-in. weld req'd min.}}$$

To be quite conservative, it is desirable to <u>double this depth</u> of weld, using <u>2</u> layers of 3/4-in. penetration welds (in offset relationship), providing continuous beam strength in an outer annulus 1-1/2 in. thick out of a total of 3-1/2-in. wall. The inner 2 in. would be machined with interlocking steps (four of 1/2-in. each) providing concentric shear rings and effective shielding pattern as illustrated.

Figure 2-37

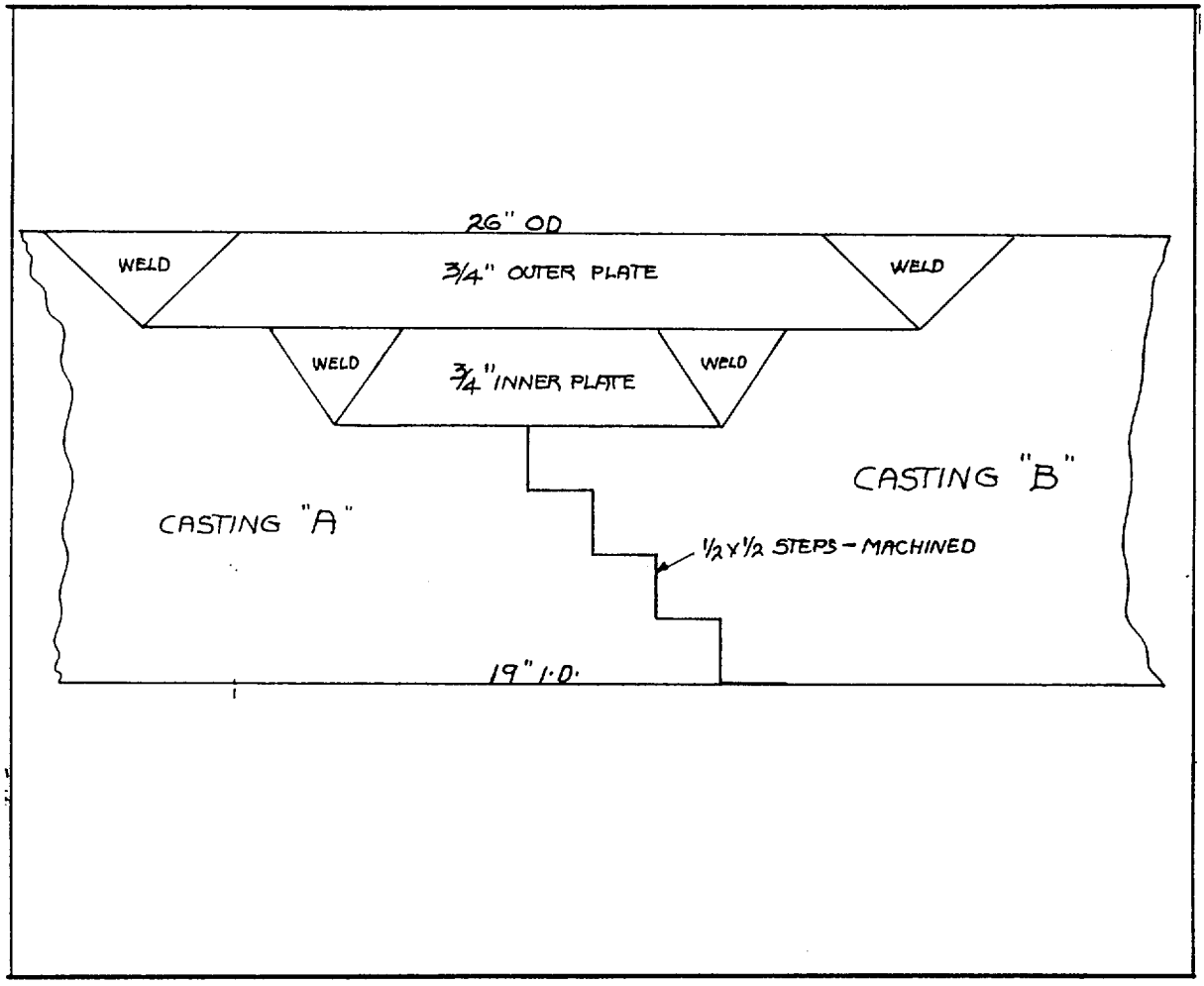
26" OD
WELD
3/4" OUTER PLATE
WELD
WELD
3/4" INNER PLATE
WELD
CASTING "B"
CASTING "A"
1/2 X 1/2 STEPS - MACHINED
19" I.D.

References

2-1. ASME Boiler and Pressure Vessel Code Section III - Nuclear Vessels, The American Society of Mechanical Engineers, United Engineering Center, NY, 1965.

2-2. ASME Boiler and Pressure Vessel Code Section IX - Welding Qualifications, The American Society of Mechanical Engineers, United Engineering Center, NY, 1965.

2-3. "Metallic O-Rings," United Aircraft Products, Inc., Bulletin No. 596191B, Dayton, Ohio, July 15, 1959.

2-4. "O-Ring Design Handbook," Plastic and Rubber Products Company, Ontario, California.

2-5. "Bolt, External Wrenching, Self-Retained by Washer," Standard Pressed Steel Company, Jenkintown, PA, Part Number and Specification 69241, Sheets 1, 2, and 3, March 6, 1968.

2-6. "Heli-Coil Screw-Lock Inserts," Heli-Coil Corporation, Danbury, Connecticut, Bulletin 900.

2-7. Aerospace Structural Metals Handbook, Dept. of Defense.

2-8. Clifford, C. B., "Design and Fabrication of a Prototype Laminated Uranium Metal Shipping Cask for Large Shipments of Co-60," USAEC Research and Development Report No. KY-521, Union Carbide Corporation, Nuclear Division, Paducah, KY, April 3, 1967.

2-9. Alloy Digest. HY-130 and HY-140(T) Steel Alloy, Filing Code: SA-280. Published by Engineering Alloys Digest Inc., September 1972.

2-10. Memo: FSV-ME:MLN:42:79, Nichols to Ketchen dated 4/3/79, "Summary of Plywood Evaluation Tests for the FSV-1 Shipping Cask Impact Limiter."

2-11. Handbook of the Engineering Sciences - Volume I, "The Basic Sciences."

2-12. Roark: "Formulas for Stress and Strain," 5th Edition.

2-13. Mantell, C. L., "Engineering Materials Handbook, 1958, McGraw.

2-14. Biggs, John M., "Introduction to Structural Dynamics," McGraw-Hill, 1964.

2-15. Clifford, C. B., "USAEC Research and Development Report Number KY-546," Union Carbide Corporation.

2-16. Lipp, Robert H., "Bolt Torque Factors," Design News Magazine, March 8, 1971 issue.

2-17. GAMD-9710. SAC Manual. Prepared by H.D. Shatoff. Dated 15 December 1969.

2-18. Parker Gask-O-Seal Handbook OSD 5411 (1977).

2-19. J. E. Shigley, "Mechanical Engineering Design," McGraw-Hill 1963.

2-20. Rack, H. J., "The Influence of Strain Rate and Temperature ___ Steele ___ Shipping Cask," SAND-75-0579. UC-79c, dated February 1976.

2-21. Burke, Colling, Gorum and Greenspan: "Physical Metallurgy of Uranium Alloys," First Ed. 1976.

2-22. SLA-74-0039, "HONDO - A Finite Element Computer Program" by S. W. Key April 1974.

2-23. Blasch, Stukenbroeker, Lusky, Bonilla, Berger: "The Use of Uranium as a Shielding Material," Nuclear Engineering and Design, Vol. 13 (1970), p. 146 and on.

2-24. Y-DA-3616, "Compilation of the Mechanical Properties of Dilute (5% maximum) Alloys of Uranium," Union Carbide Corp.

2-25. Steichen, J. M., "High Strain Rate Mechanical Properties of Type 304 stainless" HEDL-TME 71-145. Hanford Engineering Development Lab, dated September 1971.

2-26. Nuclear Systems Materials Handbook, Vol. 1. Design Data Part IV Nuclear Fuel Materials, Group 2 - Metals, Section 1 Uranium, Revision 1, 12/1/74.

2-27. Product Handbook, INCO Alloys International, Huntington, West Virginia, 1988 p. 11.

SECTION 3.0

THERMAL EVALUATION

3.0 THERMAL EVALUATION

A separate thermal evaluation for Model FSV-1 in Configurations F and G is not provided since thermal evaluation for Model FSV-1 in Configuration E will encompass all applicable thermal conditions.

3.1 DISCUSSION

Model FSV-1 in Configuration E is designed for the transport of six (6) High Temperature Gas-Cooled Reactor spent fuel elements. Each spent fuel element has a maximum decay heat output of 2322 Btu/hr after 100 days following reactor shutdown.

3.2 SUMMARY OF THERMAL PROPERTIES OF MATERIALS

Table 3-1 lists the thermal properties of the materials which constitute the cask as they were used in the analysis. In the formulas shown, T represents the temperature in °R and t in °F.

TABLE 3-1
THERMAL PROPERTIES OF MATERIALS

Helium Conductivity

$K = 0.00129\ T^{0.674}$ Btu/hr-ft°F) Ref. 3-9

Air Conductivity

$K = 0.0146 + 1.695\ E\text{-}05\ t$ Btu/hr-ft°F) Ref. 3-10

Helium-Air Mixture (50% by Volume) Conductivity

$K = 0.341 \cdot K_{He} + 0.549\ K_{Air}$ Ref. 3-11

Stainless Steel (Type 304)

Conductivity

$K = 8.0 - 0.004433\ t$ Btu/hr-ft°F) Ref. 3-12

Heat Capacity per Unit Volume

$C = 55. + 0.011458\ t$ Btu/ft^3-°F) Ref. 3-12

Emissivity

$= 0.85$ Ref. 3-8

Aluminum (Type 6061)

Conductivity

$K = 100$ Btu/hr-ft°F) Ref. 3-13

Heat Capacity per Unit Volume

$C = 39.$ (Btu/ft^3-°F) Ref. 3-13

Emissivity

$\epsilon = 0.2$ Ref. 3-7

$\epsilon = 0.85$ (with surface treatment for exposed surface)

TABLE 3-1 (continued)

Depleted Uranium Shielding Material	
Conductivity	
K = 14.8 Btu/hr-ft°F)	Ref. 3-2
Heat Capacity per Unit Volume	
C = 38. (Btu/ft^3-°F)	Ref. 3-2
Emissivity	
ϵ = 0.5	Ref. 3-2
Spent Fuel Blocks	
Conductivity	
K = 10.0 Btu/hr-ft°F)	Ref. 3-2
Heat Capacity per Unit Volume	
C = 32. (Btu/ft^3-hr)	Ref. 3-2
Emissivity	
ϵ = 0.8	Ref. 3-2
Alloy Steel (4340)	
Conductivity	
K = 20.0 Btu/hr-ft°F)	Ref. 3-12
Heat Capactiy per Unit Volume	
C = 60. (Btu/ft^3-hr)	Ref. 3-12
Emissivity	
ϵ = 0.1	Ref. 3-7

3.3. TECHNICAL SPECIFICATIONS OF COMPONENTS

A Gask-O-Seal assembly is used to seal the inner closure to the inner container body and an O-ring is used to seal the cavity gas sampling port. Both of these seals are manufactured from a silicone elastomer which has a useful temperature operating range from -80°F to +450°F and will resist temperatures up to +700°F for short periods of time.

3.4. THERMAL EVALUATION FOR MODEL FSV-1 CONFIGURATION E

The following evaluation combines the package performance during the normal conditions of transport and the hypothetical accident conditions.

3.4.1. Thermal Model

Temperatures were calculated by a finite-difference method. A digital computer code, TAC2D described in Ref. 3-2, was used to perform the numerical calculations concerning the upper half of the cask. The lower end was originally analyzed with the aid of RAT. The cask system was modeled in a form suitable for both of these codes.

TAC2D is a digital computer code that is capable of calculating temperature transients for a two-dimensional network of points. It may also be used to obtain steady state solutions asymptotically by carrying a transient calculation to the point where the time dependence of the result becomes negligible. The code version used for the present analysis differs only in array dimension statements from a certified version evaluated in Ref. 3-3. All other program adaptations relate to the particular problem at hand and are documented with the actual computer runs in Ref. 3-4.

The network is specified by establishing a grid system, assigning individual materials within that grid system, and identifying the applicable thermal parameters that represent those materials. The grid system consists of two sets of grid lines parallel to the axes in a cylindrical coordinate system.

Material blocks are defined by four bounding grid lines and a label which identifies the material they contain. Parameters that characterize each material are the pertinent thermal properties as well as the volumetric rate of heat generation within the material. Material blocks may be separated by narrow gaps that contain stagnant gases which are identified by numbers allocating the proper thermal conductivities. Heat transfer across these gaps is one-dimensional by conduction and radiation.

The various material regions and gap configurations are illustrated on Figs. 3-1 and 3-2.

Boundary conditions at external boundaries are imposed either by prescription of a sink temperature and surface conductance or by a simulated flowing coolant of given properties and flow conditions. In the present case, the interface between the plywood and the metal support structure of the impact limiter was assumed to constitute in effect an adiabatic boundary. Through the remaining cask surfaces, heat is exchanged with the surroundings by convection, radiation and, when applicable, as a prescribed heat flux due to solar irradiation.

The thermal parameters for the materials, gases in the gaps and coolants have been incorporated in the computer code in functional form. Certain dependent variables are available for use in these functions thereby permitting a nonlinear representation of the problem.

FIGURE WITHHELD UNDER 10 CFR 2.390

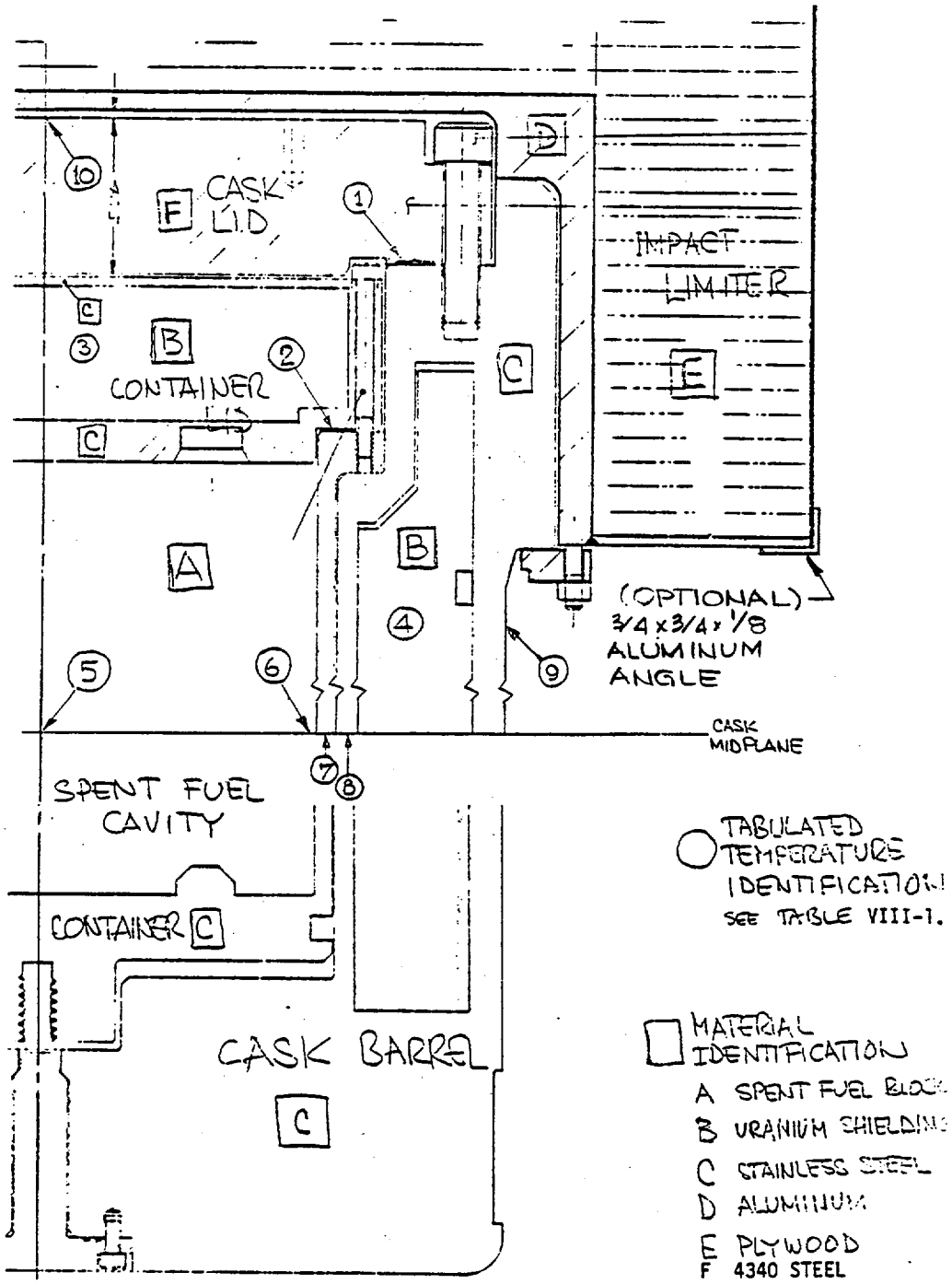

Figure 3-2. Shipping cask model

The outer closure and inner closure seal assemblies contain material of limited lifetime where this lifetime is temperature dependent. The probability that the seal fails at any time during the entire transient is obtained as the sum of the interval failure probabilities. The functional relationship between seal life and operating temperature is illustrated on Fig. 3-3, which is based on Ref. 3-5.

3.4.2. Criteria for Evaluation

The following three situations were used to define the boundary and initial conditions for the analyses:

Condition 1A. Maximum temperature day. This condition assumes an ambient temperature of 130°F around all parts of the cask. Radiation and natural convection are the mechanisms by which heat is removed from the cask. Solar heating is imposed with an effective intensity of 96 Btu/h-ft^2 on the cylindrical portion of the exposed cask surface and half of it on the exposed vertical surfaces. Decay heat generation rates for spent fuel conditions 100 days after reactor shutdown were used.

Condition 1B. Same as condition 1A except that spent fuel conditions 200 days after reactor shutdown were used.

Condition 2. Minimum temperature day. This refers to a condition of -40°F ambient temperature without solar heating. The 200 day heat generation was used for comparison with Condition 1B.

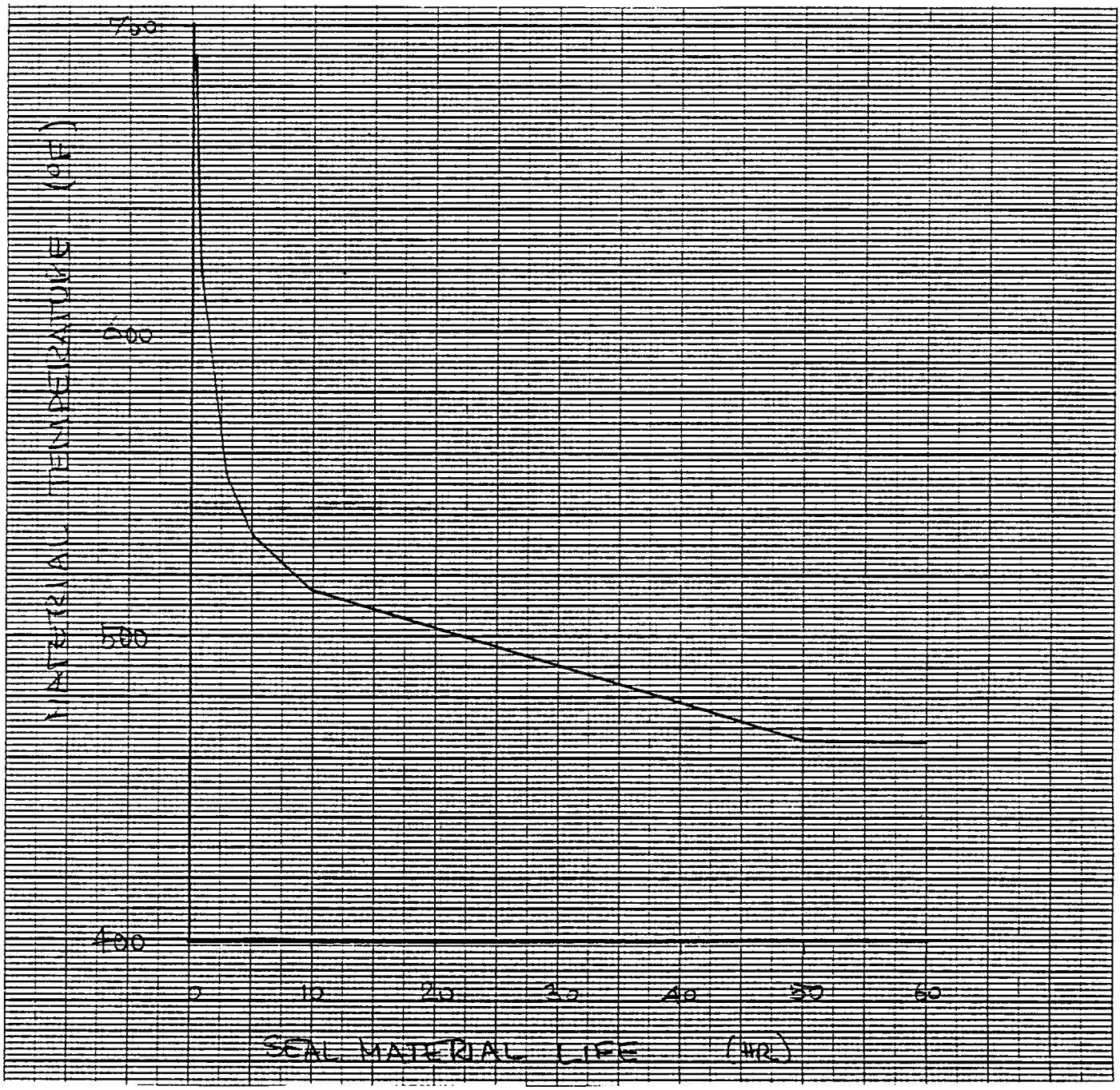

Figure 3-3. Seal material temperature limitations

Condition 3. Fire accident. This accident assumes a 1475°F fire completely surrounding the cask for a period of 30 minutes on the maximum temperature day. A convection heat transfer coefficient of 300 Btu/h-ft^2 °F was added during the fire to simulate a severe convection condition due to hot, blowing gases. After the fire, the cask is returned to the 130°F day.

3.4.3 Thermal Evaluation

a. Maximum Temperature Day: The maximum temperature day is defined as sunny and having an air and radiation background temperature of 130°F. The net solar irradiation is assumed to be constant and amount of 96 Btu/h-ft^2 on the cylindrical portion of the exposed cask and impact limiter. (This assumption permits the calculation of a representative steady-state solution in lieu of a temperature cycle for a 24-h period.) Further, it was assumed that the cask is surrounded by still air so that convective cooling is limited to free convection. Using a correlation for free convection around a horizontal cylinder, the following function was derived to calculate the surface heat transfer coefficient (Ref. 3-7):

$$h = 0.221 \left(S_t - T_a\right)^{0.25}$$

where S_t = the cask surface temperature,
T_a = the ambient temperature.

Thermal radiation from the cask to its surroundings was included utilizing a cask surface emissivity of 0.85 (Ref. 3-8) and a background absorbtivity of 1.0.

b. Minimum Temperature Day: The minimum temperature day was defined as having an air radiation background temperature of -40°F and no solar heating. This heat exchange between the cask and its surroundings is calculated on the same basis as that of the maximum temperature day.

c. Fire Accident: The fire accident is defined as a temporary radiation source of 1475°F whose iteraction with the cask is based on a fire emissivity of 0.9 and a cask surface absorptivity of 0.8. An additional surface heat transfer contribution resulting from strong convection was assumed. Heat transfer coefficients representing hot, flowing gases are expected to reach at most 300 Btu/h-ft^2-°F. The impact limiter, largely made from plywood, protects the cask from the fire. Its plywood bulk is assumed to perfectly insulate the major portion of the structural aluminum elements. There is no heat input due to solar irradiation during the fire.

Cask Dimensions:

Since the thermal analysis is performed with cask dimensions determined from manufacturing drawings, gaps cannot be defined exactly. Their actual size will fall into a range bounded by extremes which can be deduced from specific manufacturing tolerances. Sets of extreme combinations (such as all gaps of the largest possible size) as well as a mixed set which tends to affect the seal temperatures in

an adverse manner have been utilized in the calculation of the results presented here. Thermal expansion of materials and the associated variation in gap sizes were considered insignificant and therefore disregarded in the analysis.

Spent Fuel Heat Generation:

The fuel blocks to be shipped in this cask will have been irradiated and the original fissionable material partly consumed. Due to residual isotope activity in blocks that have been removed from the reactor, there is a continuing "after-heat" generation which decreases with time. It takes place predominantly in the fuel and graphite blocks and to a lesser degree in cask shielding components. This heat generation is predictable and has been used in the calculations.

It is assumed that the spent fuel is loaded into the shipping cask no sooner than 100 days after the reactor has been shut down. This represents the maximum heat generation that the cask need be designed for.

The fuel element behavior after reactor shutdown and the associated after-heat generation were evaluated at GA in unrelated analyses. The heat generation rates recommended for thermal analysis of short duration processes are listed in Table 3-1. Of these quantities, 88% are realized within the fuel block and the remaining 12% are generated within the first inch of the surrounding shielding. For the present analysis, all heat generation was assumed to be confined to the fuel blocks and distributed uniformly through their entire volume.

3.4.4 Results of Thermal Evaluation

Steady-state and transient thermal analyses were conducted with the aid of two models representing each end of the cask extending far enough along the length of the cask to ascertain valid results. No unexpected or in any way critical results were obtained from the analysis of the relatively simple lower end. Results pertaining to the upper end of the cask including the effect of the impact limiter are summarized in Table 3-2. The analytical model of the cask's thermal behavior is described in the following sections.

Three gap combinations have been constructed and employed in this analysis. The minimum gap and maximum gap combinations refer to extreme geometrical situations whereas the mixed gap combination refers to a set of gaps which was considered likely to cause high temperatures in the top of the cask under the insulating impact limiter where the critical seal assemblies are located. Temperature histories of two fire accident transients are shown on Fig. 3-4a and Fig. 3-4b, where the corresponding calculated seal life reduction due to the fire is also listed. Based on the similarity of these two results, it was concluded that other gap combinations would yield temperatures within the basic computational tolerances of those reported. Figures 3-5 through 3-8 show the complete temperature maps from the computer output for representative steady-state conditions for the extreme gap configurations.

3.4.5 Conclusions

The calculated temperatures, as provided in Table 3-2, for the three conditions evaluated do not exceed any design parameters or acceptable operating temperatures.

TABLE 3-2
TEMPERATURES AT SELECTED LOCATIONS

	Condition 1A			Condition 1B	Condition 2		Condition 3		
	130°F Ambient Air Solar Irradiation				-40°F Ambient Air		Accident: Fire of 30 min duration		
	100 Day Fuel*			200 Day Fuel**	200 Day Fuel		(Peak Values)		
	Min Gaps	Max Gaps	Mixed Gaps	Max Gaps	Min Gaps	Max Gaps	Min Gaps	Max Gaps	Mixed Gaps
1) Cask Seal	242	234	244	202	30	23	517	463	522
2) Container Seal	270	274	284	224	50	51	484	454	485
3) Closure Shielding	282	274	299	224	59	51	482	452	486
4) Body Shielding	266	275	274	227	36	46	839	831	830
5) Fuel Centerline	392	422	420	311	140	170	562	574	572
6) Fuel Surface	384	414	412	307	137	166	555	567	565
7) Container Wall	327	362	361	275	80	115	587	581	579
8) Inner Shell	296	324	322	253	57	83	656	646	645
9) Exposed Cask Surface	227	227	228	203	6	7	1440	1442	1442
10) Cask Top Centerline	247	236	247	203	33	24	481	431	487

*Equivalent Heat Generation: 2322 Btu/h/spent fuel element
**Equivalent Heat Generation: 1101 Btu/h/spent fuel element

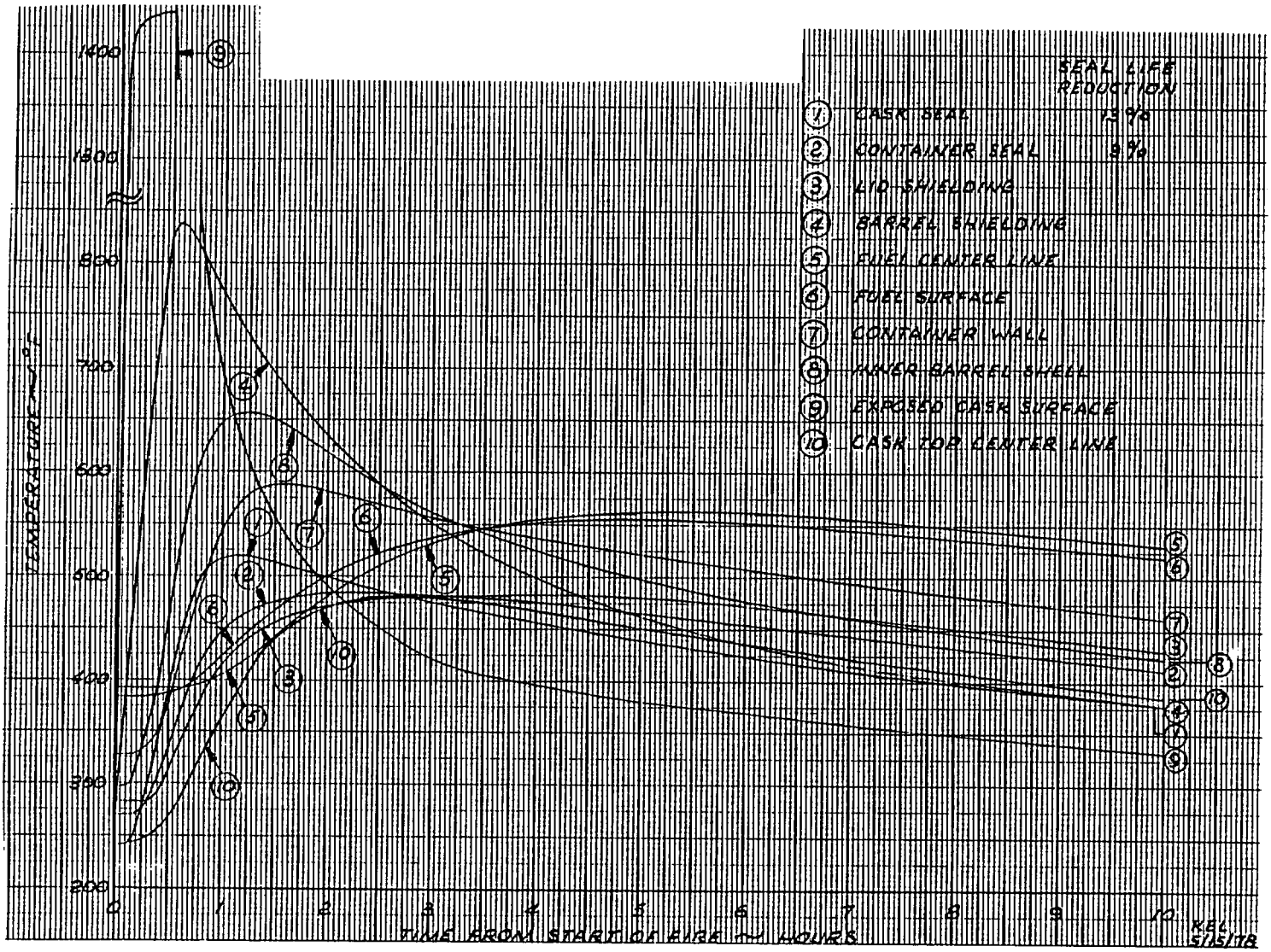

Figure 3-4a. Fire Accident (Minimum Gaps)

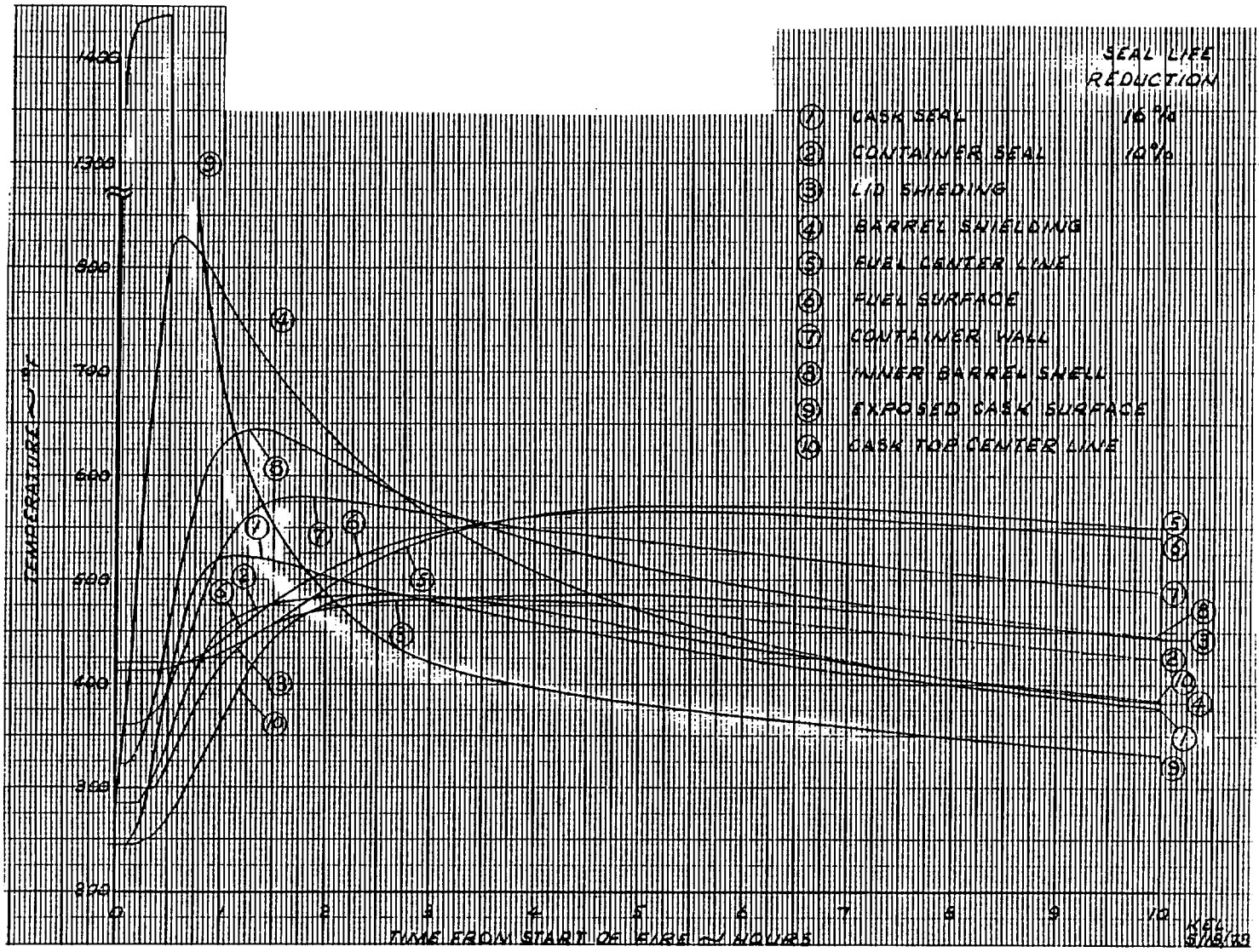

Figure 3-4b. Fire Accident (Mixed Gaps)

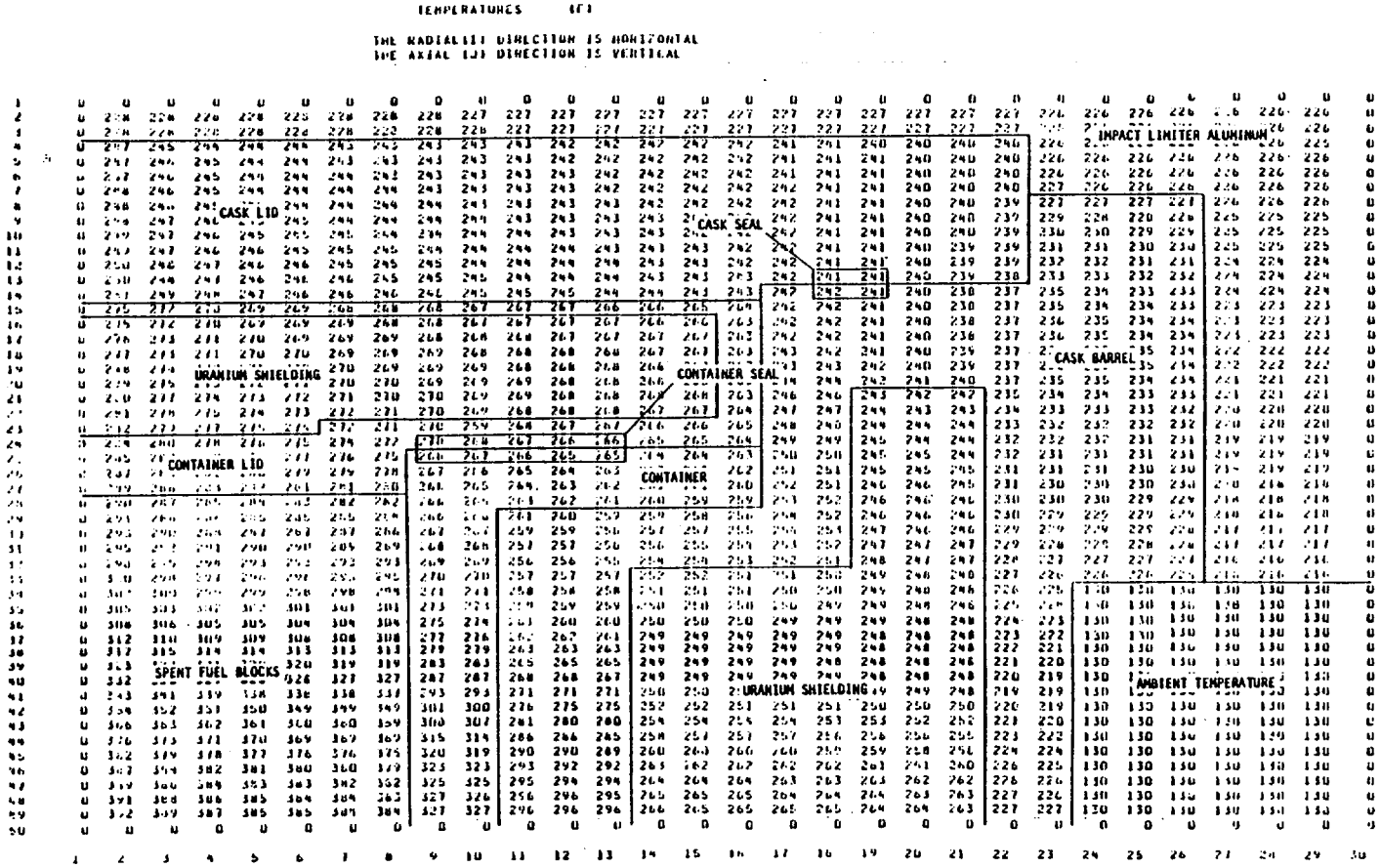

Figure 3-5. Fuel Shipping Cask Temperature Map for Steady State Condition 1A (Maximum Temperature Day) - Minimum Gap Configuration, 100 Day Fuel

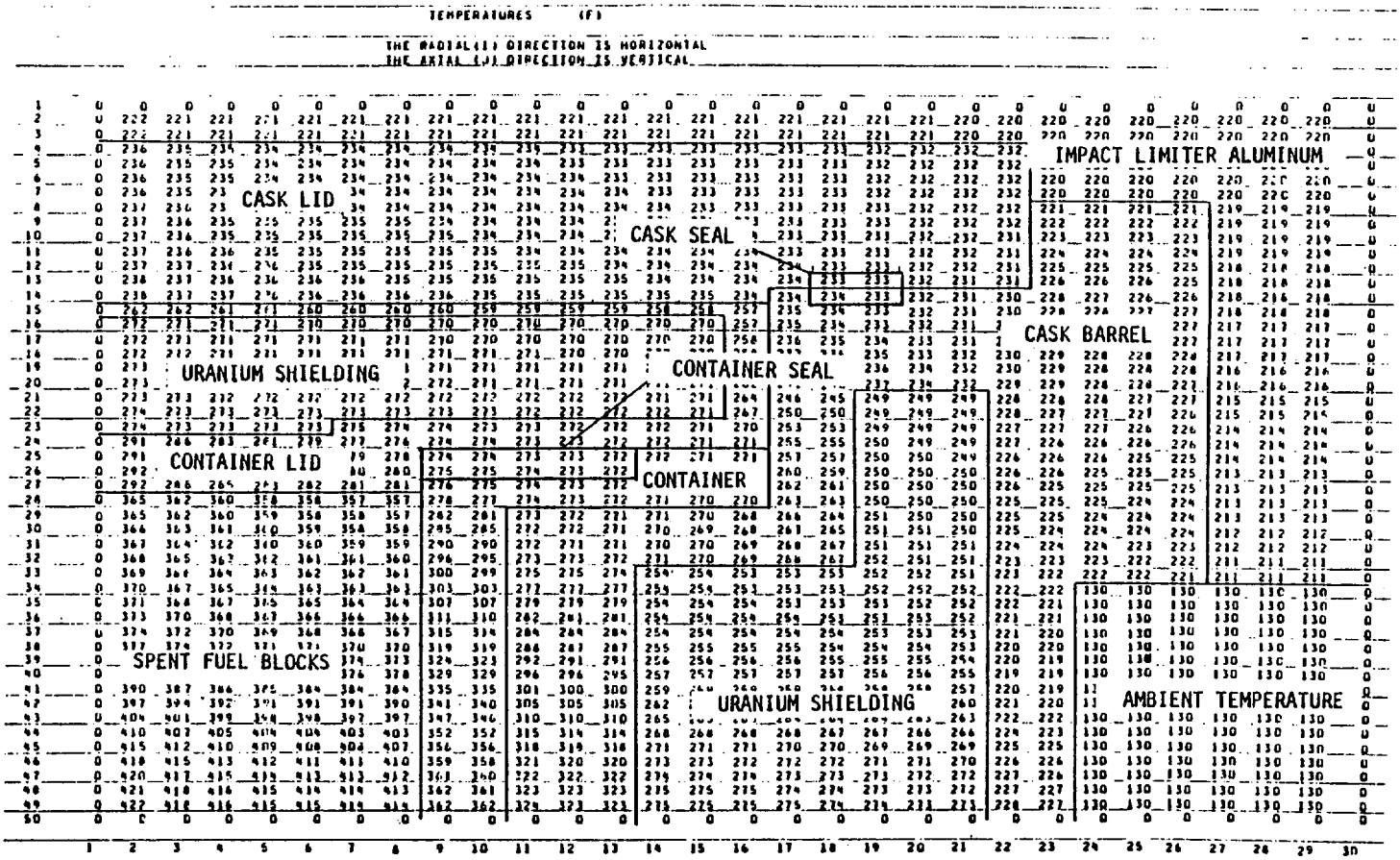

Figure 3-6. Fuel Shipping Cask Temperature Map for Steady State Condition 1A (Maximum Temperature Day) - Maximum Gap Configuration, 100 Day Fuel.

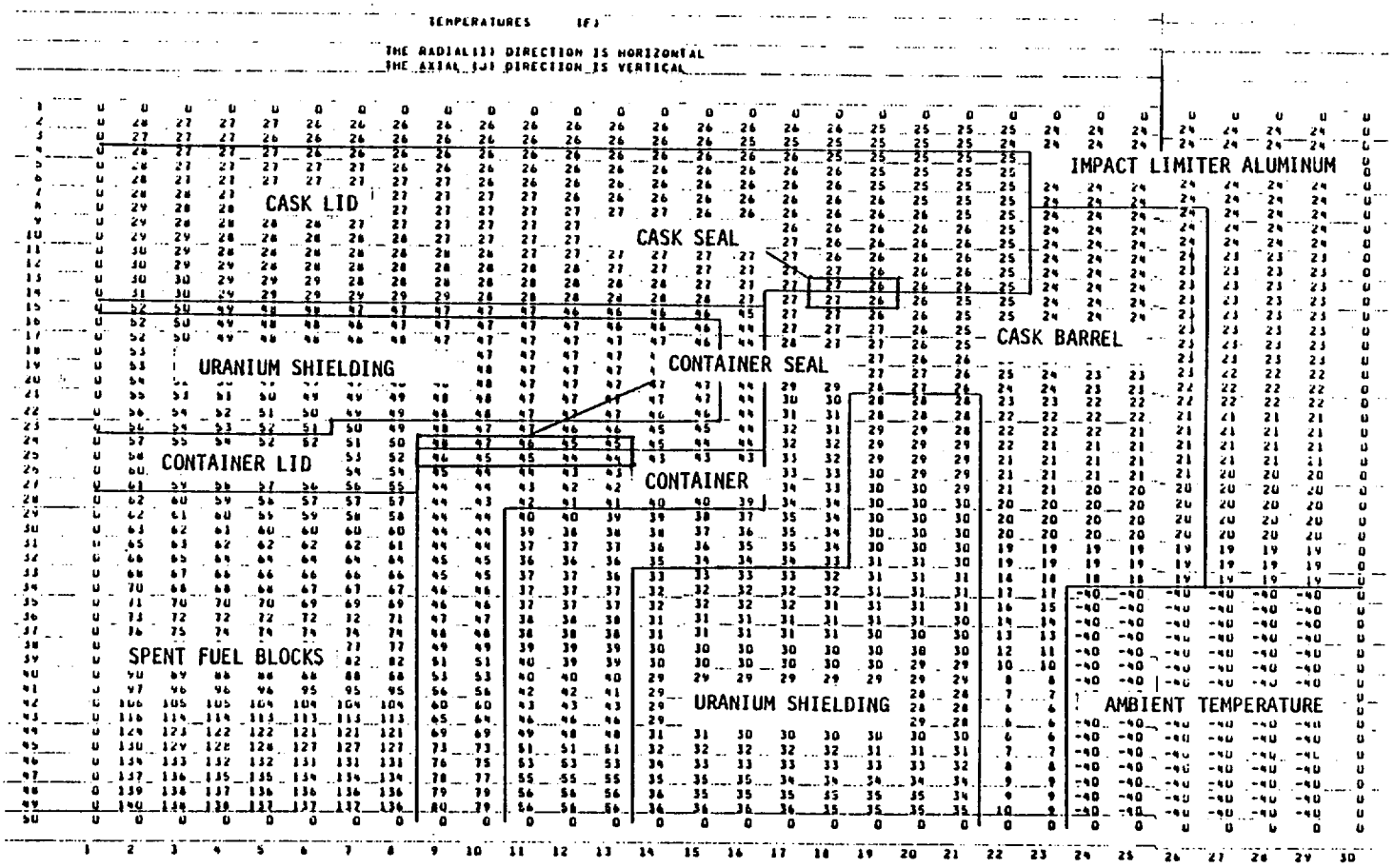

Figure 3-7. Fuel Shipping Cask Temperature Map for Steady State Condition 2 (Minimum Temperature Day) - Minimum Gap Configuration, 200 Day Fuel.

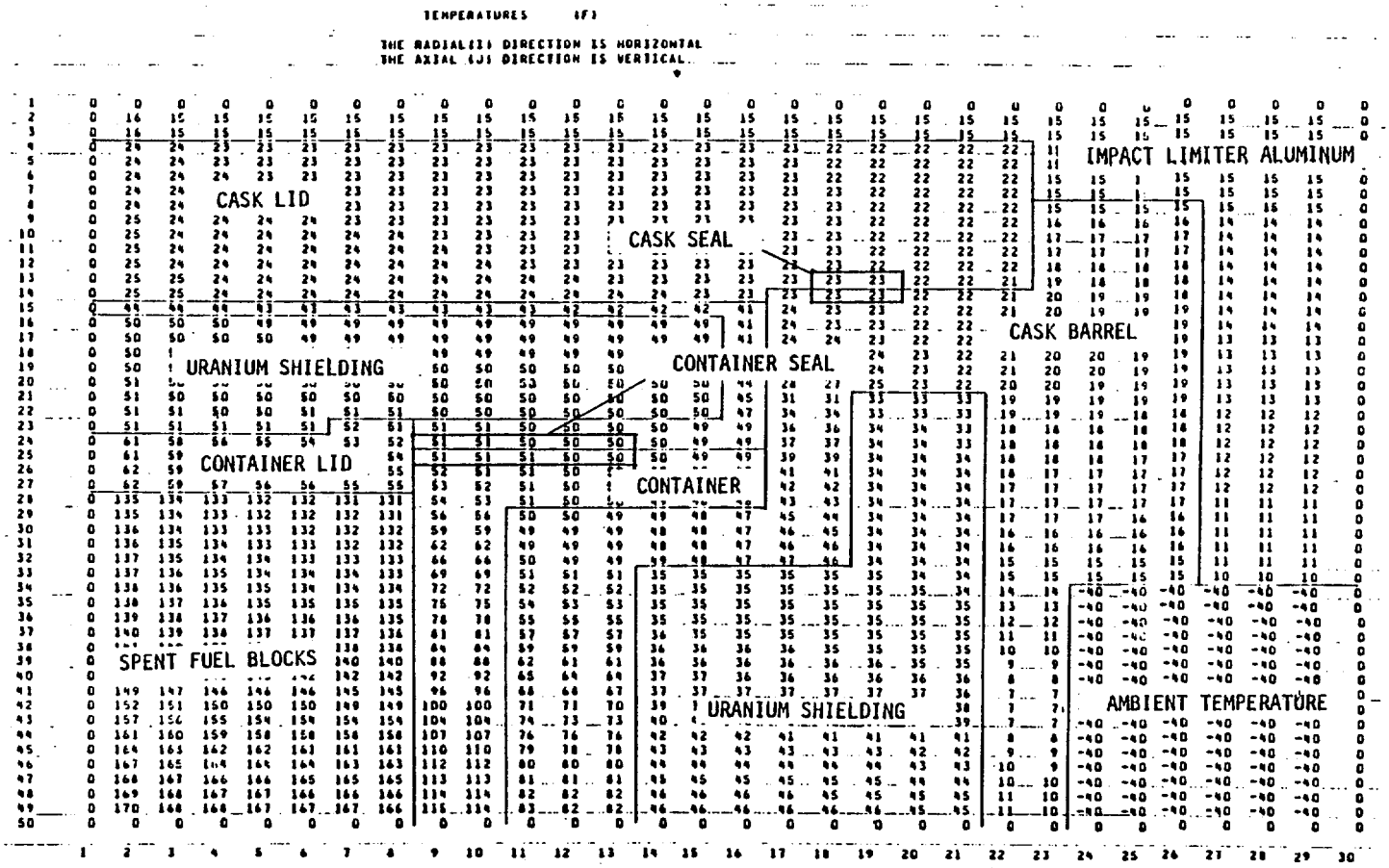

Figure 3-8. Fuel Shipping Cask Temperature Map for Steady State Condition 2 (Minimum Temperature Day) - Maximum Gap Configuration, 200 Day Fuel.

REFERENCES

3-1 U.S. Nuclear Regulatory Commission: Packaging of Radioactive Material for Transport and Transportation of Radioactive Material Under Certain Conditions; 10CFR, Part 71, Appendices A and B, April 30, 1975.

3-2 Davis, C. R., et al., Final Design Report for Fort St. Vrain Fuel Shipping Cask with "As-Built" Information; General Atomic Report GADR-55, including Supplements A, B and C.

3-3 Boonstra, R. H.: TAC2D a General Purpose Two-Dimensional Heat Transfer Computer Code - User's Manual; General Atomic Report GA-A14032, July 15, 1976.

3-4 Morcos, S. M., K. A. Williams: The TAC2D Code, Version TFMABC 75-1, Part C: Code Verification and Benchmark Problems; General Atomic Report GA-A13415, June 1975.

3-5 Freudiger, F. S., T. E. McKelvey: Cask Thermal Analysis Computer Runs; GAC Calculation File No. DEC 15001, 1978.

3-6 Anonym.: O-Ring Handbook; Parker Seal Company - Lexington KY 40509, January 1977 Edition (Page A3-36).

3-7 McAdams, W. H.: Heat Transmission; McGraw-Hill Book Company, Inc., 1954.

3-8 Shappert, L. B., et al.: A Guide for the Design, Fabrication, and Operation of Shipping Casks for Nuclear Applications; Oak Ridge National Laboratory, Oak Ridge, Tenn., February 1970.

3-9 Goodman, J., et al.: The Thermodynamic and Transport Properties of Helium, General Atomic Report GA-A13400, October 1975.

3-10 Kreith, F.: Principles of Heat Transfer; International Textbook Company, Section 1958.

3-11 Perry, R. H. (ed.): Chemical Engineer's Handbook, 4th Edition, McGraw-Hill Book Company, Inc., New York, 1963.

3-12 ASME Code: Section III, Appendix I.

3-13 Brown, W. F., Jr., in Aerospace Structural Metals Handbook, Volume III, Department of Defense, Washington, DC, 1972.